ISSN Print: 2518-4245
ISSN Online: 2518-4253
Vol. 60(3), September 2023

PROCEEDINGS
OF THE PAKISTAN ACADEMY OF SCIENCES:
A. Physical and Computational Sciences

PAKISTAN ACADEMY OF SCIENCES
ISLAMABAD, PAKISTAN

Proceedings of the Pakistan Academy of Sciences: Part A
Physical and Computational Sciences

Proceedings of the Pakistan Academy of Sciences A. Physical and Computational Sciences is the official flagship, the peer-reviewed quarterly journal of the Pakistan Academy of Sciences. This open-access journal publishes original research articles and reviews on current advances in the field of Computer Science (all), Materials Science (all), Physics and Astronomy (all), Engineering Sciences (all), Chemistry, Statistics, Mathematics, Geography, Geology in English. Authors are not required to be Fellows or Members of the Pakistan Academy of Sciences or citizens of Pakistan. The journal is covered by Print and Online ISSN, indexed in Scopus, and distributed to scientific organizations, institutes and universities throughout the country, by subscription and on an exchange basis.

Annual Subscription: **Pakistan:** Institutions, Rupees 4000/-; Individuals, Rupees 2000/- (Delivery Charges: Rupees 150/-)
Other Countries: US$ 200.00 (includes air-lifted overseas delivery)

HEC Recognized, Category Y; Scopus Indexed

Published by **Pakistan Academy of Sciences**, 3 Constitution Avenue, G-5/2, Islamabad, Pakistan
Email: editor@paspk.org; **Tel:** 92-51-920 7140 & 921 5478; **Websites:** www.paspk.org/proceedings/; www.ppaspk.org

Printed at **Graphics Point.,** Office 3-A, Wasal Plaza, Fazal-e-Haq Road Blue Area Islamabad.
Ph: 051-2806257, **E-mail:** graphicspoint16@gmail.com

PROCEEDINGS OF THE
PAKISTAN ACADEMY OF SCIENCES: PART A
Physical and Computational Sciences

CONTENTS

Volume 60, No. 3, September 2023 **Page**

Review Article

Blockchain in Healthcare: A Comprehensive Survey of Implementations and a Secure Model Proposal 1
— *Mehak Maqbool Memon, Manzoor Ahmed Hashmani, Filmann Taput Simpao, Anthony Cinco Sales, Neil Quinones Santillan, and Dodo Khan*

Research Articles

Acoustical Analysis of Insertion Losses of Ceiling Materials 15
— *Enobong Patrick Obot, Rufus Chika Okoro, Daniel Effiong Oku, Christian Nlemchukwu Nwosu, and Michael Ugwu Onuu*

Practical Analysis of Tap Water Dissolved Solids Efficient Reduction 27
— *Muhammad Imran Majid, and Naeem Shahzad*

An Intelligent Decision Support System for Crop Yield Prediction Using Machine Learning and Deep Learning Algorithms 37
— *Maryum Bibi, Saif-Ur-Rehman, Khalid Mahmood, and Rana Saud Shoukat*

Nutritional Study of Various Cow Breeds from Bhatta Chowk Lahore (Punjab), Pakistan 49
— *Asad Gulzar, Bisma Sher, Shabbir Hussain, Abdul Ahad Rasheed, Muhammad Salman, Shazma Massey, and Abdur Rauf*

Evaluation of Bending Length, Rigidity and Modulus of Woven and Knitted Fabrics 57
— *Mehreen Ijaz, Namood-e-Sahar, and Zohra Tariq*

Mathematical Analysis on Spherical Shell of Permeable Material in NID Space 63
— *Saeed Ahmed, Muhammad Akbar, Muhammad Imran Shahzad, Muhammad Ahmad Raza, and Sania Shaheen*

Instructions for Authors

Submission of Manuscripts: Manuscripts may be submitted as an e-mail attachment at editor@paspk.org or submit online at http://ppaspk.org/index.php/PPASA/about/submissions. Authors must consult the ***Instructions for Authors*** at the end of this issue or at the Website: www.paspk.org/proceedings/ or www.ppaspk.org.

Proceedings of the Pakistan Academy of Sciences: A Physical and Computational Sciences 60(3): 1-13 (2023)

ISSN (Print): 2518-4245; ISSN (Online): 2518-4253
https://doi.org/10.53560/PPASA(60-3)816

Pakistan Academy of Sciences

Review Article

Blockchain in Healthcare: A Comprehensive Survey of Implementations and a Secure Model Proposal

Mehak Maqbool Memon[1], Manzoor Ahmed Hashmani[1*], Filmann Taput Simpao[2], Anthony Cinco Sales[3], Neil Quinones Santillan[4], and Dodo Khan[1]

[1]Department of Computer and Information Sciences, Universiti Teknologi Petronas, Malaysia
[2]College of Engineering, University of Southeastern Philippines, Philippines
[3]Department of Science and Technology, Regional Office No. XI, Philippines
[4]MS3 Agriventures Corp, Philippines

Abstract: Blockchain's core attributes, including decentralization, transparency, and immutability, have positioned it as a pioneering technology in the realm of financial technology (fintech) and have rendered it highly applicable across diverse industries. The current enterprise ecosystem has faced setbacks primarily due to a lack of trust in the existing infrastructure. This issue can be traced back to the centralized management of healthcare data, making it vulnerable to tampering and fraudulent activities, resulting in financial losses. The existing enterprise ecosystem failed due to the lack of trust in the currently in-place infrastructure. This problem can be attributed to the centralized healthcare data management, which is prone to tampering and fraudulent activities leading to capital loss. The present study relates to a comprehensive survey conducted in timespan from 2018 to 2022 on the implementation of blockchain technology in the healthcare industry, identifying and discussing the key challenges facing the healthcare industry, such as fraud, and scams against healthcare data. It is found that there is an enormous inclination towards the decentralization of patient-centric data. However, a rapid decline is reported due to the privacy and security concerns of the confidential and sensitive data. Moreover, it is noticed that most of the implementations utilized either Ethereum or Hyperledger. Based on the survey's findings, the study proposed a blockchain-based healthcare framework that can address the identified challenges by providing a secure and transparent platform for collecting, storing, and sharing patient health data while prioritizing security and privacy.

Keywords: Blockchain in Healthcare, Healthcare Scams, Blockchain Solution, eHealthcare, Blockchain Architectures, Hyperledger, Enterprise Ecosystem, Ethereum, Transparency, Survey.

1. INTRODUCTION

Blockchain (BC), with its core features including decentralization, transparency, and immutability, has emerged as a leader in financial technology (fintech). These features are applicable to various industries desiring transparent and trackable practices. The enterprise blockchain provides a decentralised platform to involve stakeholders to increase gain margins. Some of the known enterprise blockchains include digital identity systems for theft reduction by providing greater ownership of the data [1], sustainable solutions for companies suffering from siloed infrastructures with multiple touchpoints [1, 2], healthcare & insurance requiring efficient data management to protect sensitive data by streamlining transparent data verification practices and distributions [3], entertainment and sports industry prone to piracy of the digital content may be benefitted by managing authentic digital distributions and fan engagement with enhanced loyalty programs and incentives [4], and real estate and supply chain involving global agencies to efficiently monitor and track the digital asset management [2, 5]. The existing enterprise ecosystem failed due to the lack of trust in the currently in-place infrastructure. A similar problem can be attributed to the centralised healthcare data management. Healthcare big data is growing rapidly, including information of patients,

Received: April 2023; Accepted: September 2023
*Corresponding author: Manzoor Ahmed Hashmani <manzoor.hashmani@utp.edu.my>

hospitals, and insurance agencies, with the medical insurance system functioning based on the data transmitted by the hospitals (including physicians and pharmacies). The insurance claims are borne by the agency based on the logs generated against the patient's health in the form of medical treatments, medicines and equipment used. Since the entire workflow is centralized and all involved use their centralized independent silos, it is easier to tamper with the data [3-9]. This form of tampering leads to easier ways of fraudulent scams against medical insurance. As per the 2020 report of the United States Sentencing Commission, losses related to healthcare scams have exponentially increased in the US over the years [4, 10]. The capital loss witnessed over the period from 2016 to 2020. Care Anti-Fraud Association (NHCAA), claims tens of billions of dollars of fraudulent scams per year. one source of fraud is from the patients themselves by identity swapping or identity theft, wherein one person's insurance is used by another person. Finally, the prescriptions are also forged and illegally used to claim the increased amount of money [5, 11]. The traditional data-sharing methods were deemed as the major cause of the scams due to centralized data stores and single-point-of-failure, which results in poor data security and privacy strategies. The second major problem is unconnected data in which a patient's information can be easily changed, leaving behind no trace leading to another security-related problem. Moreover, in healthcare scenarios, insurance claims are essentially dependent on third-party administrators. As such, sharing this information with third-party administrators over a network means exposing sensitive data to cyber-attacks [6]. Considering the current healthcare ecosystem and associated data-driven attacks. A decentralized solution such as blockchain has the potential to bring medical big data onto the decentralized ledger, where a single change is transparent to all the individuals/ organizations involved. The data on the blockchain is secure due to the usage of cryptography, where only known users can have access to the actual information. This study makes a significant contribution in two ways. Firstly, it conducted a comprehensive survey on the implementation of blockchain technology in the healthcare industry. The survey explored various aspects such as fraud, scams, and data storage techniques related to healthcare. By examining these issues, the study identified the key challenges facing the healthcare industry regarding implementing blockchain technology and the major frameworks to be implemented. Secondly, based on the findings from the survey, the study proposed a blockchain-based healthcare framework that can address the identified challenges. The proposed framework consists of different components. By integrating these components, the proposed framework aims to provide a secure and transparent platform for collecting, storing, and sharing patient health data while prioritizing security and privacy.

2. SURVEY METHODOLOGY AND CRITICAL ANALYSIS ON HEALTHCARE IMPLEMENTATIONS

The current healthcare ecosystem is susceptible to scams and fraud due to centralized regulatory entities. This centralized scenario deviates the entire healthcare insurance ecosystem from the goal of health policies to uphold the applicant's/ patient's health. Over the period of the last decade, blockchain-based solutions have been revolutionizing different domains such as supply chain, education, healthcare and so on [7, 15, 22-24]. This revolution is in terms of the minimization of single-entity dependence and ownership of data to maintain the integrity of patients.

This section critically analyzes healthcare-related blockchain-based research reported in a timespan from 2018 to 2022. At the time of compilation of this research, the main 3 (Google Scholar, IEEE, Science Direct) repositories have been queried with 3 different search queries. The search queries included the following phrases: "medical fraud detection blockchain decentralization"; "healthcare blockchain system"; and "healthcare blockchain system smart contracts". The search resulted in the retrieval of 39 indexed research articles. Figure 1 shows the blockchain-based healthcare research solution trend. In the year 2020, most of the blockchain-based solutions have been reported due to the readily available implementation resources and the hype in the domain of blockchain solutions, whereas a rapid decline was seen in the following years. One of the major reasons for this decline is the usage of architectural platforms which leads to lesser trust of stakeholders in the technology due to the shift towards public networks.

Drilling down further into the details of these researches uncovered the fact that most of the decentralized healthcare researches used Ethereum-based platforms, which raises concerns about private patient data handling as it is inherently a public blockchain network. Figure 2 shows the division of development platforms reported in the 39 Combine these paragraphs.

Figure 2 shows over 40 % of the blockchain-based healthcare solution are backed by Ethereum-based architectures which inherits features of public blockchain architecture. Whereas 28 % research focuses merely on the conceptualization of use case under consideration. Hyperledger-based implementations dominate only 17 percent of the overall research which inherits the features of the consortium blockchain solution. Finally, 5 and 10 percent represent other platforms and articles without platform specifics respectively.

The comprehensive critical analysis of these 39 blockchain-based healthcare research articles is further presented in Table 1 which shows detailed analysis of conducted research. It is seen

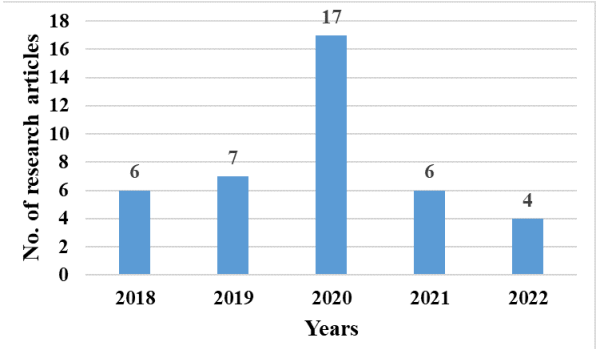

Fig. 1. Distribution of research articles in healthcare blockchain system (2018-2022)

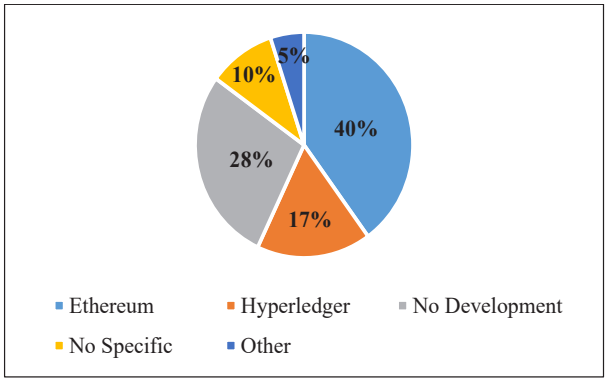

Fig. 2. Blockchain based Development Platforms for Healthcare

that there is immense inclination towards the decentralization of patient-centric data. However, most of the articles have provided the conceptual module for the healthcare sector. As stated earlier, a rapid decline in the blockchain-based studies in healthcare was witnessed leading the researchers to believe that it is due to the privacy concerns of the confidential and sensitive hospital data which otherwise is inaccessible to irrelevant identities. Most of the reported developed use cases are based on public blockchain networks which can be easily accessed by any registered node. Moreover, registration of new nodes is comparatively easy in public blockchains. Additionally, if encryption mechanisms are implemented on top of public blockchain network, it increases the computational resources. Eventually, stakeholders may lose interest in blockchain technology due to association of sensitive patient data to be handled. The private blockchain systems are still governed by a singular entity, meaning hospitals and third-party insurance companies should create their own separate ledgers which serves the purpose of traceability within respective organizations only. Whereas the consortium-based blockchains (such as Hyperledger) seem to be a promising solution as the development ecosystem is designed in such a way that all the involved entities are brought onto a single ledger and new registration of nodes is still controlled by the authorized nodes. Section 4 further discusses the details of public and consortium-based architectures of blockchain to compare the offered features with respect to the healthcare data and how they can help in reduction of healthcare scams.

3. APPLICABILITY OF BLOCKCHAIN DEVELOPMENT PLATFORMS

The most popular blockchain development platforms are Ethereum and Hyperledger. Both networks belong to different architectural schemes based on the accessibility. As mentioned earlier, Ethereum is a public blockchain while Hyperledger is a consortium blockchain. This section compares the features of both platforms with respect to enterprise business use as in the case of healthcare. Both the blockchain platforms are open source. In converting existing healthcare management systems, it is imperative to identify the correct representative platform for the implementation.

Table 1. The comprehensive critical analysis Blockchain based healthcare research.

S. No.	Title	Survey/ Use case	Year	Comments
1	Identifying fraud in medical insurance based on blockchain and deep learning [8]	Use case	2022	• Bidirectional Encoder Representations from Transformers (BERT-LE) model. • Based on consortium Blockchain • Two real datasets from two 3A hospitals • Participants: Hospital, regulatory agency, Medical insurance center, patient • Practical Byzantine Fault Tolerance (PBFT) consensus • No clear specification which blockchain architecture/ framework is used (Hyperledger/quorum etc) • Uses Machine Learning (ML) along with decentralization.
2	A survey of blockchain-based IoT eHealthcare: Applications, research issues, and challenges [9]	Survey	2022	• Reports 12 Ethereum, 6 Hyperledger, 6 others (4 without smart contract) research articles. • Future research might consider incorporating more technological characteristics to improve feasibility evaluation and narrow the gap between ideas and implementations, propelling healthcare technology.
3	Blockchain Framework for Cognitive Sensor Network Using Non-Cooperative Game Theory [10]	Use case	2022	• Ethereum-based private blockchain for medical sensory data tracing and tracking. • Keeps track of patient's illness and treatments. • Proposes a merger module based on Blockchain (BC), ML and IoT to bring in Internet of Medical Things (IOMT) scenario working. • EEG blood pressure data of patient and other details of patient and hospital are saved in the decentralized ledger. • Focuses fraud detection in medicare. • Federated Learning Aware Blockchain Enabled IoMT is proposed. • Does not mention which blockchain is used.
4	Using blockchain and semantic web technologies for the implementation of smart contracts between individuals and health insurance organizations [11]	Use case	2022	• Ethereum-based implementation for maintaining health insurance data. • With additional layer of security as the blockchain used is implicitly public.
5	Healthcare Insurance Frauds: Taxonomy and Blockchain-Based Detection Framework (Block-HI) [12]	Use case	2021	• Just a plan for blockchain implementation in medicare fraud detections. • Considers up to 12 different ways of threat in medicare to be resolved by decentralization. • Good for conceptualization.
6	Health Insurance Claim Using Blockchain [13]	Use case	2021	• Medical health report keeping via decentralization. • Implements blockchain but does not provide any information of architecture. • Provides good conceptualization.
7	Decentralized Healthcare Management System Using Blockchain to Secure Sensitive Medical Data for Users [14]	Use case	2021	• Proposes SADS (stringent authentication and decentralized storage). • Correlates the implementation with the usage for fraud detection but originally implanted for record keeping. • Uses hash function of SHA-256. • No clear mentions of blockchain architecture used.

8	HealthBlock: A secure blockchain-based healthcare data management system [15]	Use case	2021	• Detailed study with all the conceptualization diagrams. • Closely consider the aspect of privacy and security. • Hyperledger based implementation is used.
9	A Blockchain and Artificial Intelligence-Based, Patient-Centric Healthcare System for Combating the COVID-19 Pandemic: Opportunities and Applications [16]	Survey	2021	• Detailed survey for the applicability of BC in healthcare along with integration of AI. • Proposes a conceptualization module to create decentralized medicare solution. • Proposes usage of Ethereum-based blockchain which nullifies the privacy and secrecy of patient in its original form.
10	Decentralized secure storage of medical records using Blockchain and IPFS: A comparative analysis with future directions [17]	Survey	2021	• Discusses the storage issues of Medicare BC solutions. • Detailed study focusing Ethereum perspective. • Presents existing decentralized medical health data keeping solutions.
11	Implementing healthcare services on a large scale: Challenges and remedies based on blockchain technology [18]	Use case	2020	• Proposes AarogyaChain. • Uses Hyperledger. • Identifies speed throughput for transactions. • three tiers: the tier-I comprises of patients and physicians, the tier-II includes healthcare organizations, and the tier-III is the government. • Three probs speed, security, and decentralization requirements together
12	Application of Blockchain and IoT towards Pharmaceutical Industry [19]	Use case	2020	• General blockchain study. • Discusses challenges for use case no information for blockchain architecture.
13	Blockchain technology applications to postmarket surveillance of medical devices [20]	Use case (Plan only)	2020	• Focuses post market surveillance issue of the medical devices and emphasizes on the usage of blockchain technology. • Gives out 10-year long term switch plan to convert the centralized mechanism to decentralized. • No mention of recommendation for usage of type of blockchain architecture.
14	Health Care Insurance Fraud Detection Using Blockchain [21]	Use case	2020	• Uses tendermint having BFT consensus but the core is built on public blockchain, Ethereum-based. • Focuses the problem of fraud detection and in medical insurances. • Good research article for the core blockchain project implementations.
15	Blockchain solutions for healthcare [22]	Survey	2020	• Discusses the evolution of blockchain and relevance with healthcare. • Sheds light on the challenges and future directions of research.
16	Combating Health Care Fraud and Abuse: Conceptualization and Prototyping Study of a Blockchain Antifraud Framework [23]	Use case	2020	• Keeps track of fraud and theft in medical insurances. • Describes every aspect of implementation from front to backend of Decentralized Application (DApp) development. • Ethereum-based implementation with restricted permissions using Health Insurance Portability and Accountability Act (HIPAA) business associate agreement.

17	Towards a Remote Monitoring of Patient Vital Signs Based on IoT-Based Blockchain Integrity Management Platforms in Smart Hospitals [24]	Use case	2020	• Manages patient's sensory data on decentralized ledger. • In current state no mechanism for fraud detection. • Hyperledger Fabric based framework. • Mentions details of the development top-to-down.
18	A blockchain-based secure healthcare scheme with the assistance of unmanned aerial vehicle in Internet of Things [25]	Use case	2020	• Patient's UAV (unmanned vehicular data) is stored in decentralized ledger to keep the track of activity performed. • Proposed BHealth system is based on Ethereum, which is public blockchain, this raises issues related to privacy and security of patient.
19	GuardHealth: Blockchain empowered secure data management and Graph Convolutional Network enabled anomaly detection in smart healthcare [26]	Use case	2020	• Patients record maintenance meeting the aspect of privacy and confidentiality. • Consortium-based implementation. • Implicit privacy handling by implemented BC architecture. • Added intelligence by using convolutional neural networks. • More information for DApp implementation is required.
20	S2HS- A blockchain based approach for smart healthcare system [27]	Use case	2020	• Maintenance of electronic medical records on decentralized ledger. • Detailed analysis of blockchain technology growth. • Just the conceptualization, analysis of blockchain research w.r.t healthcare dept.
21	Blockchain-based electronic healthcare record system for healthcare 4.0 applications [28]	Use case	2020	• Hyperledger based implementation. • Detailed analysis of transaction time and cost for performance.
22	A Blockchain-Based Smart Contract System for Healthcare Management [29]	Use case	2020	• Detailed in terms of more participant and use cases (pharmacy, physicians, consultants, patients, and insurance agency roles) have been addressed. • Uses Ethereum-based implementation and uses Delegated PoS (Proof-of-Stake) Consensus.
23	Blockchain Based Smart Contracts for Internet of Medical Things in e-Healthcare [30]	Use case	2020	• Proposes a sensory data keeping engine to track patient's health. • Implements BC network from scratch in MATLAB networking simulator. • Does not discuss privacy concerns. • Focuses identification and comparison of packet delivery ratio, energy consumed and latency.
24	Use of Blockchain Technology to Curb Novel Coronavirus Disease (COVID-19) Transmission [31]	Use case	2020	• Implements Ethereum-based blockchain. • Proposes the data management and sharing of covid patients to help stop the spreading of virus. • This use case works well with public blockchain.
25	A remix IDE: smart contract-based framework for the healthcare sector by using Blockchain Technology [32]	Use case	2020	• Ethereum-based blockchain is used. • The specific smart contract used are mocha and chai. • Privacy concerns remains unresolved.

26	SHealth: A Blockchain-Based Health System with Smart Contracts Capabilities [33]	Use case	2020	• PBFT is used for consensus. • The blockchain is implemented from scratch, however, it is compatible with Hyperledger.
27	Applications of blockchain in ensuring the security and privacy of electronic health record systems: A survey [34]	Survey	2020	• Detailed survey with conceptual diagrams for each category of BC architecture and its relevance with distributed medicare data. • Compare and contrast discussions of private, public and consortium blockchain architectures can be extended w.r.t security.
28	A Blockchain-Based System for Anti-Fraud of Healthcare Insurance [35]	Use case	2019	• Anti-fraud service application architecture based on blockchain with cross-cloud platform. • Future work discusses implementation of Hyperledger.
29	Secure and Scalable mHealth Data Management Using Blockchain Combined With Client Hashchain: System Design and Validation [36]	Use case	2019	• Uses Hyperledger Fabric v1.0 for implementation combined with client hashchain of extra security layer. • Provides mobile based health decentralised solution (mhealth). • Tackles medical health record keeping only.
30	Fraud Detection in Medical Insurance Claim with Privacy Preserving Data Publishing in TLS-N Using Blockchain [37]	Use case	2019	• Focused research of decentralized solution for insurance related thefts. • Ethereum-based smart contract implementation. • Incorporating TLS-N in communication. • The core bc remains public.
31	Secure Electronic Medical Records Storage and Sharing Using Blockchain Technology [38]	Use case	2019	• Hyperledger with PBFT consensus algorithm-based implementation is used. • Considers security and privacy aspects of patient and hospital data. • No real data implementation so far. • No mentions of fraud detection.
32	A Secure Healthcare System Design Framework using Blockchain Technology [39]	Use case	2019	• Presents the conceptualization framework with role of different entities and amalgamation of IoT. • Discusses privacy concerns of patient but w.r.t blockchain implementation does not mention any concern.
33	Blockchain in healthcare applications: Research challenges and opportunities [40]	Use case	2019	• Discusses different theoretical aspects of blockchain networks. • Mentions privacy, consensus mechanisms but does not mention the suitable platform for development. • Compares the existing medicare data BC networks.
34	Applications of Blockchain Technology in Medicine and Healthcare: Challenges and Future Perspectives [41]	Survey	2019	• Discusses opportunities for medicare to be handled on distributed ledger. • Mentions all the possibilities & challenges of integration with AI & ML. • Can be further extended w.r.t to development platforms.
35	Geospatial blockchain: promises, challenges, and scenarios in health and healthcare[42]	Survey	2018	• Discusses possibilities of decentralization for different domains including pharmaceutical, medicine, supply chain, clinical trials, and smart cities. • Focuses on the identification of bc search interest in all the mentioned domains.

36	Privacy-friendly platform for healthcare data in cloud based on blockchain environment [43]	Use case	2018	• Ethereum-based patient record keeping. • The research is inclined towards the applicability in terms of time consumed for retrieval (speed) and cost involved. • Such sensitive data should be kept secure – Major flaw.
37	Healthcare Blockchain System Using Smart Contracts for Secure Automated Remote Patient Monitoring [44]	Use case	2018	• Covers the aspect of patient's health monitoring via decentralization. • Private blockchain based on Ethereum. • Quotes "Hyperledger is more user friendly with a UI and customer support." • Implements private Ethereum blockchain. • The use case focuses transparent information sharing between physician and the patient. • Uses extra layer of encryption as privacy mechanism.
38	A Secure Remote Healthcare System for Hospital Using Blockchain Smart Contract [45]	Use case	2018	• IoT based blockchain solution for patient's health monitoring. • Implements Ethereum-based BC • As counter mechanism for privacy of patient in public BC sets patient's identity to anonymous but his/her medical history remains on public blockchain. • Presence of data raises concerns related to hacking of the authorized nodes or fishing with random identity numbers to identify the actual one remains unresolved.
39	Blockchain and Smart Contracts in a Decentralized Health Infrastructure [46]	Use case	2018	• Assigns medical cards to the patients and connect all the involved parties (physicians, patients, insurance agencies) over single platform. • Provides the concept of BC in medicare scenario does not mention development concerns.

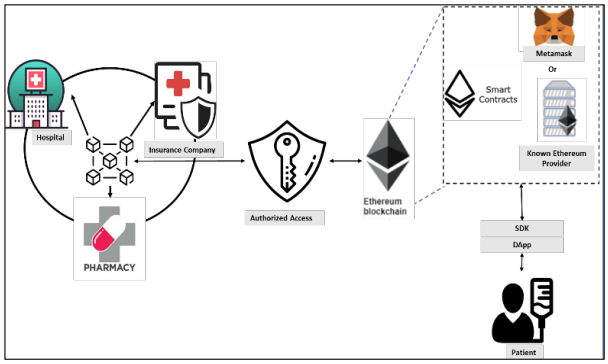

Fig 3. Implementation schema of Ethereum [14]

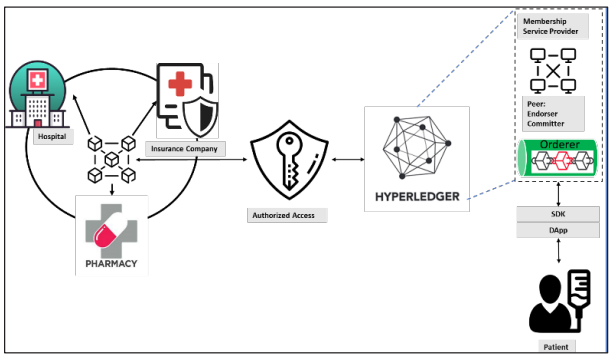

Fig 4. Implementation schema of Hyperledger [27]

3.1 Ethereum

In operating the system on Ethereum's EVM (Ethereum Virtual Machine), 'gas' is required to get the access of public network. For every transaction, Combine these paragraphs.

Implying that if the threatening entity has gas, it can easily get the access of network. Figure 3 shows the Ethereum-based implementation schema for healthcare data management. All the entities are connected over the Ethereum blockchain. A patient registers via the DApp interface, which is connected to the EVM. In getting the EVM imprint, either metamask or known providers are requested. Finally, all the existing nodes are connected via predefined smart contracts.

3.2 Hyperledger

Hyperledger is one of the consortiums blockchain architectures. It is based on the modular approach

for enterprise blockchain solutions. The consensus is based on different components including peers, MSP (Membership Service Provider), and orderer. All the peers are nominated by administrators of each organization thus no unauthorized entities can trespass the distributed ledger. The key feature of Hyperledger is freedom of selection for consensus. The consensus is divided into three steps: endorsement, ordering, and validation. Figure 4 shows the Hyperledger-based implementation schema for healthcare data management. Table 2 compares the features of Ethereum and Hyperledger. The supporting languages of Ethereum development are Go and Solidity whereas Hyperledger support several programming languages with rich functionalities and already known to the research community. Both platforms support their respective consensus. However, the consensus supported by Hyperledger is transactional level, implying tracking of every single change to be logged.

After a detailed comparative discussion of the known existing blockchain architectures and the platforms, the final argument to be addressed is the selection of a platform for enterprise data management infrastructure. Considering the requirements and workflows involved in enterprise's business logic (healthcare), specifically for insurance claims and scam tracking, the idea is to provide access only to authorized users that are also predefined/nominated peers. This ensures the decentralization of data among the organizations without affecting privacy of patient. Both the feature decentralization along with the implicit privacy feature is offered by Hyperledger.

4. PROPOSED BLOCKCHAIN BASED HEALTHCARE MODEL

The proposed blockchain-based healthcare model is designed to provide a secure and transparent framework for collecting, storing, and sharing patient health data. It aims to improve the security and privacy of patient data by utilizing blockchain technology to provide a decentralized and tamper-proof platform for storing and sharing patient health data with other entities such as insurance claims, pharmacies, prescription etc. This ensures that patient health data is secure and protected from unauthorized access, while also providing transparency in the use and sharing of the data. This model addresses the frauds, scams in the healthcare eco system (hospitals, insurances and patients). The Figure 5 illustrated Blockchain based health

Table 2. Public versus consortium Blockchain development platform

Platform	Ethereum	Hyperledger
• Type	• Permission less, public, or private (limited permissions)	• Consortium
• Database Compatibility	• Ethereum's Rust client Parity uses RocksDB Ethereum's Go, C++ and Python clients all use LevelDB • BigchainDB	• Compatible with CouchDB
• Supporting languages	• Go, Solidity	• JavaScript, Java, Go, Python, and Node.js
• Host Platform	• Ethereum developers	• IBM
• Operating System	• Linux, macOS, Windows	• Linux foundation(base) Linux, Windows
• Consensus	• Mining based on Proof of Work (PoW) • Ledger level • PoA (Aura) • PoS (Casper)	• Multiple approaches (PBFT, CFT-Kafka, Raft) • Transaction-level
• Currency	• Ether • Tokens via smart contracts	• None (Currency and tokens via chaincode)
• Smart contracts	• Smart contract code (e.g., Solidity)	• Smart contract development in JavaScript, Java, Go, and Node.js

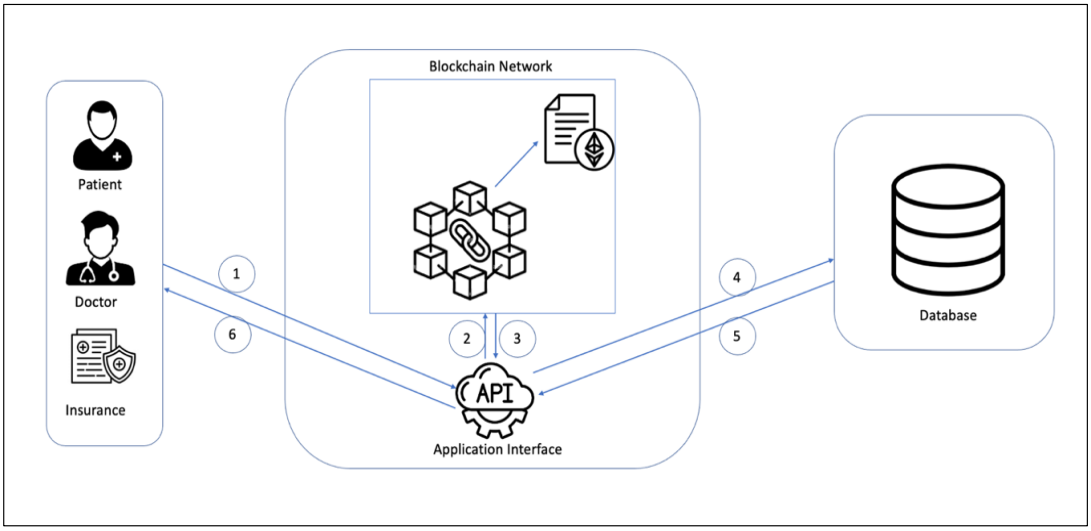

Fig. 5. Proposed healthcare model

model which is consists of six components that work together to ensure the privacy and security of patient health data while enabling healthcare providers and patients to access and utilize the data to improve healthcare outcomes [47]. Moreover, Figure 6 shows the flow of data from its origin (patient) to Blockchain and electronic health record (EHR). Initially data generates from patient's wearable or medical device, and it will be forwarded to Blockchain via API and eventually EHR in very transparent way. It also be query back to patient or healthcare provider with the same path. Any temper on data has to get a consensus from other stakeholders.

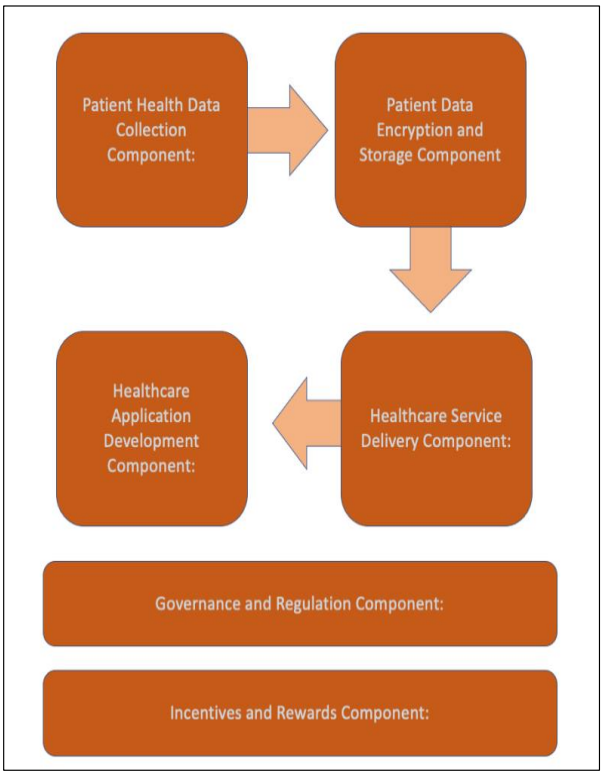

Fig 6. Flow of data in the proposed model

The model consists of six components:

- Patient Health Data Collection Component: This component is responsible for collecting patient health data from various sources, including medical devices and healthcare providers, wearables etc.
- Patient Data Encryption and Storage Component: This component receives and stores the encrypted patient health data on the blockchain. The blockchain ensures that the data is decentralized and tamper-proof, providing a secure and transparent platform for sharing patient health data.
- Healthcare Service Delivery Component: This component provides healthcare services to healthcare providers, patients, and other stakeholders based on the patient health data stored on the blockchain. These services may include telemedicine, remote monitoring, and personalized medicine.
- Healthcare Application Development Component: This component provides healthcare applications that enable healthcare providers to access and interact with the patient health data stored on the blockchain. These applications may include mobile apps, web portals, and electronic health records (EHRs).

- Governance and Regulation Component: This component provides oversight and governance of the framework, ensuring that the patient health data is accessed, used, and shared in a secure and transparent manner. This includes regulatory compliance, data privacy, and security standards.
- Incentives and Rewards Component: This component provides incentives for stakeholders to participate in the framework, encouraging the sharing of health data and use of the services provided. These incentives may include tokens, rewards, and discounts.

Overall, the proposed blockchain-based layered healthcare model is designed to prioritize security and privacy, with a focus on regulatory compliance and transparency. It aims to provide a secure and transparent platform for collecting, storing, and sharing patient health data while enabling healthcare providers and patients to access and utilize the data to improve healthcare outcomes. The model is designed to prioritize security and privacy, with a focus on regulatory compliance and transparency.

5. CONCLUSIONS

The present survey shows that the decentralized, transparent, and immutable features of Blockchain have made it a leading technology in fintech and applicable to various industries. However, the lack of trust in the existing enterprise ecosystem has led to problems, such as centralized healthcare data management being prone to tampering and fraudulent activities, causing capital loss. To address these challenges, a comprehensive survey was conducted and a blockchain-based healthcare framework was proposed that provides a secure and transparent platform for collecting, storing, and sharing patient health data while prioritizing security and privacy. This framework has the potential to revolutionize the healthcare industry and bring about a new era of trust and transparency in data management.

6. ACKNOWLEDGEMENT

This research work is a part of an ongoing research project jointly funded and facilitated by the Universiti Teknologi PETRONAS, Malaysia, University of Southeastern Philippines, Philippines, Department of Science and Technology, Philippines, and MS3 Agri-ventures Corporation, Philippines (Grant Number: 015ME0-307). Authors also acknowledge support, guidance, and advise of Prof. Dr. Mohd Shahir Liew and Assoc. Prof. Dr. Mohd Fadzil Hassan in the completion of this work.

7. CONFLICT OF INTEREST

The authors declare no conflict of interest.

8. REFERENCES

1. D. Khan, L.T. Jung, and M.A. Hashmani. Systematic literature review of challenges in blockchain scalability. *Applied Sciences* 11(20): 9372 (2021).
2. D. Khan, M.M. Memon, M.A. Hashmani, F.T. Simpao, A.C. Sales, and N.Q. Santillan. A Critical Review on Blockchain Frameworks for Dapp. *International Journal of Technology Management and Information System* 5(1): 1-10 (2023).
3. D. Khan, L.T. Jung, M.A. Hashmani, and M.K. Cheong. Blockchain Enabled Diabetic Patients' Data Sharing and Real Time Monitoring. *In CS & IT Conference Proceedings* 12(6): (2022).
4. D. Khan, L.T. Jung, M.A. Hashmani, and A. Waqas. A critical review of blockchain consensus model. *3rd international conference on computing, mathematics and engineering technologies (iCoMET):* 1-6 (2020).
5. D. Khan, L.T. Jung, and M.A. Hashmani. Proof-of-Review: A Review based Consensus Protocol for Blockchain Application. *International Journal of Advanced Computer Science and Applications* 12(3): 290-300 (2021).
6. K.C. Moke, T.J. Low, and D. Khan. IoT blockchain data veracity with data loss tolerance. *Applied Sciences* 11(21): 9978 (2021).
7. D. Khan, L.T. Jung, M.A. Hashmani, and M.K. Cheong. Empirical performance analysis of hyperledger LTS for small and medium enterprises. *Sensors* 22(3): 915 (2022).
8. G. Zhang, X. Zhang, M. Bilal, W. Dou, X. Xu, and J. Rodrigues. Identifying fraud in medical insurance based on blockchain and deep learning. *Future Generation Computer Systems* 130: 140-154 (2021).
9. M.S. Rahman, M.A. Islam, M.A. Uddin, and G. Stea. A survey of blockchain-based IoT eHealthcare: Applications, research issues, and challenges. *Internet of Things* 19(8): 100551 (2022).
10. S. Surekha, and M.Z.U. Rahman. Blockchain framework for Cognitive Sensor Network using

Non-Cooperative Game Theory. *IEEE Access* 10: 60114-60127 (2022).
11. E. Chondrogiannis, V. Andronikou, E. Karanastasis, A. Litke, T. Varvarigou. Using blockchain and semantic web technologies for the implementation of smart contracts between individuals and health insurance organizations. *Blockchain: Research and Applications* 3(2): 100049 (2022).
12. L. Ismail and S.J.I.p. Zeadally. Healthcare insurance frauds: Taxonomy and blockchain-based detection framework (Block-HI). *IT professional* 23(4): 36-43 (2021).
13. J. Kuckreja, P. Nigde, and P. Patil. Health Insurance Claim using Blockchain. *International Research Journal of Engineering and Technology (IRJET)* 8(5): 2406-2409 (2021).
14. N. Deepa, T. Devi, N. Gayathri, and S.R. Kumar. Decentralized Healthcare Management System Using Blockchain to Secure Sensitive Medical Data for Users. *Blockchain Security in Cloud Computing* 265-282 (2022).
15. B. Zaabar, O. Cheikhrouhou, F. Jamil, M. Ammi, and M.J.C.N. Abid. HealthBlock: A secure blockchain-based healthcare data management system. *Computer Networks* (200): 108500 (2021).
16. M.Y. Jabarulla, and H.N. Lee. A blockchain and artificial intelligence-based, patient-centric healthcare system for combating the COVID-19 pandemic. *Opportunities and applications In Healthcare* 9(8): 1019 (2021).
17. S. Kumar, A.K. Bharti, and R. Amin. Decentralized secure storage of medical records using Blockchain and IPFS: A comparative analysis with future directions. *Security and Privacy* 4(5): 162 (2021).
18. P. Pandey, and R. Litoriya. Implementing healthcare services on a large scale: challenges and remedies based on blockchain technology. *Health Policy and Technology* 9(1): 69-78 (2020).
19. A. Premkumar, and C. Srimathi. Application of blockchain and IoT towards pharmaceutical industry. *In 2020 6th International Conference on Advanced Computing and Communication Systems (ICACCS)*: 729-733 (2020)
20. J. Pane, K.M. Verhamme, L. Shrum, I. Rebollo, and M.C.J.M. Sturkenboom. Blockchain technology applications to postmarket surveillance of medical devices. *Expert Review of Medical Devices* 17(10): 1123-1132 (2020).
21. G. Saldamli, V. Reddy, K.S. Bojja, M.K. Gururaja, Y. Doddaveerappa, and L. Tawalbeh. Health care insurance fraud detection using blockchain. *Seventh International Conference on Software Defined Systems*: 145-152 (2020).
22. P. Zhang, and M.N.K. Boulos. Blockchain solutions for healthcare. In Book: Precision Medicine for Investigators, practitioners and providers. *Academic Press:* 519-524: (2020).
23. T.K. Mackey, K. Miyachi, D. Fung, S. Qian, and J. Short. Combating health care fraud and abuse: Conceptualization and prototyping study of a blockchain antifraud framework. *Journal of medical Internet research* 22(9): e18623 (2020).
24. F. Jamil, S. Ahmad, N. Iqbal, and D.H. Kim. Towards a remote monitoring of patient vital signs based on IoT-based blockchain integrity management platforms in smart hospitals. *Sensors* 20(8): 2195 (2020).
25. A.I. Abhi, and S.Y. Shin. A blockchain-based secure healthcare scheme with the assistance of unmanned aerial vehicle in Internet of Things. *Computers & Electrical Engineering* 84: 106627 (2020).
26. Z. Wang, N. Luo, and P. Zhou. GuardHealth: Blockchain empowered secure data management and Graph Convolutional Network enabled anomaly detection in smart healthcare. *Journal of Parallel and Distributed Computing* 142: 1-12 (2020).
27. G. Tripathi, M.A. Ahad, and S. Paiva. S2HS-A blockchain based approach for smart healthcare system. *Healthcare* 8(1): 100391 (2020).
28. S. Tanwar, K. Parekh, and R. Evans. Blockchain-based electronic healthcare record system for healthcare 4.0 applications. *Journal of Information Security and Applications* 50: 102407 (2020).
29. A.J.E. Khatoon. A blockchain-based smart contract system for healthcare management. *Electronics* 9(1): 94 (2020).
30. A. Sharma, Sarishma, R. Tomar, N. Chilamkurti, and B.G. Kim. Blockchain based smart contracts for internet of medical things in e-healthcare. *Electronics* 9(10): 1609 (2020).
31. A. Khatoon. Use of blockchain technology to curb novel coronavirus disease (COVID-19) transmission. *Available at SSRN* 3584226: (2020).
32. R.M.A. Latif, K. Hussain, N.Z. Jhanjhi, A. Nayyar, and O. Rizwan. A remix IDE: smart contract-based framework for the healthcare sector by using Blockchain technology. *Multimedia tools and applications*: 1-24 (2020).
33. M. Zghaibeh, U. Farooq, N.U. Hasan, and I. Baig. Shealth: A blockchain-based health system with smart contracts capabilities. *IEEE Access* 8: 70030-70043 (2020).
34. S. Shi, D. He, L. Li, N. Kumar, M.K. Khan, and K.R. Choo. Applications of blockchain in ensuring the security and privacy of electronic health record systems: A survey. *Computers & security* 97: 101966 (2020).
35. W. Liu, Q. Yu, Z. Li, Z. Li, Y. Su, and J. Zhou. A blockchain-based system for anti-fraud of healthcare insurance. *IEEE 5th International Conference on Computer and Communications (ICCC)*: pp. 1264-1268 (2019).

36. T. Motohashi, T. Hirano, K. Okumura, M. Kashiyama, D. Ichikawa, and T. Ueno. Secure and scalable mhealth data management using blockchain combined with client hashchain: system design and validation. *Journal of medical Internet research* 21(5): e13385 (2019).
37. T. Mohan and K. Praveen. Fraud detection in medical insurance claim with privacy preserving data publishing in TLS-N using blockchain. *International Conference on Advances in Computing and Data Sciences*: pp. 211-220 (2019).
38. M. Usman and U. Qamar. Secure electronic medical records storage and sharing using blockchain technology. *Procedia Computer Science* 174: 321-327 (2020).
39. S. Chakraborty, S. Aich, and H.C. Kim. A secure healthcare system design framework using blockchain technology. *21st International Conference on Advanced Communication Technology (ICACT)*: pp. 260-264 (2019).
40. T. McGhin, K.R. Choo, C.Z. Liu, D. He. Blockchain in healthcare applications: Research challenges and opportunities. *Journal of network and computer applications* 135: 62-75 (2019).
41. A.A. Siyal, A.Z. Junejo, M. Zawish, K. Ahmed, A. Khalil, and G. Soursou. Applications of blockchain technology in medicine and healthcare: Challenges and future perspectives. *Cryptography* 3(1): 3 (2019).
42. M.N.K. Boulos, J.T. Wilson, and K.A. Clauson. Geospatial blockchain: promises, challenges, and scenarios in health and healthcare. *International journal of health geographics* 17: (2018).
43. A. Al Omar, M.Z.A. Bhuiyan, A. Basu, S. Kiyomoto, and S. Rahman. Privacy-friendly platform for healthcare data in cloud based on blockchain environment. *Future generation computer systems* 95: 511-521 (2019).
44. K.N. Griggs, O. Ossipova, C.P. Kohlios, A.N. Baccarini, E.A. Howson, and T. Hayajneh. Healthcare blockchain system using smart contracts for secure automated remote patient monitoring. *Journal of medical systems* 42: 1-7 (2018).
45. H. Pham, T. Tran, and Y. Nakashima. A secure remote healthcare system for hospital using blockchain smart contract. *IEEE globecom workshops* (GC Wkshps): pp. 1-6 (2018).
46. S.P. Novikov, O. Kazakov, N. Kulagina, and N. Azarenko. Blockchain and smart contracts in a decentralized health infrastructure. *IEEE International Conference -- Quality Management, Transport and Information Security, Information Technologies* (IT&QM&IS): pp. 697-703 (2018).
47. D. Khan, T.J. Low, and V.T.B. Dang. Challenges and Application of Blockchain in Healthcare Systems. *International Conference on Digital Transformation and Intelligence (ICDI)*: pp. 15-20 (2022).

Proceedings of the Pakistan Academy of Sciences: A Physical and Computational Sciences 60(3): 15-25 (2023)

ISSN (Print): 2518-4245; ISSN (Online): 2518-4253
https://doi.org/10.53560/PPASA(15-25)635

Pakistan Academy of Sciences

Research Article

Acoustical Analysis of Insertion Losses of Ceiling Materials

Enobong Patrick Obot[1*], Rufus Chika Okoro[2], Daniel Effiong Oku[2], Christian Nlemchukwu Nwosu[1], and Michael Ugwu Onuu[1]

[1]Department of Physics, Alex Ekwueme Federal University Ndufu-Alike, Ebonyi State, Nigeria
[2]Department of Physics, University of Calabar, Cross River State, Nigeria

Abstract: This study concentrates on measuring, analyzing and recommending the ceiling materials most suited for the reduction of distinct frequency noise levels with focus on rain noise. A frequency analyzer has been used to measure and obtained accurate sound level (L_p) data of the rain noise outside, and inside five buildings with diverse acoustical ceiling materials in South Eastern Nigeria. It was done with and without the ceiling partition (or noise barrier) for the audio and narrow frequency band without contribution from other outdoor-related noise sources. Insertion losses of the ceiling materials were calculated using the data obtained from the measured L_p. Result obtained from the analysis indicated that the ceiling material found to effectively reduce the noise levels from external noise source. The type for speech reception threshold frequencies of more than 125 Hz and higher audiometric range was moabi wood with peak L_p of 21.20 dB at 500 Hz. While for lower frequencies where the ears are least responsive was plaster of Paris (POP) with peak L_p of 12.61 dB at 62.5 Hz. This makes "moabi wood" most suitable in lecture rooms, conference halls and large auditoriums as ceiling material, in consideration of its capability to provide notable attenuation of rain noise within the building. This is in accordance with several other studies done on this subject. In general, at much low frequencies and frequencies greater than 2k Hz significant reduction in the rain noise level was observed.

Keywords: Sound Enclosure, Acoustic Insertion Loss, Sound Pressure Level, Acoustic Ceiling Material, Frequency Analyser.

1. INTRODUCTION

The world is really noisy. Individuals are exposed to sounds twenty-four hours per day, seven days per week, twelve months per year – sounds they do not need, desire, or profit from. Every person continually fantasizes about living in a pleasant environment free of annoying noises [1]. Workers in loud industrial sites are subjected to continuous noise over the course of the workday. This unease could prompt some health disorders like heart issues, temporary or permanent hearing failure, internal tissue pain, nerve damage, and significantly higher circulatory strain in the long haul [2, 3]. According to World Health Organization (WHO), people exposed to prolong noise will adversely suffer hearing failure, sleep disturbance and even immune system problems [4]. Noise as one of the core air contaminants has a significant effect on living creatures, and the fast-industrial development and an ever-growing road traffic are the main factors [5].

The effect of acoustics on building's architecture can be seen over the centuries from the Roman amphitheaters to the contemporary structures, where people exhaust their flextime and free time. However, the major contrast between life in primeval Rome and life in the overcrowded urban towns is the prevalence of noise from a rising variety of sources, including factory, residents and traffic [6]. Acoustic enclosures are vast efficient methods of noise reduction to minimize noise generated from sources such as diesel engines, rain, turbines, air compressors and so on. Its performance is characterized by an insertion loss (IL), which can be defined as the variation in sound pressure levels at the receiver's end with and without the presence of a barrier (the enclosure walls in place), given that the source sound level is not altered [7].

Received: October 2021; Accepted: September 2023
*Corresponding author: Enobong Patrick Obot <enobong_youngprof@yahoo.co.uk>

$$IL = 10\log (I_1/I_2) = L_1 - L_2 \text{ dB} \qquad (1)$$

where I_1 & I_2 are the intensities and L_1 & L_2 are the source sound pressure level and receiving end sound pressure level.

The sound pressure level at the measurement location resulting from the *i*th path can be written either with or without the partition in terms of the loss of the *i*th path insertion, IL_i as:

$$IL_i = 10\log_{10} \sum_{i=1}^{n} 10^{-(IL_i/10)} \qquad (2)$$

Introducing subscripts to indicate cases 1 (without partition) and 2 (with partition), the total partition insertion loss ($IL = L_1 - L_2$) is expressed,

$$IL = 10\log_{10}\sum_{i=1}^{n_1} 10^{-(L_{1i}/10)} - 10\log_{10}\sum_{i=1}^{n_2} 10^{-(L_{2i}/10)} \qquad (3)$$

The acoustic enclosure insertion loss is resolved by the combination of source field movement and the wall panel vibrations. Bies and Hansen [8] determined a sole blockade indoors and outdoors insertion loss in accordance with "ISO 9613-2, ISO 10847, and ISO 11821". They found that in a higher reverberating condition, the blockades were ineffectual, but the indoor blockades performance enhanced by inserting specifically on the ceiling sound absorbing materials or by suspending ceiling assimilation baffles. Martinez-Orozco and Barba [9] investigated the in-situ performance of extant noise barriers using the indirect insertion loss technique outlined in the International Standard ISO 10847:1997. They performed the measurements at thirty sample locations, distributed among the three most prevalent forms of construction material (metal, concrete, and earthen berm walls). Their findings showed that the three different kinds of barriers had comparable insertion loss levels. The noise reduction effect was most effective in the 125 Hz – 8 kHz frequency band. Field measurements was conducted by May [10] on the balconies of a highway building. In spite of the fact that no balcony insertion loss calculation was made directly, these findings demonstrated that the balcony's ceiling reflection would greatly compensate the balcony's noise screening impact, and additionally the various reflections inside the balcony. Elden and Woloszyn [11, 12] used the pyramid tracing approach to investigate how the balcony ceiling and breastwork affected sound insertion loss. They also used a scale prototype to show that the configuration of the front parapet and the balcony's inclination and profundity could affect the balcony's overall sound insertion loss. The insertion loss of the balcony showed a rising pattern, they discovered, in conjunction with rising balcony profundity. No pattern was detected for either the angle of ceiling disposition or the impact of floor height on the insertion loss, which is most likely due to reflections from the "sensitive angle of incident". The insertion loss in the balcony was discovered to shift between 0.5 dB and 6 dB. Be that as it may, for balconies with depths of 1 m, 2 m, and 3 m respectively, the overall insertion loss when the front parapet was kept vertical, was found to be 2 dB, 4 dB and 6 dB [11]. An addition of 0.5 dB to 4 dB of noise reduction from a slant front parapet was also discovered [12]. Nonetheless, a 3-metre-deep balcony is by no means typical in a city filled with congested tall buildings. With the aid of simulations and a 1:50 scale ideal construction for a 16-storey building, Lee *et al.* [13] demonstrated the consolidated impact of front parapet configuration, ceiling tilt, and sound assimilation on noise reduction within an elevated building balcony. They utilized a sound-absorbing material made of 3 mm-thick polystyrene. They discovered a noise decrease of up to 23 dB, and described the noise reduction as the variation in balcony noise levels with and without the unique remedies mentioned above. On the balcony's rear wall, however, there was just a single measurement and consequently, the vulnerability in their analysis might be lofty. According to Rylander and Dunt [14], who conducted research on the subject of environmental noise control, noise levels can be decreased by installing effective noise barriers surrounding homes and entrance ramps. Application of noise barriers is one of the most pertinent mitigation strategies since reducing the sources of noise is a major concern for lowering ambient noise levels. Among other variable characteristics, noise barriers can be constructed from a variety of materials, as can their shapes or elevations [15-17].

Speech clarity is a concern in lecture rooms, conference halls, doctor's office, etc. It is a concern in our region where universities are built with lecture rooms without or with inferior ceiling material. More often than not, conference halls are built for their aesthetic value or cutting-edge

ceiling design instead of the practicality of the ceiling material. Choices of ceiling materials and acoustical wall treatment have a significant effect on the noise level within this space. Statistical data on the sound pressure level within the building with and without a ceiling partition for the audio and narrow frequency band was obtained for the insertion losses of the ceiling materials to be analyzed and determine which one can be used to achieve a desired sound level within a building. The calculated insertion losses of the measurements for the acoustical ceiling materials are compared to confirm the accuracy of the calculation.

2. MATERIALS AND METHODS

Measurements were taken in five buildings with various acoustic ceiling materials as enclosure, as well as the appropriate instruments, digital sound level meter and real-time spectrum analyzer (Figure 1), required to assist in the measurements. The enclosures were about 4.66 m x 4.05 m (L x W) and the building dimensions about 3.58 m x 3.04 m x 2.95 m (L x W x H). Dimensions of the rooms (L x W) are different in each case. But similar acoustical problems exist in both small and large rooms, just on a different scale and level. Surface boundary reflections in small rooms can seriously affect the sound, particularly from side walls. The overall reverberation levels are impacted by large-room reflection problems. The building data/information is given in Table 1. Some sides of the buildings were surrounded with disposition of trees and vegetation, and the other side by other buildings. The particular types of materials for the buildings with moabi wood, plaster of Paris (POP), polyvinyl chloride (PVC), and asbestos ceiling materials (Figures 2, 3, 4 and 5) include reinforced concrete walls, tile floors, and normal (uncoated) aluminum glass windows. While that of the raffia palm ceiling material (Figure 6) is made up of mud walls, concrete floors, and wooden windows. The thickness of the building's wall was about 9" inches. The main objective has been to obtain statistical data on the sound pressure level within and outside the building with and without the ceiling partition (or noise barrier). Conclusions regarding the insertion losses of the ceiling materials would then be drawn.

2.1 Sound Level Meter (SLM)

The Mastech digital SLM (model MS6700) with a measurement range of 30 dB to 130 dB and automatic ranging, a resolution of 0.1 dB, and a precision of ±1.5 dB, operates over a frequency response of 31.5 Hz to 8 kHz. It is a precision instrument used for the measurement of sound pressure level. It comprises of an array, a frequency response network range (weighting), a microphone, and an amplifier with graduated logarithm attenuator.

2.2 Frequency Analyzer

A real-time spectrum analyzer (RTA) allows precise measurement of the amplitude of the input signal versus the frequency enclosed by the analyzer's peak frequency scale. It is a software-based instrument used within the audio spectrum to analyze signals. This tool was installed in a personal computer with fundamental capabilities for sound input and output. A sound level meter, a low-distortion signal generator, a peak factor meter, a high-resolution real-time analyzer, and a double-trace oscilloscope are incorporated into the true RTA instrument.

Table 1. Building information

Building with ceiling materials	Dimension of the rooms (m^3)	Number of rooms	Interior description
Moabi wood	3.68 x 3.05 x 2.95	6	Normal residential rooms with reinforced concrete walls, tile floors and normal (uncoated) aluminum glass windows.
Plaster of Paris (POP)	4.20 x 3.87 x 2.95	6	Normal urban residential rooms with polished concrete walls, tile floors and normal (uncoated) aluminum glass windows.
Polyvinyl chloride (PVC)	3.63 x 3.00 x 2.95	5	Normal residential rooms with reinforced concrete walls, tile floors and normal (uncoated) aluminum glass windows.
Asbestos ceiling board	3.65 x 3.20 x 2.95	8	Normal residential rooms with reinforced concrete walls, tile floors and normal (uncoated) aluminum glass windows.
Raffia palm	2.75 x 2.10 x 2.95	4	Normal rural residential rooms with reinforced mud walls, concrete floors and wooden windows.

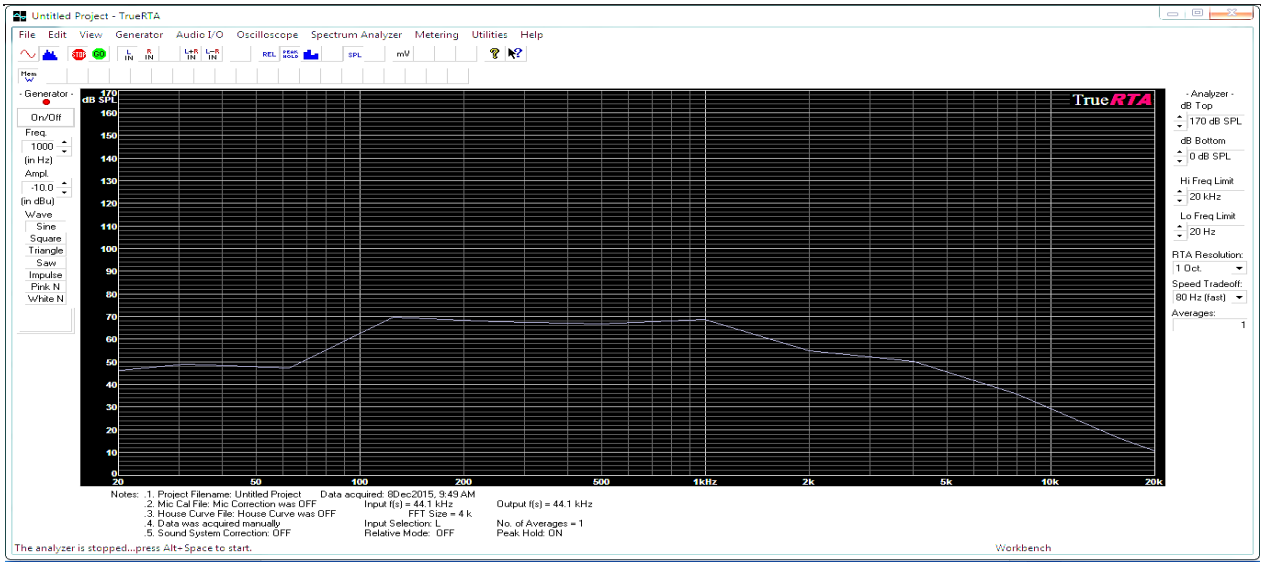

Fig. 1. True RTA audio frequency analyzer

Fig. 2. Moabi wood material

Fig. 3. Plaster of Paris

Fig. 4. Polyvinyl chloride material

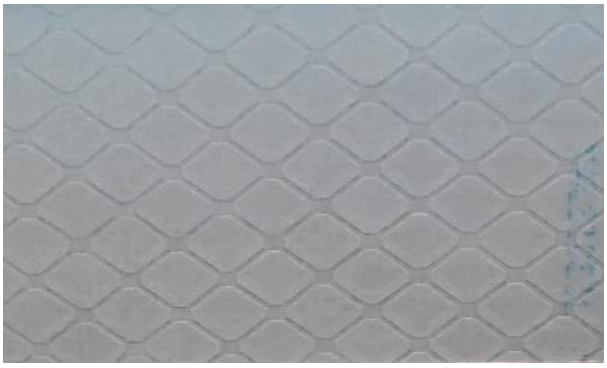

Fig. 5. Asbestos ceiling board

Fig. 6. Raffia palm material

2.3 Ceiling Materials

The measurements were carried out in five buildings with different acoustical ceiling materials. The materials specification is given in Table 2.

2.4 Measurement Method

For sound level measurements, a digital SLM and the RTA were used. The meter was synchronized

Table 2. Materials specification

Ceiling materials	Thickness (mm)	Mass per unit area (kg/m²)
Moabi wood	10	0.0427
Plaster of Paris (POP)	10	0.0521
Polyvinyl chloride (PVC)	6	0.0081
Asbestos ceiling board	4	0.0096
Raffia palm	10	0.0062

with the RTA, and the one-octave band readings were taken. Measurements were made in four different rooms for each of the buildings at four different points, and the average values of the measuring points were used. Within the building, measurements were made prior to and during the rain. The sound level meter's weighting network was calibrated to "A" position and the meter's dynamic features calibrated to "slow" response. The microphone's axis of highest sensitivity was oriented towards the source of the noise, and all measurements were made at 3.5 m away from any vertical reflecting surface and a height of 1.5 m altitude. A windshield was used to protect and shield the most precious part of the sound level meter, the microphone, from external signal effects such as wind and electrical interference.

3. RESULTS AND DISCUSSION

3.1 Results for Moabi Wood

Figure 7 shows the measurements of the average noise level obtained and their characteristics within the moabi wood ceiling partition one-octave band. The first aspect observed is that without the partition, at most of the distinct frequencies, the ambient noise outside was attenuated within the building in the one-octave band. But with the partition, the building's ambient noise was reduced at all one-octave band distinct frequencies, with the highest attenuation occurring at 1 kHz, at 4.07 dB.

The noise level inside without the partition was higher at all one-octave band distinct frequencies when there was rain fall, relative to ambient noise inside without the partition, with a highest value of 86.63 dBA at 62.5 Hz. However, at all the distinct frequencies in the one-octave band, attenuation was observed with the partition, with a highest value of 21.20 dB at 500 Hz. One possible explanation for this observation is the spreading introduced by the building structure and interior [18].

3.2 Results for Asbestos Ceiling Board

In Figure 8, the same observation as in the case of moabi wood could be made. The difference

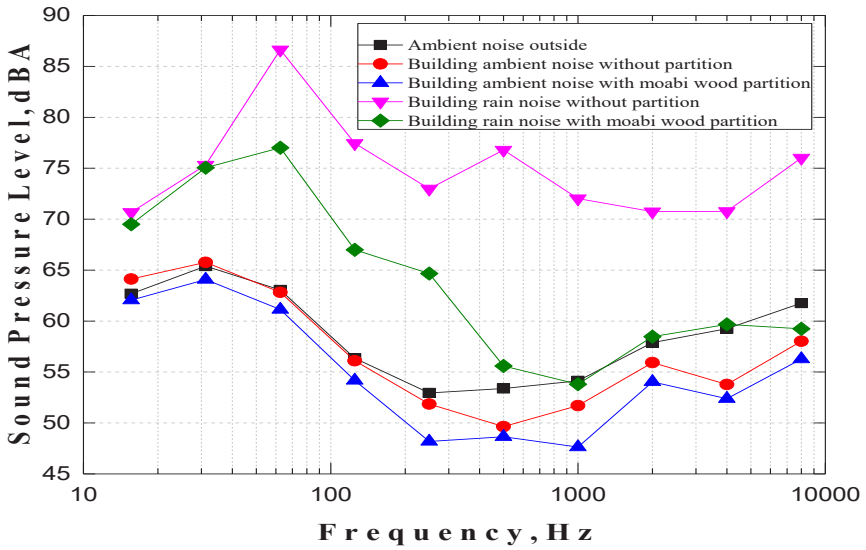

Fig. 7. Measurements of the average noise level for moabi wood

here was that, with the partition, at all one-octave band distinct frequencies, the building's ambient noise was not attenuated aside from 1 kHz and a considerably higher frequency spectrum. In other words, asbestos ceiling boards resonate the acoustic waves due to reflection, material composition, and spreading introduced by the building structure and interior. But at all the distinct frequencies in the one-octave band, attenuation was observed with the partition when there was rainfall with a highest value of 12.46 dB at 8 kHz, except at lower frequencies range of 31.2 Hz and below.

3.3 Results for Polyvinyl Chloride

Figure 9 shows the corresponding variations of the average measured noise level and their characteristics within the one-octave band for PVC ceiling partition. The results of PVC are similar to that of moabi wood. However, at all the distinct frequencies in the one-octave band, attenuation was observed with the partition when there was rainfall, with a highest value of 14.53 dB at 500 Hz.

3.4 Overall Experimental Results

Table 3 and Figure 10 show an overview of the calculated insertion losses for each ceiling materials based on the average measured rain noise level within the building, with and without the partition. The results of average noise level for each material investigated in the present study are given in appendixes (A to E).

3.5 Discussion of Results

As shown in Figures 7, 8 and 9, the noise level was attenuated by all the ceiling materials examined. For each ceiling materials, the insertion losses increase (in a particular case slightly) to a maximum value before decreasing and again increases with the frequency. At the initial stage in each of the ceiling materials, the system undergoes transient behaviors. From Table 3 and Figure 10, it is observed that at 15.6 Hz and 31.2 Hz asbestos ceiling board had the least insertion loss compared to others. As mentioned earlier, explanation was given for the insertion loss due to the composition of the material, reflection, and the spreading introduced by the building structure and the interior. At 62.5 Hz, in contrast to other materials, POP and raffia palm materials losses were slightly higher, but the differences were not notable. Again, apart from moabi wood which undergoes a little increment in insertion loss at 125 Hz, all the other materials undergo a substantial decrease in insertion loss. For other materials, except moabi wood which was higher at 250 Hz, the same pattern was encountered, although it also has a slight decrease. At 500 Hz, moabi wood has the highest value, as all materials witnessed a rise in insertion loss. Although its curve rises to a peak and then falls, its range of high attenuation is wider

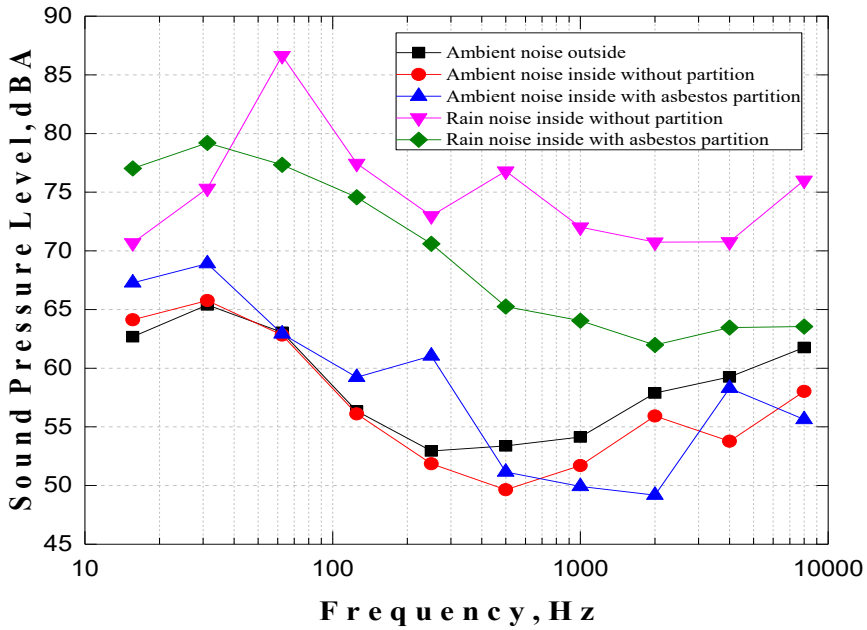

Fig. 8. Measurements of the average noise level for asbestos ceiling board

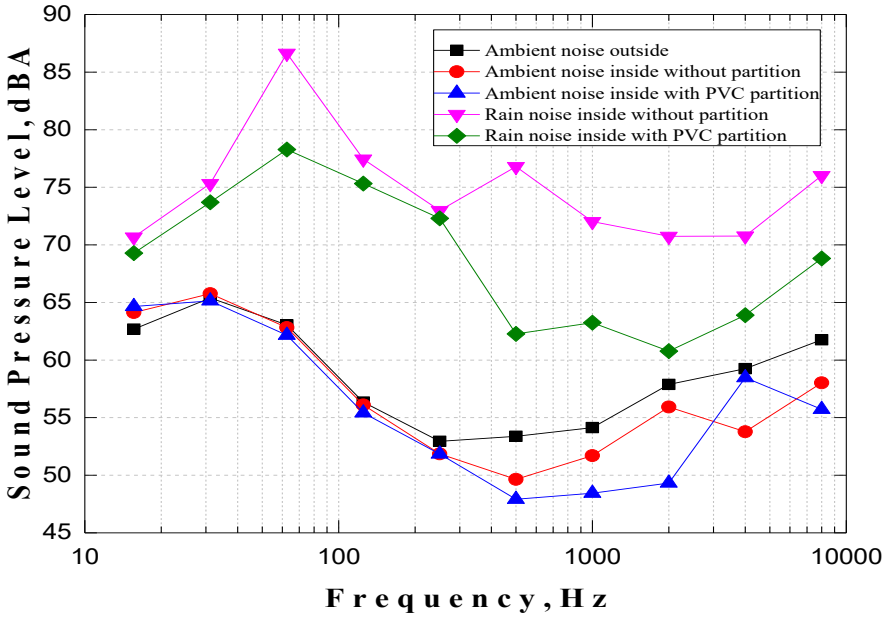

Fig. 9. Measurements of the average noise level for polyvinyl chloride

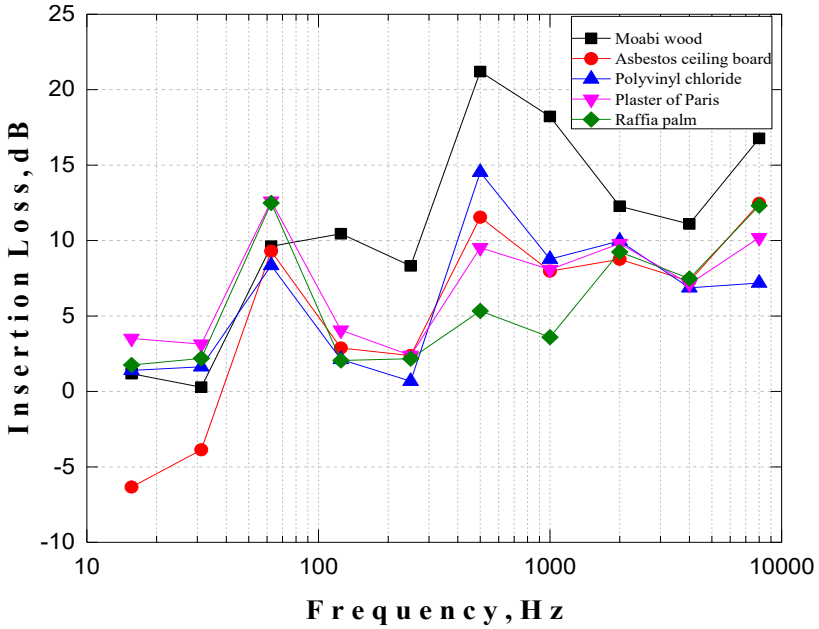

Fig. 10. Overall comparison results of insertion losses for the ceiling materials

than that shown by asbestos ceiling board, PVC, POP, and raffia palm materials. Their profiles of high attenuation are rather narrow, and confined to the middle range of the frequency spectrum. From 1 kHz to 8 kHz, moabi wood insertion loss was significantly higher than the other materials. In general, the curves are in sequence with noise criterion curve which shows that sound can be perceived at lower frequency with higher intensity of signal.

From these results, it has been perceived that the range of useful attenuation depends on the composition of the material, by weight or by thickness, microstructure of the material, and the spreading introduced by the building structure and interior. Results obtained show that, of all the ceiling materials examined, moabi wood has the best capability of attenuating sound, with a peak value of 21.20 dB from an external noise source of this type. This relates to the speech reception threshold frequency ranges of 500 Hz and higher audiometric frequency ranges. However, POP, which peaks at 62.5 Hz at 12.61 dB, is higher at lower frequencies

Table 3. Overall results of the calculated insertion loss per ceiling material

Frequency (Hz)	Insertion loss (dB) of the materials				
	Moabi wood	**Asbestos ceiling board**	**Polyvinyl chloride**	**Plaster of Paris**	**Raffia palm**
15.6	1.18	-6.34	1.39	3.51	1.75
31.2	0.28	-3.87	1.63	3.14	2.19
62.5	9.62	9.30	8.35	12.61	12.49
125	10.45	2.88	2.12	4.06	2.05
250	8.32	2.38	0.68	2.39	2.17
500	21.20	11.55	14.53	9.53	5.34
1000	18.22	7.97	8.77	8.08	3.59
2000	12.27	8.76	9.97	9.80	9.25
4000	11.10	7.31	6.87	7.13	7.49
8000	16.77	12.46	7.19	10.19	12.31

where the ears are slightly sensitive. Therefore, moabi wood can effectively be employed as ceiling material in lecture rooms, conference halls and large auditoriums in consideration of its capability to provide notable attenuation of rain noise level within the building. These results are in accordance with that of the work reported earlier by Lee *et. al*. [13].

The mean ambient noise level measured outside, adjacent to each room, and the room (with partition) mean ambient noise level measured were compared using the correlation coefficient, R. The overall computed correlation coefficient was approximately 0.9. This means that the ambient noise levels measured just outside the room and the ambient noise levels measured inside the room (with a partition) have a strong correlation.

4. CONCLUSIONS

Noise occurs when unwelcomed sounds encroach into the surroundings. Again, one is not only frequently greeted with a wide range of noise caused by rain when one stays in a shelter for safety, but also experiences varying degrees of frustration and discomfort from the same rain. In this study, measurements were taken with and without the ceiling partition (or noise barrier) to obtain sound pressure level statistical data outside and within the building. Conclusions were drawn regarding the insertion loss of the materials. Results from the measurements taken in five buildings with diverse acoustical ceiling materials in South Eastern Nigeria indicated a peak insertion loss of 21.20 dB with moabi wood. This relates to the speech reception frequency and other higher audiometric frequencies range. The insertion losses of the other ceiling materials examined show an increase in frequency, up to a maximum value, after which they fall and then rise again with further increases in frequency. Therefore, moabi wood can effectively be employed as ceiling material in lecture halls, conference rooms and large auditoriums. The correlation between the outdoor and indoor (with partition) measured ambient noise levels showed a close relation between the room sound pressure level recorded and the sound pressure level recorded just outside the room.

In general, a significant reduction of distinct frequency rain noise levels within the building was observed at much lower frequencies and other higher audiometric frequencies. The range of useful reduction depends on the composition of the material, by weight or by thickness, microstructure of the material, as well as the spreading introduced by the building structure and interior.

5. CONFLICT OF INTEREST

The authors declare no conflict of interest.

6. REFERENCES

1. L.A. AL-Rahman, R.I. Raja, and R.A. Rahman. Attenuation of noise by using absorption materials and barriers: A review. *International Journal of Engineering and Technology* 2(7): 1207–1217 (2012).

2. W. Babisch. Traffic noise and cardiovascular disease: Epidemiological review and synthesis. *Noise and Health* 2(8): 9–32 (2000).
3. R.R. Davis, P. Kozel, and L.C. Erway. Genetic influences in individual susceptibility to noise: A review. *Noise and Health* 5(20): 19–28 (2003).
4. A.A. Abiodun, O.T. Oyelola, E.O. Popoola, and A.I. Babatunde. Assessing noise levels in a commercial and industrial centres of Lagos Metropolis. *Continental Journal of Water, Air and Soil Pollution* 2(2): (2012).
5. L. Goines, and L. Hagler. Noise pollution: A modern plague. *Southern Medical Journal* 100(3): 287–294 (2007).
6. Brüel & Kjaer. *Measurements in building acoustics.* Brüel & Kjaer Booklet, DK – 2850, Naerum, Denmark (1988).
7. H-S Kim, J-S Kim, S-H Lee, and Y-H Seo. A simple formula for insertion loss prediction of large acoustical enclosures using statistical energy analysis method. *International Journal of Naval Architecture and Ocean Engineering* 6(4): 894–903 (2014).
8. D.A. Bies, and C.H. Hansen. *Engineering noise control: Theory and practice* (2nd edition). E and FN Spon., London (1996).
9. J.M. Martinez-Orozco, and A. Barba. Determination of insertion loss of noise barriers in Spanish roads. *Applied Acoustics* 186(3): 108435 (2022).
10. D.N. May. Freeway noise and high-rise balconies. *Journal of the Acoustical Society of America* 65: 699–704 (1979).
11. H.H. Eldien, and P. Woloszyn. Prediction of the sound field into high-rise building facades due to balcony ceiling form. *Applied Acoustics* 63: 431–440 (2004).
12. H.H. Eldien, and P. Woloszyn. The acoustical influence of balcony depth and parapet form: Experiments and simulations. *Applied Acoustics* 66: 533–551 (2005).
13. P.J. Lee, Y.H. Kim, J.Y. Joen, and K.D. Song. Effects of apartment building facade and balcony design on the reduction of exterior noise. *Building Environment* 42: 3517–3528 (2007).
14. R. Rylander, and D.R. Dunt. Traffic noise exposure planning. *Journal of Sound and Vibration* 151(3): 54–56 (1991).
15. X. Song, and Q. Li. Numerical and experimental study on noise reduction of concrete LRT bridges. *Science of the Total Environment* 643: 208–224 (2018).
16. W. Sun, L. Liu, H. Yuan, and Q. Su. Influence of top shape on noise reduction effect of high-speed railway noise barrier. *IOP Conference Series Materials Science and Engineering* 493: 012043 (2019).
17. J. Lázaro, M. Pereira, P.A. Costa, and L. Godinho. Performance of low-height railway noise barriers with porous materials. *Applied Sciences* 12(6):2960 (2022).
18. E.P. Obot, and D.E. Oku. Propagation of electromagnetic waves in some public buildings in Cross River State, Nigeria. *European Scientific Journal* 10(3): 474–484 (2014).

APPENDICES

Appendix A. Result of average noise level measurement for moabi wood.

Frequency (Hz)	Ambient noise outside (dBA)	Building ambient noise without partition (dBA)	Building ambient noise with partition (dBA)	Building rain noise without partition (dBA)	Building rain noise with partition (dBA)
15.6	62.68	64.13	62.05	70.68	69.50
31.2	65.39	65.76	64.08	75.33	75.05
62.5	63.05	62.82	61.14	86.63	77.01
125	56.35	56.11	54.17	77.45	67.00
250	52.94	51.86	48.19	72.98	64.66
500	53.38	49.64	48.65	76.80	55.60
1000	54.13	51.70	47.63	72.02	53.80
2000	57.88	55.93	54.03	70.74	58.47
4000	59.26	53.78	52.38	70.77	59.67
8000	61.76	58.02	56.27	76.01	59.24
				R	**0.95**

Appendix B. Result of average noise level measurement for asbestos ceiling board.

Frequency (Hz)	Ambient noise outside (dBA)	Building ambient noise without partition (dBA)	Building ambient noise with partition (dBA)	Building rain noise without partition (dBA)	Building rain noise with partition (dBA)
15.6	62.68	64.13	67.28	70.68	77.02
31.2	65.39	65.76	68.91	75.33	79.20
62.5	63.05	62.82	62.93	86.63	77.33
125	56.35	56.11	59.23	77.45	74.57
250	52.94	51.86	61.04	72.98	70.60
500	53.38	49.64	51.16	76.80	65.25
1000	54.13	51.70	49.93	72.02	64.05
2000	57.88	55.93	49.18	70.74	61.98
4000	59.26	53.78	58.30	70.77	63.46
8000	61.76	58.02	55.63	76.01	63.55
				R	**0.66**

Appendix C. Result of average noise level measurement for polyvinyl chloride.

Frequency (Hz)	Ambient noise outside (dBA)	Building ambient noise without partition (dBA)	Building ambient noise with partition (dBA)	Building rain noise without partition (dBA)	Building rain noise with partition (dBA)
15.6	62.68	64.13	64.65	70.68	69.29
31.2	65.39	65.76	65.14	75.33	73.70
62.5	63.05	62.82	62.16	86.63	78.28
125	56.35	56.11	55.42	77.45	75.33
250	52.94	51.86	51.85	72.98	72.30
500	53.38	49.64	47.92	76.80	62.27
1000	54.13	51.70	48.44	72.02	63.25
2000	57.88	55.93	49.32	70.74	60.77
4000	59.26	53.78	58.47	70.77	63.90
8000	61.76	58.02	55.72	76.01	68.82
				R	**0.88**

Appendix D. Result of average noise level measurement for Plaster of Paris.

Frequency (Hz)	Ambient noise outside (dBA)	Building ambient noise without partition (dBA)	Building ambient noise with Partition (dBA)	Building rain noise without partition (dBA)	Building rain noise with partition (dBA)
15.6	62.68	64.13	63.83	70.68	67.17
31.2	65.39	65.76	66.50	75.33	72.19
62.5	63.05	62.82	62.28	86.63	74.02
125	56.35	56.11	51.51	77.45	73.39
250	52.94	51.86	49.98	72.98	70.59
500	53.38	49.64	48.53	76.80	67.27
1000	54.13	51.70	48.50	72.02	63.94
2000	57.88	55.93	49.36	70.74	60.94
4000	59.26	53.78	58.90	70.77	63.64
8000	61.76	58.02	55.81	76.01	65.82
				R	**0.92**

Appendix E. Result of average noise level measurement for raffia palm.

Frequency (Hz)	Ambient noise outside (dBA)	Building ambient noise without partition (dBA)	Building ambient noise with partition (dBA)	Building rain noise without partition (dBA)	Building rain noise with partition (dBA)
15.6	62.68	64.13	63.52	70.68	68.93
31.2	65.39	65.76	64.34	75.33	73.14
62.5	63.05	62.82	60.87	86.63	74.14
125	56.35	56.11	53.86	77.45	75.40
250	52.94	51.86	50.61	72.98	70.81
500	53.38	49.64	48.59	76.80	71.46
1000	54.13	51.70	48.55	72.02	68.43
2000	57.88	55.93	49.20	70.74	61.49
4000	59.26	53.78	58.06	70.77	63.28
8000	61.76	58.02	56.32	76.01	63.70
				R	**0.91**

Proceedings of the Pakistan Academy of Sciences: A Physical and Computational Sciences 60(3): 27-36 (2023)

ISSN (Print): 2518-4245; ISSN (Online): 2518-4253
https://doi.org/10.53560/PPASA(60-3)799

Pakistan Academy of Sciences

Research Article

Practical Analysis of Tap Water Dissolved Solids Efficient Reduction

Muhammad Imran Majid*, and Naeem Shahzad

Department of Electrical Engineering & Engineering Management,
Institute of Business Management, Karachi, Pakistan

Abstract: Water is an essential component in the manufacturing of oral solid dosage forms in the pharmaceutical industry. The objective of the present study is to develop a compact and easy-to-maintain one-platform solution for generating high-purity water with near to zero Total Dissolved Solids (TDS) and low conductivity for pharmaceutical applications. To achieve this objective, different purification methods were explored and integrated into a single platform. The purification process involved the use of Electro-Deionization (EDI) in combination with double-pass Reverse Osmosis (RO), an activated carbon filter, water softeners, and micron filtration. The resource water was carefully selected based on specific criteria to ensure the quality of the final purified water. The developed one-platform solution successfully produced purified water with near to zero TDS and a conductivity level below 1 micro siemens/cm^2. The integrated approach involving EDI and double-pass RO, along with supplementary filtration and treatment steps, proved to be highly effective in achieving the desired purity levels. The study demonstrated that the suggested one-platform solution is a reliable and efficient method for the production of high-purity water in the pharmaceutical industry. This system offers an easily maintainable and compact solution, making it suitable for various other industries such as semiconductor manufacturing and electric power generation where purified water with zero TDS is required. By providing a robust water purification process, this solution contributes to enhancing the quality and safety of pharmaceutical products and other critical applications that rely on ultra-pure water.

Keywords: Double Pass Reverse Osmosis, Electro-Deionization, Pre-Filtration, Production of Purified Water, Zero Total Dissolved Solid.

1. INTRODUCTION

The resource water with the lack of quality grades does not meet the required standards of pharmaceutical use. To meet such requirements, there is a need to have a real solution that can lead to the production of water with near zero total dissolved solids (TDS) [1]. Past studies on the production of purified water have focused on water treatment with a limited production rate rather than the complete solution to produce purified water with a production rate of almost 3000 Liter/Hour. Systems integrated with RO can achieve a such rate of production easily because two-stage RO can produce purified water at 80 % of the rate of production [1]. This phase-by-phase water treatment provides a one-platform solution for individuals to produce water with near zero TDS under certain source water parameters.

Conventionally, ion exchange techniques are used for purifying water, but micron filtration and membrane filtration are becoming very popular to demineralize water, followed by electro-deionization (EDI) which offers nonstop operation [2]. The polarity and hydrogen bonding in water give it special chemical characteristics. It can thus dissolve, absorb, adsorb, or suspend a wide variety of substances, including pollutants [3]. So, dissolved water ions can easily be separated into dilute and concentrated columns of EDI. EDI technology emerged almost 50 years ago, latterly it was utilized to remove metallic elements from radioactive wastewater [4]. Furthermore, novel tailored applications are specifically addressed, including heavy metal ion removal, water desalination, and low-level radioactive waste removal [5]. The continuous EDI (CEDI) technology has been used for over 20 years and is

Received: January 2023; Accepted: September 2023
*Corresponding author: Muhammad Imran Majid < imran.majid@iobm.edu.pk >

well-acknowledged for producing ultrapure water for industrial use [5]. EDI contains ion exchange resin beads that enhance the water flow rate and transfer cations and anions from a dilute column to a concentrated column. A stream of water passes through the concentrated column, and all absorbed cations and anions are washed away and returned to the feed tank. A pure water stream from the dilute column is fed to the storage tank for product usage.

An auto-chlorination system is a water treatment system that uses chlorine to disinfect organic and inorganic compounds found in water [6]. Chlorine is a powerful disinfectant that is effective at killing a wide range of microorganisms, including bacteria, viruses, and algae. It is commonly used in water treatment systems to purify drinking water, swimming pool water, and industrial process water. An auto-chlorination system typically consists of a chlorine storage tank, a feed pump, and a control panel. The feed pump is used to deliver a precise amount of chlorine to the water being treated, based on the specific needs of the system. The control panel is used to monitor and adjust the chlorine dosage as needed. Auto chlorination systems are designed to be easy to use and maintain, with automated controls and monitoring systems that make it easy to maintain the correct chlorine levels in the water. They are often used in a variety of applications, including drinking water treatment, swimming pool water treatment, and industrial process water treatment. Chlorine disinfection treatment of resource water has been widely employed in wastewater reclamation plants to control RO membrane biofouling [7]. There are some chlorine-resistant bacteria (CRB) that can survive even in the presence of residual chlorine such as there is a risk of pathogenicity, antibiotic resistance, and microbial growth. But there is still no accepted method to evaluate chlorine resistance germs and CRB [8].

A feed water pre-treatment plant is a system that is used to prepare raw water for use in a steam boiler or other industrial process of pharmaceutical. The purpose of the pre-treatment plant is to remove impurities from the raw water that could cause problems in the downstream equipment, such as corrosion or scaling. There are several different types of pre-treatment plants, depending on the specific needs of the process and the quality of the raw water. Chemicals are added to the raw water to cause small particles to clump together, forming larger flocs that are easier to remove. The flocculated water is then allowed to settle so that the heavier flocs will sink to the bottom of the tank and can be removed. The water is then passed through a filter, which removes any remaining particles or impurities. The specific treatment steps and equipment used in a feed water pre-treatment plant will depend on the quality of the raw water and the specific needs of the process. In general, the goal of the pre-treatment plant is to provide clean, pure water for use in the industrial process, while also protecting the downstream equipment from corrosion and other problems caused by impurities in the water. The added chlorine is disinfected in the feed water pre-treatment plant, resulting in the water being odorless, and lowering its hardness. A pretreatment unit, a treatment unit, a structure for storing and distributing water, equipment for monitoring and controlling the process, and chemical cleaning and sanitation systems are all included in a water treatment system used in the pharmaceutical industry [3].

A form of water treatment device called an activated carbon filter makes use of activated carbon to purify water. It is especially effective at adsorbing pollutants from water because activated carbon is an extremely porous, ultra-fine type of carbon with a very large surface area. Water pollutants, such as chemicals, contaminants, and odors, are frequently removed from water using activated carbon filters. These are particularly good at getting rid of heavy metals as well as organic and inorganic substances like chlorine, pesticides, and herbicides. Water is passed over a bed of activated carbon in activated carbon filters by high-pressure pumps which then absorb the pollutants from the water. Pressure-driven processes are used when the removal of suspended solid and organic elements like bacteria are the primary targets [4]. A prevalent issue is the high groundwater hardness that generates scale deposition on electrodes that irreversibly affects the treatment effectiveness and their lifetime. Electrochemical water softening as a preliminary step for electro bioremediation of nitrate-contaminated groundwater. The contaminants are subsequently trapped in the carbon and the water is collected on the other side of the filter. Both a solo treatment system and a bigger water treatment

system can make use of the activated carbon filter [9]. Activated carbon filters are commonly used in a variety of applications, including drinking water treatment, industrial water treatment, and air purification. They are generally easy to maintain and operate, and they can be an effective way to improve the quality of water by removing a wide range of impurities. They can also be aligned in carbon nanotube for capacitive deionization for effective utilization [10].

Ultraviolet (UV) water treatment is a process in which water is exposed to UV light to kill or inactivate microorganisms such as bacteria, viruses, and protozoa. This process can be used to treat drinking water, swimming pool water, and wastewater [11]. UV water treatment systems typically consist of a UV lamp and a chamber through which the water is passed. The UV lamp emits UV light, which is absorbed by the water as it flows through the chamber. UV light damages the DNA or RNA of any microorganisms present in the water, rendering them harmless. UV water treatment is a chemical-free method of water treatment that is effective at reducing the concentration of a wide range of microorganisms in water. It is commonly used as a supplement to other forms of water treatment, such as filtration and disinfection with chemicals like chlorine.

Ecosystems are becoming increasingly polluted, necessitating sustainable pollution removal techniques. Ultra-pure water is ideal for various industries, and electro-deionization (CEDI) is an effective method for removing ionic chemicals from polluted waters. CEDI offers promising wastewater treatment technologies, eradicating contaminants like ionizable compounds and hazardous chemicals. Innovative materials are being developed to improve CEDI's performance, with ion-exchange resins and membranes being the focal point [13, 14].

An EDI plant typically consists of a series of modular cells that contain ion exchange resins and electrodes. The water to be treated is passed through the cells, and the ions in the water are attracted to the oppositely charged electrodes and exchanged with the ions in the resin. This process removes the ions from the water, leaving behind pure, deionized water. EDI plants are often used to produce high-purity water for a variety of applications, including laboratory use, pharmaceutical manufacturing, and electronics manufacturing. They are known for their high efficiency and low maintenance requirements and are often preferred over other water purification technologies due to their ability to produce water with very low levels of impurities. EDI plants are often used as a final step in water purification systems after the water has already been treated by other methods such as RO or ion exchange. They are particularly useful for producing high-purity water because they can remove a wide range of impurities, including ions, dissolved solids, and organics, to very low levels. Pretreatment, treatment, water storage, distribution, and loop structure, as well as chemical cleaning and sanitization systems, make up the four units that make up the water treatment system. Deionization and RO are the two steps that make up the treatment unit [3].

Cartridge filter is used to remove impurities from water. The filter cartridge is made of a porous material, such as a synthetic fiber or a sintered metal, and has very small pores that are typically measured in microns. Different concentration technologies and energy supply systems are compared to find economically feasible and environmentally friendly treatment systems. The investigated chains include Multi-Effect Distillation (MED), Membrane Distillation (MD), and the coupling of Reverse Osmosis and Membrane Distillation (RO-MD) [12].. The filter cartridge is placed in a housing, and the water is passed through the cartridge as it flows through the housing. The impurities in the water are trapped on the surface of the cartridge, while the purified water passes through and is collected on the other side. Micron cartridge filtration systems are used in a variety of applications, including drinking water treatment, industrial water treatment, and swimming pool water treatment. They are generally easy to operate and maintain, and they can be an effective way to improve the quality of water by removing a wide range of impurities. There are many different types of micron cartridge filters available, with different pore sizes and materials to suit different water treatment needs. It is important to choose the appropriate filter for the specific impurities that need to be removed from the water. Emerging contaminants, including pharmaceuticals, pesticides, and nanomaterials, are found in various water sources and can cause endocrine disruption

and toxic effects. Nano-particles, known as new generation nano absorbents, are used to remove these pollutants [13].

In the context of sanitization, a heat exchanger can be used to heat water or other fluids to a high temperature to kill bacteria and other microorganisms. This is often done as part of a water treatment process to produce clean, sanitized water for use in industrial processes or drinking. Several different types of heat exchangers can be used for sanitization, including shell and tube heat exchangers, plate and frame heat exchangers, and spiral heat exchangers. The specific type of heat exchanger used will depend on the specific needs of the application, such as the flow rate and temperature of the water, the type of heat source being used, and the space available for the heat exchanger. Heat exchangers for sanitization are typically designed to be easy to operate and maintain, with automated controls and monitoring systems to ensure that the water is heated to the appropriate temperature for the required amount of time.

RO is a water treatment technology that uses a semi-permeable membrane to remove impurities from water. It is often used to produce purified water for a variety of applications, including drinking water, laboratory water, and industrial process water. In a double-pass RO system, the water is passed through the RO membrane twice. The first pass removes a large portion of the impurities from the water, while the second pass further purifies the water by removing any remaining impurities. The double-pass RO membrane system is an alternative efficient method to remove total organic carbon (TOC) in the production of pure water [14]. This two-step process can produce water with a very low TDS level, making it suitable for applications that require extremely pure water. Double-pass RO systems are generally more efficient and effective at purifying water than single-pass systems, as they can remove a higher percentage of impurities. RO can reduce conductivity and TDS reaches 81 % and 82 %, even the conductivity and TDS of water produced can reach zero micro siemens/cm^2, 0 ppm [15]. However, these are also more expensive and require more space and equipment than single-pass systems.

Caustic soda, also known as sodium hydroxide, is a chemical that is often used in water treatment plants to adjust the pH of the water and remove impurities. In a purified water plant, a caustic soda dosing system may be used to add a precise amount of caustic soda to the water to adjust the pH or to remove impurities such as dissolved solids or organic contaminants. A caustic soda dosing system typically consists of a storage tank for the caustic soda, a pump to deliver the caustic soda to the water, and a control panel to monitor and adjust the dosage as needed. The caustic soda is typically added to the water in a controlled manner, to avoid over-dosing or under-dosing the water. Caustic soda dosing systems are often used as part of a larger water treatment process, in conjunction with other treatment methods such as filtration, RO, or ion exchange. These are generally easy to operate and maintain, and can be an effective way to adjust the pH of water or remove impurities. However, it is important to use caution when handling caustic soda, as it is a strong alkali that can be harmful to the skin and eyes. In the present research work, a series of water treatment methods are used jointly to get purified water of TDS near zero and conductivity < 1micro Siemens/cm^2 but also purified water free of several undesired organic elements.

2. MATERIALS AND METHODS

In the present study various water treatment methods have been used, which are described here. The first one is sand filtration, where instead of passing water through small orifices through which particles are unable to pass, water runs through a bed of filtration media measuring 0.45 mm. The installation layout of the sand filter is shown in Figure 1.

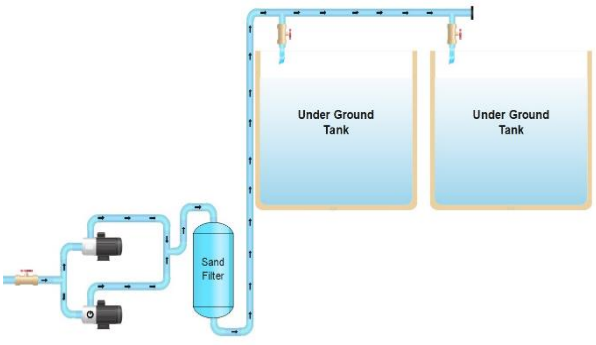

Fig. 1. Water circulation through the Sand filter

Table 1. Specifications of Equipment & material used for the sand filter system

S. No.	Description	Range
1	Power	4HP
2	Flow Rate	100 GPM
3	Pump Material	SS-304
4	Pressure Drop	5 Psi
5	Flow Rate	100 GPM
6	Filtration Chamber	42” x 72”
7	Valve System	5 Valve Battery
8	Pipeline Material	UPVC Sch-80
9	Media	Gravels and Silica Sand

There is an automatic vent device, which helps to remove excess air, created due to water turbulent flow inside the filtration chamber. This excess air can cause jerks during the continuous operation of the filtration chamber. A mixture of filtration media up to a depth of 3 ft was used, which added more clarity to the water up to 20–25 microns. The details of the sand filter are given in Table 1.

A multifaceted filtration method was used by the sand filter. Near the top of the filter bed, coarser, lighter media were used to capture large particle debris. Particles that were as small as 25 microns were trapped by finer, heavier media at successively lower media levels as smaller particles continued to descend. Following backwashing, layer separation is possible because of the disparities in medium densities. The shape of the filter is both attractive and functional. The spherical top and bottom ends of the tank was designed to give uniform flow from both the inlet distribution and outlet collection assemblies. The system provided adequate distribution to uniformly expand the filter bed during backwash, and the entire media bed was utilized during the filter cycle. High-quality, cleaned, and graded silica, 0.45 mm grade, and in the sand filter shell, accurate bedding in sizes of 1/2”, 3/4”, and 1/4” was used.

The auto-chlorination system helps to maintain the chlorine level in the water as per water testing results and the microbial growth rate. Low-pressure circulation pumps were installed in parallel, one operational, and the other on standby, to circulate the water.

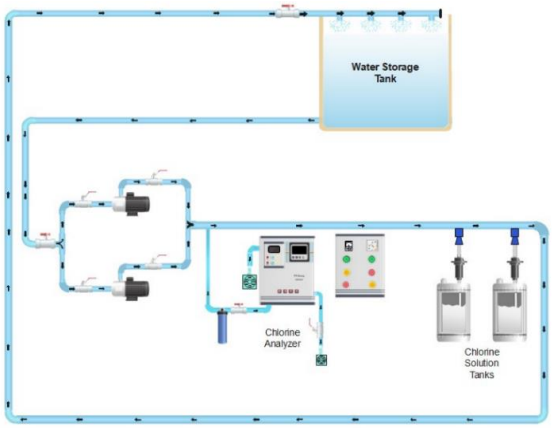

Fig. 2. Schematic diagram of auto chlorination system

During circulation, liquid chlorine was added through dosing pumps. The circulation pumps have alternated their operation after some time to avoid overheating. The dosing pumps was kept running until the desired chlorine level was achieved in the water reservoir. When the desired level of chlorine is achieved, the dozing pump stops automatically, and when the chlorine level drops, it restarts automatically. A chlorine analyzer sensor was installed in this circulation circuit to analyze the chlorine level. The chlorine dosing system layout is shown in Figure 2. The specifications of the equipment are given in Table 2.

Table 2. Specifications of equipment used in auto chlorination system

S. No	Description	Range
1	Power	1HP
2	Flow Rate	30-40 GPM
3	Pump Material	SS-304
4	Capacity	5 L/H at >5bar
5	Chlorine Sensor	1
6	PH sensor	1
7	Temperature Sensor	1
8	% Of Active Chlorine	12% - 15%
9	Chemical Name	Sodium Hypo chloride
10	Flammability	Non-Flammable

The third method is pre-treatment system, the equipment details are as follows: Polypropylene cable, wound around a polypropylene core, makes up these wound cartridges. They are suitable for the removal of fine materials, such as sand, silt, scale, invisible sludge, and rust particles, and they work

Fig. 3. Schematic layout of water Pre-treatment plant

well with the majority of acids, alkalis, corrosive fluids, and gases. As a result, they are an excellent yet affordable option for residential, commercial, and agricultural uses. The details of the cartridge filters are given in Table 3.

An activated carbon filtration using granular activated carbon (GAC) has been selected as the technique to remove organic pollutants from water. Additionally, GAC filters can be used to remove chlorine and hydrogen sulfide, two elements that give water a bad taste and smell.

Table 3. Specifications of equipment used in Pre-treatment plant

S. No	Description	Range
1	Pump Power	3HP
2	Water Flow Rate	50 GPM
3	Pump Material	SS-304
4	Filter Length	20”
5	Level of filtration	5-Micron & 1-Micron
6	Cartridge Qty.	20” – 7 No.
7	Chemical Name	Sodium Metabisulphite
8	Dosing rate	5 L/H
9	Solution Tank Capacity	80 Liter or as per operation hours

The layout of the water softening system is shown in Figure 3. While, the specifications of the GAC filter are given in Table 4. As water passes through softener vessels, water minerals can be removed from the water by using strong cation-resin beads that attract and hold them. The water transferred to the next step for further purification.

It is usually necessary that the hardness of EDI feed water should be less than 1.0 ppm [16]. As the water passes through softener vessels, strong cation-resin beads attract and holds water minerals, removing them from the water. The softened water

Table 4. Technical specifications of GAC filter

S. No	Description	Range
1	Vessel Size	30” x 72”
2	Media	Activated carbon
3	Flow Rate	50 GPM
4	Iodine Number	950
5	Feed water PH	6.6 to 7.8

then moves on to the next stage of treatment. So, for the sake of the production of purified water, the layout of the procedure is shown in (Figure 4). The technical parameters for consideration of water softeners are listed in Table 5.

3. RESULTS

3.1 Conductivity Test Results

Conductivity is a measure of a substance’s ability to conduct electric current. A conductivity test is a laboratory test that measures the electrical conductivity of a substance. This test is often used to measure the concentration of ions in a solution, as the concentration of ions is directly related to the conductivity of the solution. Conductivity tests can

Table 5. Water softener vessel and used material specifications

S. No	Description	Range
1	Type	Automatic twin alternating
2	Flow	50 GPM
3	Feed Hardness	170 ppm
4	Output Hardness	< 2ppm
5	Resin	Strong Cation
6	Vessel Size	30” x72”
7	Resin in Vessel	400 Liters
8	Salt per Regeneration	60 Kg
9	Regeneration After	10 Hrs.

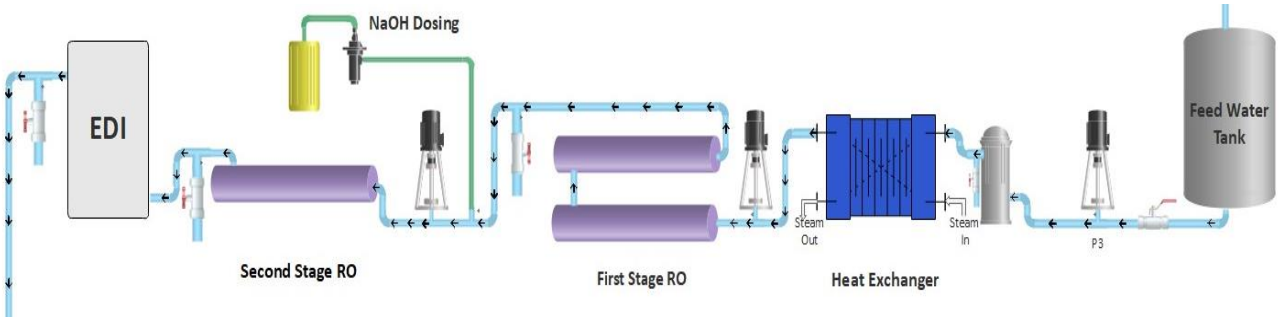

Fig. 4. The layout of EDI-based purified water plant

be used to measure the purity of water, determine the presence of contaminants in a sample, and monitor the quality of water in industrial processes. The fourteen days' conductivity test results are shown in Figure 5.

3.2 Microbiological Test Results

A microbiological test is a type of laboratory test that is used to identify, quantify, or detect the presence of microorganisms in a sample. These tests can be used to identify the presence of bacteria, fungi, viruses, or other types of microorganisms. Microbiological tests are often used in the medical field to diagnose infections, as well as in the food and water industries to ensure the safety and quality of products. After the performance qualification of the purified water plant, fourteen days of purified water testing was executed to identify the presence of any kind of harmful microorganisms. These results are shown in Figure 6.

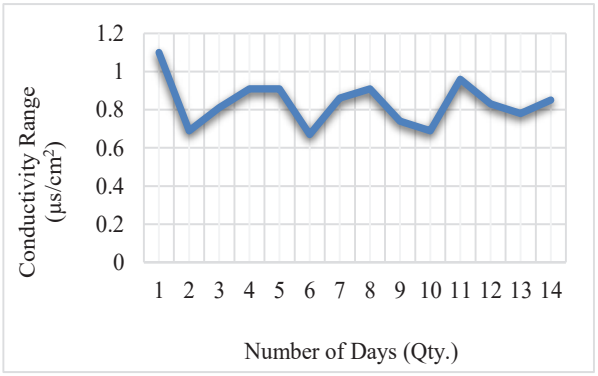

Fig. 5. Purified water conductivity testing results

3.3 TDS Results

TDS is a measure of the amount of dissolved inorganic and organic substances present in a water sample. A total dissolved solids test is a laboratory test that measures the concentration of dissolved solids in a water sample. This test is often used to determine the quality of drinking water and to monitor the concentration of contaminants in water sources.

TDS cannot be easily measured, except under controlled conditions. TDS are measured by the well-known expression: TDS = K. EC

The electrical conductivity (EC) is multiplied with factor "K" depending upon the salinity of water, the value of 0.5 to 0.75 is used depending

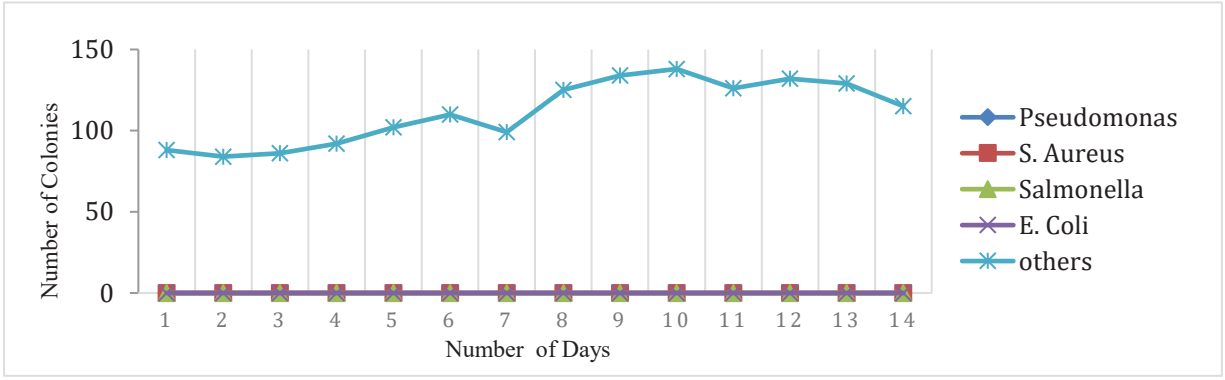

Fig. 6. Purified water Microorganism testing results

on the salinity of the water [17]. In this study we used a value of 0.5, the fourteen days' test results are shown in Figure 7.

4. DISCUSSION

The research paper discusses the production of purified water with near-zero TDS and low conductivity for use in the pharmaceutical industry and other applications. Water quality is crucial for the safety and efficacy of pharmaceutical products, and the widespread adoption of purified water with zero TDS is evident in various industries. The study investigates various purification methods, including EDI integrated with double-pass RO, microfiltration, and UV filtration. The experimental setup is used to produce purified water with near-zero TDS and conductivity below 1 micro siemens/cm^2. The proposed one-platform solution is compact and easy to maintain, offering practical and cost-effective water purification solutions.

As discussed in TDS results and graphically demonstrated in Figure 3 and Figure 4, tap water is used in various industries, however purification is necessary. Ultrafiltration, nanofiltration, reverse osmosis, and membrane distillation processes affect treated water quality. Nano filtration removes dissolved organic carbon, and RO rejects TDS at 99.7% Micropollutants are a growing concern in municipal wastewater treatment plants, posing a threat to aquatic ecosystems and drinking water resources. Powder activated carbon (PAC) is a promising technology to reduce micropollutants and ecotoxicity in receiving waters [18]. Furthermore, effective layout of water treatment equipment also played important role. Like, sand filter removes salinity and does micron filtration of tap water. Same is the case with water pre-treatment system, it reduces water pungent smell, extra chlorine and hardness making water odorless.

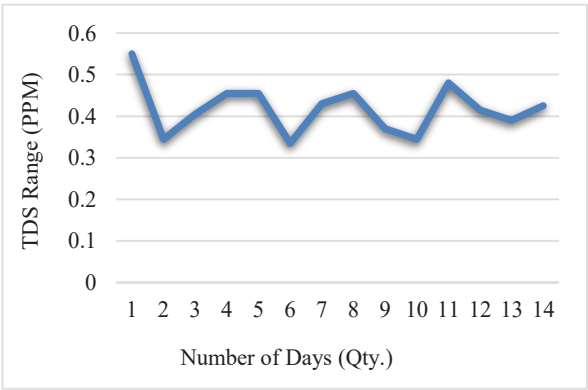

Fig. 7. Purified water TDS testing results

To determine if the water quality is adequate for pharmaceutical industry mass production, fourteen days of water testing, including TDS identification and microbiological growth, were undertaken. We can simply determine the total dissolved solids value, which is not easily calculated by other generally available equipment, close to decimals using the results displayed and the relation between TDS and conductivity that is given. The TDS value fluctuates depending on the type of tap water used and how frequently the equipment used in water treatment needs to be maintained.

The study investigates the correlation between TDS and Electrical Conductivity in natural waters like fresh water, sea water, and tender coconut. Results show that 96% of TDS variability can be attributed to EC in sea water [19]. The study's success opens up new possibilities for pharmaceutical manufacturers and other industries, potentially leading to more efficient and sustainable water purification practices. The discussion acknowledges limitations and suggests avenues for future research to improve the proposed system, explore other purification methods and address specific challenges in industrial settings.

5. CONCLUSIONS

In the pharmaceutical sector, particularly in the creation of oral solid dosage forms like creams, ointments, and gels, water is essential. Pharmaceutical, semiconductor, and electric power generation industries all depend on pure water with no TDS. This research paper has highlighted the method of generating high-purity water with near-zero TDS from resource water that meets specific criteria. The study demonstrated that different purification methods, such as EDI integrated with double-pass RO, ultrafiltration, microfiltration, and UV filtration, are beneficial in achieving this goal. The research work has provided a reliable and efficient method for producing high-purity water with near to zero Total Dissolved Solids (TDS) and low conductivity, which is crucial for manufacturing oral solid dosage forms in the pharmaceutical

industry. This advancement ensures the quality and safety of pharmaceutical products, ultimately benefiting patients who rely on these medications for their health. By developing a one-platform solution that produces purified water of such high purity levels, the research work contributes to enhancing the quality and safety of pharmaceutical products. High-purity water is essential for ensuring that medications are free from contaminants that could adversely affect patients' health. The developed water purification system has potential applications beyond the pharmaceutical industry. Industries such as semiconductor manufacturing and electric power generation, which also require ultra-pure water with zero TDS, can benefit from this compact and easily maintainable solution. This broadens the impact of the research across various critical sectors. The integrated approach involving Electro-Deionization (EDI) and double-pass Reverse Osmosis (RO) can contribute to resource conservation. By effectively removing impurities and achieving high-purity water, the system may reduce water wastage and optimize the utilization of available resources. The one-platform solution can lead to cost savings in water purification processes for the pharmaceutical industry and other sectors. By streamlining different purification methods into a single system, the need for multiple equipment and maintenance costs may be minimized.

Future research could focus on assessing the scalability of the one-platform solution and its applicability in large-scale industrial settings. Investigating the challenges and opportunities for implementing this system on an industrial scale could be beneficial. Research could be conducted to evaluate the long-term performance and reliability of the one-platform solution. Assessing how the system performs over extended periods and under different operating conditions would help build confidence in its stability and effectiveness. Understanding the environmental impact of the water purification process is crucial. Future research could explore the energy consumption and waste generation associated with the developed system, aiming to optimize the process to minimize its environmental footprint. Conducting comparative studies between the developed one-platform solution and other existing water purification technologies would help identify strengths and weaknesses. Such studies could guide industries in selecting the most suitable water purification method based on their specific requirements and constraints. Research efforts could be directed toward automating the purification system and incorporating advanced monitoring and control technologies. Automation can lead to improved efficiency, reduced human error, and increased overall system performance. Investigating the potential for water reuse and recycling within the developed system could further enhance resource sustainability. Research could focus on identifying safe and effective ways to recycle purified water for other non-critical applications within the industries.

6. CONFLICT OF INTEREST

Authors declare no conflict of interest.

7. REFERENCES

1. Y. Li, J. Fang, and L. Hou. Design and application of purified water preparation device for chemical analysis. *E3S Web of Conferences* 261: 4–7 (2021).
2. J. Wood, J. Gifford, J. Arba, and M. Shaw. Production of ultrapure water by continuous electrodeionization. *Desalination* 250: 973–976 (2010).
3. F.R.M. da Silva, D.A. de M. Fonsêca, W.L.A. da Silva, E.R.L. Villarreal, G.A.E. Espinoza, and A.O. Salazar. System of sensors and actuators for the production of water used in the manufacture of medicines. *Sensors* 19(20): 1–22 (2019).
4. L. Alvarado, and A. Chen. Electrodeionization: Principles, strategies and applications. *Electrochimica Acta* 132: 583–597 (2014).
5. Z.U. Khan, M. Moronshing, M. Shestakova, and A.A. Othman. Electro-deionization (EDI) technology for enhanced water treatment and desalination: A review. *Desalination* 548: 583-597 (2023).
6. M. Deborde, and U. von Gunten. Reactions of chlorine with inorganic and organic compounds during water treatment—Kinetics and mechanisms: A critical review. *Water Research* 42(1–2): 13–51 (2008).
7. Y.H. Wang, Y.H. Wu, T. Yu, X.H. Zhao, X. Tong, Y. Bai, Z.Y. Huo, and H.Y. Hu. Effects of chlorine disinfection on the membrane fouling potential of bacterial strains isolated from fouled reverse osmosis membranes. *Science of the Total Environment* 693: 133579 (2019).
8. L.W. Luo, Y.H. Wu, T. Yu, Y.H. Wang, G.Q. Chen, X. Tong, Y. Bai, C. Xu, H.B. Wang, N. Ikuno, and H.Y. Hu. Evaluating method and potential risks of chlorine-resistant bacteria (CRB): A review. *Water*

Research 188: 116474 (2021).
9. A. Ceballos-Escalera, N. Pous, M.D. Balaguer, and S. Puig. Electrochemical water softening as pretreatment for nitrate electro bioremediation. *Science of the Total Environment* 806: 150433 (2022).
10. M. Li, S. Liang, Y. Wu, M. Yang, and X. Huang. Cross-stacked super-aligned carbon nanotube/activated carbon composite electrodes for efficient water purification via capacitive deionization enhanced ultrafiltration. *Frontiers of Environmental Science and Engineering* 14(6):1–10 (2020).
11. J. Ippolito, K. Barbarick, and H. Elliott. Drinking Water Treatment Residuals: A Review of Recent Uses. *Journal of Environmental Quality* 40(1): 1–12 (2011).
12. M. Micari, M. Moser, A. Cipollina, A. Tamburini, G. Micale, and V. Bertsch. Towards the implementation of circular economy in the water softening industry: A technical, economic and environmental analysis. *Journal of Cleaner Production* 255: 120291 (2020).
13. B. Rai, and A. Shrivastav. Removal of emerging contaminants in water treatment by nanofiltration and reverse osmosis. *Development in Wasterwater Treatment Research and Process: Removal of Emerging Containments from Waster water through Bio-nanotechnology* 605–628 (2022).
14. P. Zhao, Y. Bai, B. Liu, H. Chang, Y. Cao, and J. Fang. Process optimization for producing ultrapure water with high resistivity and low total organic carbon. *Process Safety and Environmental Protection* 126: 232–241 (2019).
15. R. Junaidi, A. Hasan, M. Yerizam, and I. Purnamasari. The Performance of Reverse Osmosis (RO) Membrane in Producing Pure Water. *Journal of Physics: Conference Series* 1500: 012057(2020).
16. A.K. Wardani, A.N. Hakim, Khoiruddin, and I.G. Wenten. Combined ultrafiltration-electrodeionization technique for production of high purity water. *Water Science and Technology* 75(12): 2891–2899 (2017).
17. N.R.G. Walton. Electrical Conductivity and Total Dissolved Solids—What is Their Precise Relationship? *Desalination* 72(3): 275–292 (1989).
18. M. Boehler, B. Zwickenpflug, J. Hollender, T. Ternes, A. Joss, and H. Siegrist. Removal of micropollutants in municipal wastewater treatment plants by powder-activated carbon. *Water Science and Technology* 66(10): 2115–2121 (2012).
19. S. Thirumalini, and K. Joseph. Correlation between Electrical Conductivity and Total Dissolved Solids in Natural Waters. *Malaysian Journal of Science* 28(1): 22452 (2009).

Proceedings of the Pakistan Academy of Sciences: A Physical and Computational Sciences 60(3): 37-48 (2023)

ISSN (Print): 2518-4245; ISSN (Online): 2518-4253
https://doi.org/10.53560/PPASA(60-3)825

Pakistan Academy of Sciences

Research Article

An Intelligent Decision Support System for Crop Yield Prediction Using Machine Learning and Deep Learning Algorithms

Maryum Bibi[1], Saif-Ur-Rehman[1*], Khalid Mahmood[2], and Rana Saud Shoukat[1]

[1]University Institute of Information Technology,
PMAS - Arid Agriculture University Rawalpindi, Pakistan
[2]Institute of Computing and Information Technology, Gomal University, D.I. Khan, Pakistan

Abstract: Agriculture is crucial to economic growth and development. Crop yield forecasting is critical for food production which includes vegetables, fruits, flowers, and cattle. Artificial Intelligence (AI) is rising in agriculture, providing farmers with real-time or long-term insights about their fields. It allows us to identify the areas that require irrigation, fertilization, or pesticide treatment. Statistical models struggle to track complex relationships in crop yields due to numerous factors. Machine Learning (ML) and Deep Learning (DL) algorithms can solve this problem by training themselves in these relationships, enabling accurate predictions in agricultural yield prediction methods. Predicting product performance in agriculture is challenging due to various factors, but profit forecasting improves decision-making, production, economics, and food safety. The present study focuses on the use of ML and DL algorithms to suggest a novel decision support system for crop yield prediction with the objectives to develop a robust, accurate model, investigate algorithm effectiveness, and create a user-friendly system for informed crop production decisions. According to the results, the developed system is capable of making precise predictions, which can support farmers in making better decisions about how to manage their crops. The simulation results demonstrate that the intelligent decision support system proposed for crop yield prediction using ML and DL algorithms is capable of achieving high accuracy and precision. The system can be used to help farmers make better decisions about crop planting and management, which can lead to increased crop yields and profits. The results of our experiment show that our model is better than the others and it achieves an accuracy of 99.82 %. Additionally, we utilized ML to condense the input space while preserving high accuracy.

Keywords: Machine Learning Algorithm, Deep Neural Network, Deep Learning Algorithm, Crop Yield Forecasting, Artificial Intelligence, Agricultural Productivity.

1. INTRODUCTION

Digitization is having a major impact on many different areas of life including medicine, agriculture, consensus platforms, and weather forecasting, etc., [1]. Weather affects agrarian yield, food security, GDP, and environmental protection. ML and DL techniques improve the prediction of agricultural production by capturing complex correlations between crop output and environmental parameters [2]. Remote sensing improves agricultural yield prediction, but noisy data challenges accuracy [3]. ML enhances agricultural planning and production, but challenges remain in dataset quality, algorithms, and decision-making integration [4, 5]. AI aids industrial sectors, while agriculture faces climate change risks. Climate change impacts agricultural industry, affecting livelihoods and food security [6]. Post-hoc methods clarify trained predictions, process methods improve interpretation. Agricultural planning optimizes land use and yields using machine learning algorithms [7, 8]. Precision agriculture uses GPS, remote sensing, and internet technologies to manage crops, reduce fertilizers, pesticides, and water usage [9]. As such the precision agriculture ensures crop-specific product quality control. Maximizing resources and predicting yields using ML algorithms and DL techniques. The aim is to make the most of what we have while conserving resources. Yield predictions

Received: June 2023; Accepted: September 2023
*Corresponding Author: Saif-Ur-Rehman <Saif@uaar.edu.pk>

were made using ML algorithms and DL such as linear regression and multiple regressions. ML techniques such as RF, SVM, multiplexer, logistic regression, and DL techniques such as DCNN and LSTM can provide quick and accurate solutions to this problem [10]. Agricultural sustainability, food availability, productivity, and farmers' cultural familiarity are imperative for food safety and food security [11-13]. The UN Sustainable Development Goals (SDGs) for 2030 include zero hunger and sustainable agriculture. DL techniques predict crops using Convolution Neural Networks (CNNs) and Recurrent Neural Networks (RNNs) [14, 15]. Smart farming consists of advance precision in agriculture with intelligent, remote solutions [16-18]. The rubber market grows because deep learning aids rubber yield forecasts with accuracy and robustness [19]. Traditional methods overlook complex factors affecting yields [20]. The parameters that have had a major impact on crops are water, ultraviolet (UV) radiations, pesticides, fertilizers, and the area of land covered by the area. A proposed ML model illustrating the use of NN and related ANN algorithms was evaluated. The dataset consists of 140 data points that represent the effect of the attribute on crop yield. Predicting crop yields is crucial for informed decisions in agriculture, but traditional methods rely on limited statistical models that are unable to capture the complex relationship between yield and factors like weather, soil conditions, and pests [21, 22]. Traditional methods struggle with predicting crop yields due to limited statistical models. DL effectively performs image classification, speech recognition, and crop yield forecasting using CNN and weather parameters [23]. US soybean yield prediction using neural networks and CNN outperforms remote sensing by 15 % on average MAPE (mean absolute percentage error), incorporating spatiotemporal features. [24, 25]. IoT technology offers diverse applications in smart homes, cities, traffic management [26, 27]. Technology integrates agricultural equipment for optimal planting and fertilization decisions [28]. Smart machines enhance plant and animal growth monitoring accuracy [29, 30].

Satellite missions, remote sensing sensors, big data, artificial intelligence, and machine learning offer new opportunities for understanding crop processes and monitoring yield using remote sensing. Figure 1 shows that a thorough site survey is crucial

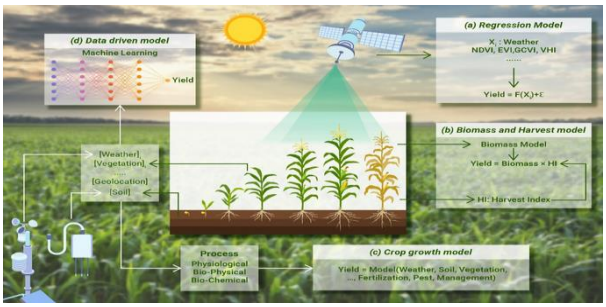

Fig. 1. IoT sensors on the ground and in farm equipment [31]

for construction plans, with drones simplifying the process and achieving impressive results [31-33]. Satellite remote sensing enhances monitoring efficiency for large, multi-scale applications [34, 35]. In recent development, satellite remote sensing has been successfully used for crop monitoring to forecast output, accurately describe location, weather, and temporal changes, and estimate yields per pixel [36-39]. Machine vision technology has gained importance in agricultural automation [40].

Figure 2 shows the use of remote sensing for monitoring and yield estimation. The plant material used is reddish-orange *Vitis vinifera L. cv.* Bhopal was vaccinated at 110 degrees Richter. The land was planted in 2002 with dimensions of 2.5 × 1.4 m (2857 vines ha-1) with ropes connected to the north-south vertical trusses. Remote sensing, big data, AI, and ML tools were adopted for sustainable agriculture [41]. AI advancements and Graphics Processing Unit (GPU) and Deep Belief Network (DBN) technologies have significantly improved plots with 1.2 drip nozzles [42]. Computer vision technology enhances resource efficiency in agricultural production through decision support [43, 44]. The approach challenges noise and distortion in underwater photographs by creating a

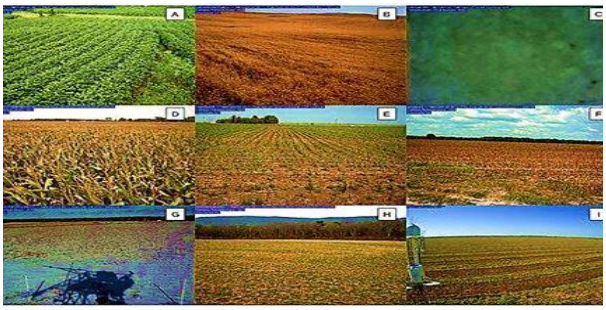

Fig. 2. Remote Sensing for Crop Monitoring and Yield Estimation [41]

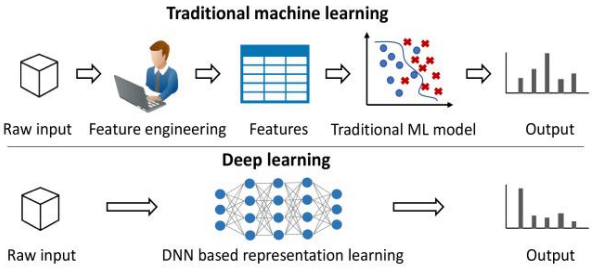

Fig. 3. Techniques for ML and DL model [46]

3D model using depth maps, overlapping tiles, and mosaic images [45]. Figure 3 categorizes ML models into feature engineering-based and end-to-end Deep Neural Network (DNN) pipelines, highlighting similarities in interpretation paradigms, focusing on understanding neural representations [46].

The typical objectives and contributions of the present study are as follows:

1) Estimation of winter wheat yields using data from multiple sources at both district and pixel levels in large areas by comparing multiple ML and DL methods, including RNN and Random Forest (RF) algorithms.
2) To explore factors such as soil, weather, and crops that are important in predicting yield.
3) Finally, we propose a scalable, simple, and cost-effective operating modeling approach for accurate and fast yield estimation.

The present study also reviews the literature on crop forecasting, analyzes planning strategies, and discusses experiments, results, and ongoing research. Table 1 depicts a summary of different studies on agricultural yield using various techniques, approaches, and models, utilizing diverse datasets. The research utilized Support Vector Machine (SVM), CNN, Long Short-term Memory Networks (LSTM), and other ML algorithms. The performance and accuracy of each algorithm is being varied.

2. MATERIALS AND METHODS

The proposed method uses data from the Kaggle database to estimate crop yield predictions [56]. Precipitation, temperature, air pressure, vapor pressure, and the frequency of rainy days are all examples of climatic parameters. The information in this document is geographically organized by latitude and county. Random Forest (RF) and Artificial Neural Network (ANN) algorithms are powerful ML tools for crop yield analysis, combining ensemble learning and AI networks to make decisive decisions and recognize complex relationships between inputs and outputs. The random forest-based crop mapping framework utilizes various data sources and remote sensing data to enhance crop classification accuracy and efficiency. This method aids in land use planning, precision agriculture, environmental monitoring, advancing agriculture, and remote sensing. RF and ANN are chosen for crop yield analysis due to their efficiency in handling large data sets, ability to learn complex relationships, and easy training, making them suitable for time-consuming tasks. ML approaches like Bayes and Decision Trees are not suitable for this task due to their probabilistic nature and limited handling of large datasets [57]. Decision Trees are unsupervised learning algorithms for classification and regression tasks, but they lack complex relationship learning capabilities. The use of existing datasets and various ML and DL approaches for crop yield prediction at different measures in high-yield agricultural manufacturing locations requires increased limited attention [58].

DL, which uses neural networks to learn features directly from the data, is the basis of present work. The DL approach is more flexible and enables to achieve better results for a series of tasks [59]. In terms of robustness, scalability and interpretation ability, the present work is better than the other because it is based on DL techniques, which are much more powerful and flexible than traditional methods of ML.

Figure 4 shows the framework for the present study using DL approach. Modules for feature extraction, Decision Support System (DSS), and data preprocessing are all included in the framework. Performance measurement and forecasting are also included in the DSS module. With ML and DL, predictions can be made, and performance can be evaluated by looking at the DSS's accuracy.

2.1 Dataset

The dataset used in the present study is from Kaggle, hypothetical data is used which is a public data repository [56]. The MSMD feature selection method improves agricultural classification efficiency and accuracy by reducing redundancy

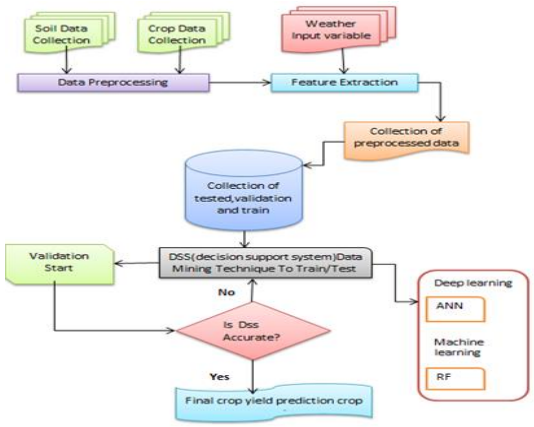

Fig. 4. The framework for the proposed methods

and focusing on optimal features. It enhances precision in farmland mapping using multi-source imagery, making it a significant addition to remote sensing and land cover categorization. The dataset contains information on crop yield, climate, and other factors.

Figure 5 depicts a visual representation of the dataset in the combined bi-temporal optical radar data for crop distribution in pictorial form recorded by Rapid Eye (optical) satellites and polarization radar data captured by UAVSAR (Unmanned Aerial Vehicle Synthetic Aperture Radars) in a rural area close to Winnipeg, Canada and are used in the present study. At harvest

Table 1. Prediction algorithm as applied in ML and DL

Ref No	Algorithm	Dataset Used	Results
[47]	Deep neural network	Each model was first trained with 900,000 data sets.	The 10-neuron, 5-layer Bayesian DNN model is the same as the original 400-neuron 10-layer DNN model, although the number of neural networks is reduced by about 80.
[48]	Hybrid machine learning, (ANN-ICA), (ANN-GWO)	Wheat, barley, potato, sugar beet	ANN-GWO showed better prediction results than the ANN-ICA model with R = 0.48, RMSE = 3.19, and MEA = 26.65.
[49]	Convolutional neural network with 1-D Convolutional operation	Meteorological, soil, and plant phenology data from 271 German districts over 21 years (1999–2019).	RMSE 7-14% lower, MAE 3-15% lower, and correlation coefficient 4-50% higher than the best-performing reference factor on all test data.
[50]	(ML): XGBoost Algorithm, (CNN), Deep (DNN), CNNXGBoost, (RNN), and CNN (LSTM).	The soybean dataset contains 25345 samples and 395 factors, such as climate and soil parameters.	CNN and DNN hybrid models have rmse 0.276, mse 0.071, mae 0.199, and R2 0.87; The XGBoost models are better than other models.
[51]	BPA with FFNN and ANN	regional soil parameter	Regional soil factors may have a critical role in enriching the CYP.
[52]	Deep Recurrent Q-Network model	Vellore district in the southern	Accuracy of 93.7%.
	Wheat crop simulation model (CSM), remote sensing (RS)	The use of Sentinel 2A and Landsat 8 imagery and in-person LAI measurements is used for verification	NE increases by 2%, 5%, 3%, and 1% more on simulated days until flowering.
[53]	Imagery satellite, (NDVI), (SAVI).	East Java with various spatial and remote sensing datasets	NDVI (R2=77.81%) and SAVI (R2=72.8%).
[54]	Backpropagation Neural Networks (BPNN) and Genetic Algorithms (GA)	When combining the three main tobacco growth metrics (plant density, nitrogen fertilization, and leaf count), prepare to plant goals (yield or QC), weather, and soil information.	77.66 kg/mu of smoke is produced, and the CQ is 81.02. The main objective is to smoke QC with a wait of 80.
[55]	Information and communication technologies (ICTs), DSSPIM	Southern Spain's greenhouses are home to orange and tomato trees.	Orange plants demonstrate how 20 % less water is used when implementing a water management method for tree crops.

Fig. 5. The visual illustration of the sample images used in this study

time, seven crops were grown in the region: corn, peas, canola, soybeans, oats, wheat, and hardwoods.

Predict crop yields for five Gulf-grown crops: potatoes, melons, dates, wheat, and maize (corn). A prediction model was developed using five independent variables: year, rainfall, pesticide, temperature fluctuations, and nitrogen fertilizer. Crop prediction is crucial for decision-making in agriculture and uses input variables to determine food availability for the upcoming years.

2.2 Data preprocessing and feature extraction

In order to address the various issues, which come due to incompleteness, inconsistency and missing of values against various features of the dataset, a data preprocessing technique known as normalization is introduced. After the data is preprocessed, it can generate promising results from simulations. Following feature extraction and data pre-processing, there are 12 features in the dataset, including derived features. These include longitude, latitude, altitude, and day length, quantity of precipitation, minitemp, maxitemp, ndvi, wind speed, mean temperature, standardized temperature, and yield are among the functions.

2.3 Model Selection

It is intended to develop an intelligent DSS for crop yield monitoring using RF and ANN.

2.3.1 Random Forest (RF)

We have used the RF Classifier from scikit-learn to simulate RF-based engines. With a few exceptions indicated below, the default set of settings is utilized initially:

- 'n estimators'- (n shows the trees that makeup the forest, default size is 10);
- 'Max depth' - The maximum depth of the tree (default: none). If the setting is 'None,' the documentation indicates that "tree vertices are expanded until all the Childs are pure or until all child node contain less than min samples split";
- 'Min samples split' – This parameter shows the required least number of samples to separate an internal node in the tree (it is set to 2 by default);
- 'Min samples leaf' - The very bare least number of nodes, correspondingly);
- One seven-node output layer.

Since entities are standardized real numbers, `ReLU was chosen as the activation function of optimal hidden layers. Also, since this is a multiclass classification exercise, where the output is intended to be binary ('1' for the specified class, '0' for all other classes), choosing 'softmax' makes the layer output trigger function seem appropriate. This is a multi-class classification exercise, and "categorical_crossentropy" is selected as the loss function. Adaptive performance is evaluated using "accuracy" as a metric for selection. For samples in freshly formed leaves, the default is one.

2.3.2 Artificial Neural Network (ANN)

The ANN design has a sequential structure that includes:

- 1-Input layer (102 input nodes);
- 3-Hidden layers (204, 204 and 102 nodes, respectively);
- one seven-node output layer

Figure 6 represents the adaptive performance being assessed using "accuracy" as a selection criteria. Because entities are standardized real numbers, the activation function 'relu' was used for buried layers. Also, because, this is a meticulous classification exercise with binary output ('1' for the chosen class, '0' for all other classes), choosing 'softmax' makes the layer output trigger function seem appropriate. This is a multi-class classification task with "categorical_crossentropy", as the loss function.

3. RESULTS AND DISCUSSION

In this section, various evaluation matrices used for the proposed technique are discussed.

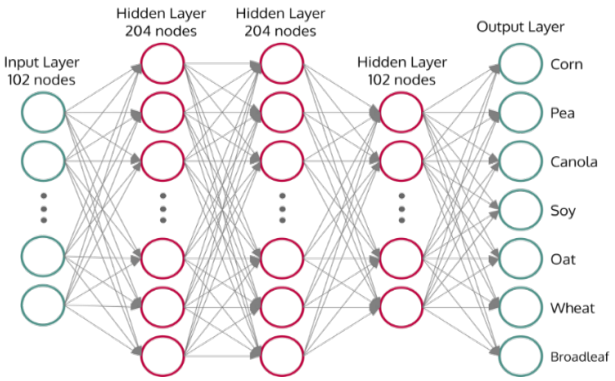

Fig. 6. The proposed Artificial Neural Network Model

3.1 Evaluation Matrices

The performance here is measured with both the evaluation and confusion matrices for both models (Random Forest and Neural Network) of the confusion matrix.

- Columns represent expected classes;
- whereas rows represent actual classes

3.1.1 Confusion Matrix

A confusion matrix is a 2x2 matrix structure that is useful for visualizing an algorithm's performance. The true positive rate (TPR) is defined as the entire number of positives that have been given that classification.

$$\text{TPR} = \frac{TP}{TP+FN} \quad (1)$$

Where TP denotes the true positive and FN shows false negative.

The true negative rate is the proportion of conditions that qualify as negative.

$$\text{TNR} = \frac{TP}{TN+FN} \quad (2)$$

The false positive rate is the proportion of instances that are misclassified or anticipated as being negative.

$$\text{FPR} = \frac{FP}{FP+TN} \quad (3)$$

The false negative rate is the proportion of positive cases reported or anticipated as negative.

$$\text{FNR} = \frac{FN}{FN+TP} \quad (4)$$

3.1.2 Accuracy

It measures the proportion of accurate predictions to all calculations.

$$\text{Accuracy} = \frac{TP+TN}{TP+FP+FN+TN} \quad (5)$$

3.1.3 Precision

It is the ratio between TPs combined with a number of TPs and FPs.

$$\text{Precision} = \frac{TP}{TP+FP} \quad (6)$$

3.1.4 Recall

It is defined as the product of the ratio of TPs and the sum of the TP and FN numbers.

$$\text{Recall} = \frac{TP}{TP+FN} \quad (7)$$

3.1.5 F1-score

Recall and accuracy are averaged mathematically, and it takes into consideration both false positive and false negative (FN) outcomes.

$$\text{F1} - \text{score} = 2 * \frac{(precision*recall)}{(precision+recall)} \quad (8)$$

Figure 7 depicts the data visually, revealing a substantial variance in agricultural yields across different locations, with a focus on autumn-sown winter crops. What sticks out is that winter crops have a substantially higher amount of variance from year to year, indicating that their yields fluctuate more pronouncedly than other crop types.

Figure 8 focuses on training an algorithm utilizing multispectral satellite photos containing

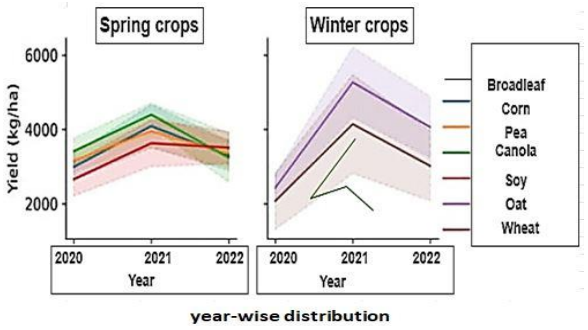

Fig. 7. Crop production statistics

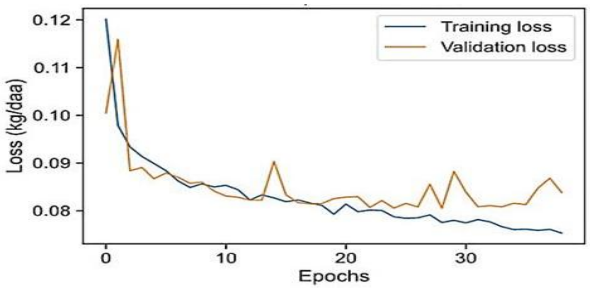

Fig. 8. Training and validation loss for the multi-temporal ANN model

information on crop kinds and their respective areas. Only these photos with crop type and area encoding were used to train the algorithm in this scenario. The training and validation losses of the multi-temporal Artificial Neural Network (ANN) model are evaluated. The best results from the single-image ANN trials served as the foundation for the training process, and subsequent photos with a pixel mask inserted as a separate channel were employed in this context. To test how well these models work, both statistics matrices and confusion matrices are used in this evaluation.

It is important to mention how crucial good data preparation is. The dataset used in present studies was originally found hampered by high feature intercorrelation, but it eventually proved to be fairly robust and representative. The neural network outperformed the random forest by a little margin. The accuracy scores for each crop variety were usually comparable, all of which were greater than 99 %. The "broadleaf" class was an outlier, having much lower accuracy values. This is to be expected that this class (with the fewest observations) is the most erroneously represented. Deep learning proved clearly superior at forecasting such harvests when focusing on the "broadleaf" class, indicating that it might be a more effective option in dealing with misrepresented classes in general.

According to Figures 9 and 10, the lowest loss was achieved at 77.53 kg/1000m^2. This figure demonstrates a 5.3% improvement over individual multi-temporal ANN findings and a 6.6% improvement over the crop classes Random Forest (RF) model. These graphs are created by mapping the distribution patterns of specific features and investigating their correlations with the dependent variable, given as "score." This study is made possible by using a custom function named "training example." This function, in particular, allows us to acquire insight into how these attributes are related with the "score." This analysis is performed on the seven attributes that have the strongest relationships with the dependent variable "score" to provide an initial comprehension of the data's behavior.

Figures 11 and 12 provide a comparison that focuses on evaluating the performance of two distinct models in predicting the same item. This evaluation entails adding farm-scale yields into predictions and then comparing these predictions to anticipated and actual crop production at the commune scale. The findings of this analysis confirm the presence of biases in numerous factors. However, it is vital to highlight that no changes will be made in advance to address these biases. The analysis is carried out with the assumption that these biases exist and will be considered throughout

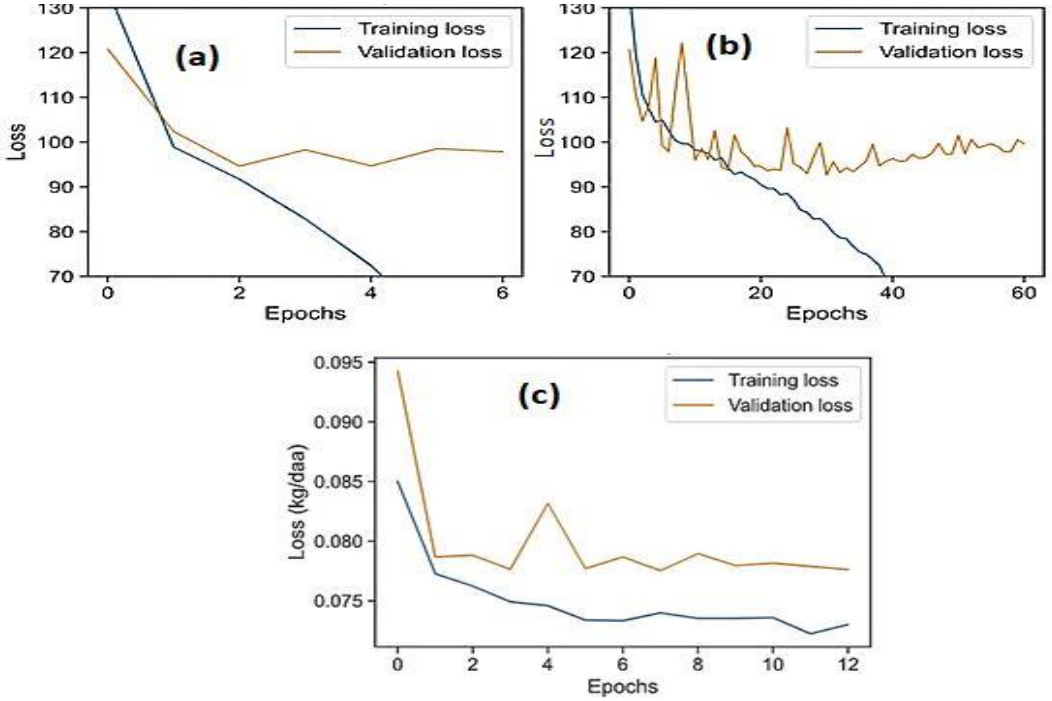

Fig. 9. Training and validation loss for the Illustration of stochastic epoch sampling (a) Simulated normal epochs, (b) With stochastic epoch sampling, and (c) Pre-trained ANN and RF.

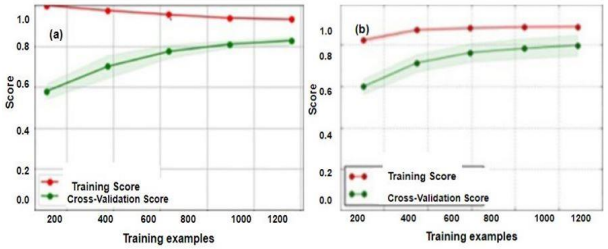

Fig. 10. Learning Curve of (a) ANN vs (b) RF

the review. It's worth noting that the sample size for each set of data points is 64 for each batch of data used. In every epoch, model has to interpretation to more than 5,000 diverse bunches. Few epochs may suffice to lead to top accuracy, minimum loss levels already in the start of the model training. Depending on how well trained classifiers performed overall, this choice might be reconsidered later. To compare deep neural networks and traditional random forests machine learning approaches, two separate sets of tensors will be produced and used in each learning experiment. After highly correlated characteristics were eliminated, this dataset now comprises 325,834 observations, which include one column for labels (integers ranging from 1 to 7); 102 columns for features. Following that, the unique features tensor and the two label tensors are divided into training and testing sets. The training set will have 80% of the observations, with the testing set holding the remaining 20%.

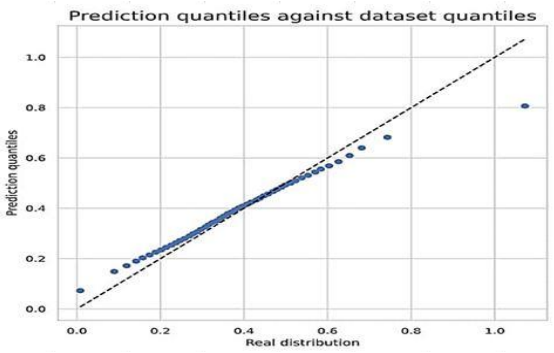

Fig. 11. ANN prediction quantiles versus real quantiles.

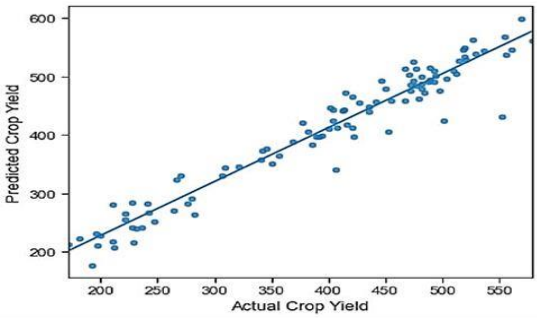

Fig.12. Comparison between actual and predicted crop yields on a commune-scale.

Table 2 represents that the grouping of optical and radar-based information produces extremely precise distant cropland mapping. It is important to note, however, that selecting the appropriate number of trees and depth parameters may have a significant influence on the results. Experiments with fewer trees and lower depth topologies revealed some deterioration, as predicted/expected. When utilized correctly, random forests are good predictors, with performance equivalent to more sophisticated, complicated algorithms. From the simulation results, it is crystal clear that NN-based model outperformed the RF-model to some extent.

Figure 13 and 14 show that the performance of the random forest classification will be preserved, with original labels (integers ranging from 1 to 7) being accommodated into one unidimensional array. The label column for neural network classification will be encoded one-hot using the "Pandas' get_dummies method" (/kaggle/input/cropland-mapping). As a result, labels will now be made up of seven binary parts, each of which refers to a different crop class, allowing for final class identification based on the array member with the greatest anticipated value.

Table 2. Comparison results

RF	Percentage	ANN	Percentage
Accuracy	99.64	Accuracy	99.82
Precision	99.29	Precision	99.79
Recall	99.29	Recall	99.38
F-Score	99.29	F-Score	99.58

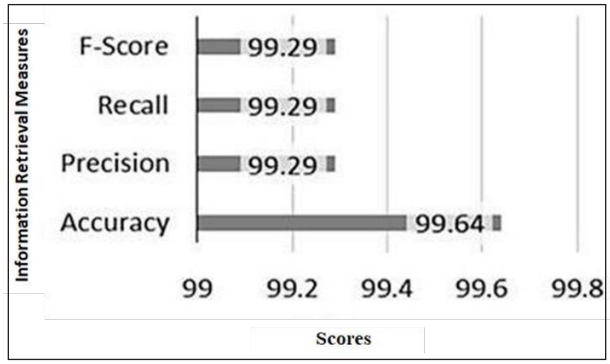

Fig. 13. RF and ANN results

Table 3: Results comparison of current and related study

Study	Year	Technique	Dataset	Precision	Recall	F1 Score	Accuracy
Zhang, et al., [60]	2022	Deep neural networks	Winter wheat (Landsat 8 imagery, Sentinel-2 imagery)	82	74	73	76
Akbar, et al., [61]	2022	CNN AlexNet, ResNet-50, VGG16	Wheat	86	77.1	76.9	85
Proposed Methodology	2023	ML + DL	Wheat	99.79	99.38	99.58	99.82

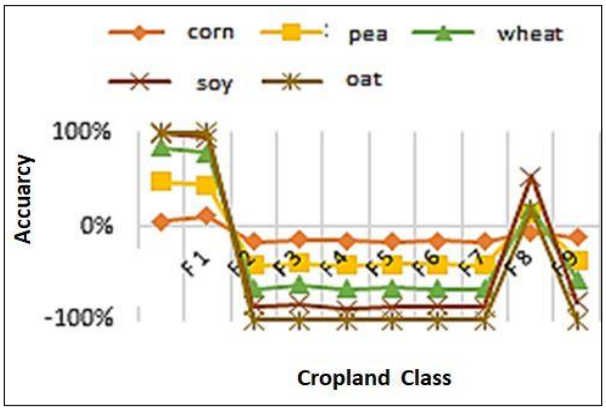

Fig. 14. The performance indicators of RF and ANN for cropland mapping

We have made comparisons with existing related studies to show that our results outperform in terms of accuracy using the different technique and the same type eof data. The empiricla evaluation of the proposed model with the existing studies, as depicted in Table 3, showed that the suggested model have achived more accuracy then the model in comparison. The suggested approach achieved the accuracy of 99.82% and super-passed all the other approaches.

4. CONCLUSIONS

AI is a technology that is emerging in the field of agriculture. It can give farmers real-time or overtime insights into their field. This allows farmers to identify areas that require irrigation, fertilization, or pesticide treatment. AI businesses are creating agricultural robots that can effortlessly do a variety of duties. These robots are programmed to harvest crops and kill plants more quickly than people. These can predict crop yield monitoring using precision farming technique that use–data sensors, connected devices, remote control devices, and other technologies to allow farmers to control their fields. It is concluded from the present studies that the RF and ANN models based decision support system can be potentially used to generate cropland mapping for crop yield prediction. It is also revealed that the ANN model outperformed in crop yield prediction as compared to other models. Future research is required to look into hybrid machine learning algorithms like random forest, support vector machine, multiple regressor, logistic regressor, and deep learning algorithms like Deep convolution neural network (DCNN) and LSTM to see whether they can give rather quicker and more accurate solutions in the domain of precise agriculture. It is suggested that the DCNN and LSTM models be used in pre-foliar disease prediction to estimate crop yield, taking into account the latest large-scale data from several nations to predict fruit quality, etc. Farmers and agricultural experts may test the results.

5. ACKNOWLEDGEMENTS

The authors would like to thank Dr. Tahir Iqbal, Chairman Depatment of Farm Machinery and Precision Engineering, PMAS Arid Agriculture University for helping us in collecting and analysing the dataset and all the experimentations.

6. CONFLICT OF INTEREST

The authors declare no conflict of interest.

7. REFERENCES

1. K.S.M. Anbananthen, S. Subbiah, D. Chelliah, P. Sivakumar, V. Somasundaram, K.H. Velshankar, and M.A. Khan. An intelligent decision support system for crop yield prediction using hybrid machine learning algorithms. *F1000Research* 10: 1143 (2021).
2. K. Jhajharia, P. Mathur, S. Jain, and S. Nijhawan. Crop yield prediction using machine learning and deep learning techniques. *Procedia Computer Science* 218: 406-417 (2023).

3. S. Boonprong, C. Cao, W. Chen, X. Ni, M. Xu, and B.K. Acharya. The classification of noise-afflicted remotely sensed data using three machine-learning techniques: effect of different levels and types of noise on accuracy. *ISPRS International Journal of Geo-Information* 7: 1-21 (2018).
4. B. Devika, and B. Ananthi. Analysis of crop yield prediction using data mining technique to predict annual yield of major crops. *International Research Journal of Engineering and Technology* 5: 1460-1465 (2018).
5. S. Iniyan, V.A. Varma, and C.T. Naidu. Crop yield prediction using machine learning techniques. *Advances in Engineering Software* 175: 103326 (2023).
6. Anshul, and R. Singh. Crop Yield Prediction and Climate Change Impact Assessment Using Machine Learning Technology in Agriculture. In *Information and Communication Technology for Competitive Strategies (ICTCS 2022) Intelligent Strategies for ICT* 349-362 (2023).
7. D. Paudel, A. de Wit, H. Boogaard, D. Marcos, S. Osinga, and I.N. Athanasiadis. Interpretability of deep learning models for crop yield forecasting. *Computers and Electronics in Agriculture* 206: 107663 (2023).
8. A. Nigam, S. Garg, A. Agrawal, and P. Agrawal. Crop yield prediction using machine learning algorithms. In *2019 Fifth International Conference on Image Information Processing (ICIIP),* 125-130 (2019).
9. F. Abbas, H. Afzaal, A.A. Farooque, and S. Tang. Crop yield prediction through proximal sensing and machine learning algorithms. *Agronomy* 10: 1046 (2020).
10. V. Pandith, H. Kour, S. Singh, J. Manhas, and V. Sharma. Performance evaluation of machine learning techniques for mustard crop yield prediction from soil analysis. *Journal of scientific research* 64: 394-398 (2020).
11. A. McBratney, B. Whelan, T. Ancev, and J. Bouma. Future directions of precision agriculture. *Precision agriculture* 6: 7-23 (2005).
12. E. Manjula, and S. Djodiltachoumy. A model for prediction of crop yield. *International Journal of Computational Intelligence and Informatics* 6: 298-305 (2017).
13. S. Bhanumathi, M. Vineeth, and N. Rohit. Crop yield prediction and efficient use of fertilizers. In *2019 International Conference on Communication and Signal Processing (ICCSP)*: 0769-0773 (2019).
14. C. Bojtor, S.M.N. Mousavi, A. Illés, A. Széles, J. Nagy, and C. L. Marton. Stability and adaptability of maize hybrids for precision crop production in a long-term field experiment in Hungary. *Agronomy* 11: 2167 (2021).
15. L. Meng, H.L. Liu, S. Ustin, and X. Zhang. Predicting maize yield at the plot scale of different fertilizer systems by multi-source data and machine learning methods. *Remote Sensing* 13: 3760 (2021).
16. U. Hampicke. Germany's Agriculture and UN's Sustainable Development Goal 15. *SUSTAINABLE LIFE ON LAND*, 18: 103(2021).
17. S. Khaki, L. Wang, and S. V. Archontoulis. A cnn-rnn framework for crop yield prediction. *Frontiers in Plant Science* 10: 1750 (2020).
18. S. Toomula, and S. Pelluri. An Extensive Survey of Deep learning-based Crop Yield Prediction Models for Precision Agriculture. In *Proceedings of the International Conference on Cognitive and Intelligent Computing: ICCIC 2021, Volume 1* (pp. 1-12). Singapore: Springer Nature Singapore (2022).
19. L.R. Varghese, and K. Vanitha. Deep Reinforcement Learning and Model Predictive Control in Hybrid Deep Learning for Rubber Yield Forecast. *Revue d'Intelligence Artificielle* 35: 367-374 (2021).
20. E. Kalaiarasi, and A. Anbarasi. Multi-parametric multiple kernel deep neural network for crop yield prediction. *Materials Today: Proceedings* 62: 4635-4642 (2022).
21. S. Wolfert, D. Goense, and C.A.G. Sørensen. A future internet collaboration platform for safe and healthy food from farm to fork. *2014 annual SRII global conference* 266-273 (2014).
22. S. Khaki, and L. Wang. Crop yield prediction using deep neural networks. *Frontiers in plant science* 10: 621 (2019).
23. F.F. Haque, A. Abdelgawad, V.P. Yanambaka, and K. Yelamarthi. Crop Yield Prediction Using Deep Neural Network. 2020 *IEEE 6th World Forum on Internet of Things (WF-IoT)* 1–4 (2020).
24. M. Qiao, X. He, X. Cheng, P. Li, H. Luo, L. Zhang, and Z. Tian. Crop yield prediction from multi-spectral, multi-temporal remotely sensed imagery using recurrent 3D convolutional neural networks. *International Journal of Applied Earth Observation and Geoinformation* 102: 102436 (2021).
25. L. Gong, M. Yu, S. Jiang, V. Cutsuridis, and S. Pearson. Deep learning based prediction on greenhouse crop yield combined TCN and RNN. *Sensors* 21: 4537 (2021).
26. J. You, X. Li, M. Low, D. Lobell, and S. Ermon. Deep gaussian process for crop yield prediction based on remote sensing data. In *Proceedings of the AAAI conference on artificial intelligence* (2017).
27. K. Gavahi, P. Abbaszadeh, and H. Moradkhani. DeepYield: A combined convolutional neural network with long short-term memory for crop yield forecasting. *Expert Systems with Applications* 184: 115511 (2021).
28. M. Samaila, G. Neto, M. Fernandes, D.A. Freire, M.M, and P.R. Inácio. Challenges of securing Internet of Things devices: A survey. *Security and Privacy* 1: e20 (2018).
29. E.S. Mohamed, A.A. Belal, S.K. Abd-Elmabod, M.A. El-Shirbeny, A. Gad, and M.B. Zahran. Smart farming for improving agricultural management. *The Egyptian Journal of Remote Sensing and Space Science* 24: 971-981 (2021).
30. M.S. Farooq, S. Riaz, A. Abid, T. Umer, and Y.B. Zikria. Role of IoT technology in agriculture: A systematic literature review. *Electronics* 9: 319 (2020).
31. A. James, A. Saji, A. Nair, and D. Joseph.

CropSense–A Smart Agricultural System using IoT. *Journal of Electronic Design Engineering* 5**:** 3 (2019).
32. J.M.O. Jayamanne, R. Vandebona, and J.M.I. Karalliyadda. 2020. Optimization of Conventional Land Survey Techniques Using Modern Technology (2020).
33. K. Guan, J. Wu, J.S. Kimball, M.C. Anderson, S. Frolking, B. Li, C.R. Hain, and D.B. Lobell. The shared and unique values of optical, fluorescence, thermal and microwave satellite data for estimating large-scale crop yields. *Remote sensing of environment* 199: 333-349 (2017).
34. Q. Yang, L. Shi, J. Han, Y. Zha, and P. Zhu. Deep convolutional neural networks for rice grain yield estimation at the ripening stage using UAV-based remotely sensed images. *Field Crops Research* 235: 142-153 (2019).
35. L. Wei, Y. Luo, L. Xu, Q. Zhang, Q. Cai, and M. Shen. Deep convolutional neural network for rice density prescription map at ripening stage using unmanned aerial vehicle-based remotely sensed images. *Remote Sensing* 14: 46 (2022).
36. Y. Shen, B. Mercatoris, Z. Cao, P. Kwan, L. Guo, H. Yao, and Q. Cheng. Improving Wheat Yield Prediction Accuracy Using LSTM-RF Framework Based on UAV Thermal Infrared and Multispectral Imagery. *Agriculture* 12: 892 (2022).
37. F. Wang, M. Yang, L. Ma, T. Zhang, W. Qin, W. Li, Y. Zhang, Z. Sun, Z. Wang, F. Li, and K. Yu. Estimation of above-ground biomass of winter wheat based on consumer-grade multi-spectral UAV. *Remote Sensing* 14: 1251 (2022).
38. H. Tian, T. Wang, Y. Liu, X. Qiao, and Y. Li. Computer vision technology in agricultural automation—A review. *Information Processing in Agriculture* 7: 1-19 (2020).
39. T. Wang, B. Chen, Z. Zhang, H. Li, and M. Zhang. Applications of machine vision in agricultural robot navigation: A review. *Computers and Electronics in Agriculture* 198: 107085 (2022).
40. N. Ismail, and O.A. Malik. Real-time visual inspection system for grading fruits using computer vision and deep learning techniques. *Information Processing in Agriculture* 9: 24-37 (2022).
41. H. Li, Z. Li, W. Dong, X. Cao, Z. Wen, R. Xiao, Y. Wei, H. Zeng, and X. Ma. An automatic approach for detecting seedlings per hill of machine-transplanted hybrid rice utilizing machine vision. *Computers and Electronics in Agriculture* 185: 106178 (2021).
42. R. Ballesteros, D.S. Intrigliolo, J.F. Ortega, J.M. Ramírez-Cuesta, I. Buesa, and M.A. Moreno. Vineyard yield estimation by combining remote sensing, computer vision and artificial neural network techniques. *Precision Agriculture* 21: 1242-1262 (2020).
43. K. Mochida, S. Koda, K. Inoue, T. Hirayama, S. Tanaka, R. Nishii, and F. Melgani. Computer vision-based phenotyping for improvement of plant productivity: a machine learning perspective. *GigaScience* 8: giy153 (2019).
44. M. Vázquez-Arellano, H.W. Griepentrog, D. Reiser, and D. S. Paraforos. 3-D imaging systems for agricultural applications—a review. *Sensors* 16: 618 (2016).
45. Y. Li, C.J. Randall, R. van Woesik, and E. Ribeiro. Underwater video mosaicing using topology and superpixel-based pairwise stitching. *Expert Systems with Applications* 119: 171-183 (2019).
46. L. Haalck, and B. Risse. Embedded dense camera trajectories in multi-video image mosaics by geodesic interpolation-based reintegration. In *Proceedings of the IEEE/CVF Winter Conference on Applications of Computer Vision* 1849-1858 (2021).
47. E. Casoli, D. Ventura, G. Mancini, D.S. Pace, A. Belluscio, and G. Ardizzone. High spatial resolution photo mosaicking for the monitoring of coralligenous reefs. *Coral Reefs* 40: 1267-1280 (2021).
48. M. Du, N. Liu, and X. Hu. Techniques for interpretable machine learning. *Communications of the ACM* 6: 68-77 (2019).
49. B. Saravi, A.P. Nejadhashemi, P. Jha, and B. Tang. Reducing deep learning network structure through variable reduction methods in crop modeling. *Artificial Intelligence in Agriculture* 5: 196-207 (2021).
50. S. Nosratabadi, F. Imre, K. Szell, S. Ardabili, B. Beszedes, and A. Mosavi. Hybrid machine learning models for crop yield prediction. *arXiv preprint arXiv:2005.04155* (2020).
51. J. Arshad, M. Aziz, A.A. Al-Huqail, M. Husnain, A.U. Rehman, and M. Shafiq. Implementation of a LoRaWAN based smart agriculture decision support system for optimum crop yield. *Sustainability* 14: 827 (2022).
52. S.S. Dahikar, and S.V. Rode. Agricultural crop yield prediction using artificial neural network approach. *International journal of innovative research in electrical, electronics, instrumentation and control engineering* 2: 683-686 (2014).
53. F. Abbas, H. Afzaal, A.A. Farooque, and S. Tang. Crop yield prediction through proximal sensing and machine learning algorithms. *Agronomy* 10: 1046 (2020).
54. D. Elavarasan, and P.D. Vincent. Crop yield prediction using deep reinforcement learning model for sustainable agrarian applications. *IEEE access* 8: 86886-901 (2020).
55. R. Dhakar, V.K. Sehgal, D. Chakraborty, R.N. Sahoo, J. Mukherjee, A.V. Ines, S.N. Kumar, P.B. Shirsath, and S.B. Roy. Field scale spatial wheat yield forecasting system under limited field data availability by integrating crop simulation model with weather forecast and satellite remote sensing. *Agricultural Systems* 195: 103299 (2022).
56. I. Khosravi, and S.K. Alavipanah. A random forest-based framework for crop mapping using temporal, spectral, textural and polarimetric observations. *International Journal of Remote Sensing* 40: 7221-7251 (2019).
57. I.H. Sarker. Machine learning: Algorithms, real-world applications and research directions. *SN computer science* 2: 160 (2021).
58. L. Alzubaidi, J. Zhang, A.J. Humaidi, A. Al-Dujaili,

Y. Duan, O. Al-Shamma, J. Santamaría, M.A. Fadhel, M. Al-Amidie, and L. Farhan. Review of deep learning: Concepts, CNN architectures, challenges, applications, future directions. *Journal of Big Data* 8: 1-74 (2021).

59. H.F. Assous, H. AL-Najjar, N. Al-Rousan, and D. AL-Najjar. Developing a Sustainable Machine Learning Model to Predict Crop Yield in the Gulf Countries. *Sustainability* 12: 9392 (2023).
60. S. Zhang, H. Feng, S. Han, Z. Shi, H. Xu, Y. Liu, and J. Yue. Monitoring of Soybean Maturity Using UAV Remote Sensing and Deep Learning. *Agriculture* 13: 110 (2022).
61. S. Akbar, K.T. Ahmad, M.K. Abid, and N. Aslam. Wheat Disease Detection for Yield Management Using IoT and Deep Learning Techniques. *VFAST Transaction on Software Engineering* 10: 80-89 (2022).

Proceedings of the Pakistan Academy of Sciences: A Physical and Computational Sciences 60(3): 49-55 (2023)

ISSN (Print): 2518-4245; ISSN (Online): 2518-4253
https://doi.org/10.53560/PPASA(60-3)652

Pakistan Academy of Sciences

Research Article

Nutritional Study of Various Cow Breeds from Bhatta Chowk Lahore (Punjab), Pakistan

Asad Gulzar[1], Bisma Sher[1,2], Shabbir Hussain[3*], Abdul Ahad Rasheed[4], Muhammad Salman[4], Shazma Massey[5], and Abdur Rauf[6]

[1]Department of Chemistry, Division of Science and Technology (DSNT), University of Education Lahore, Pakistan
[2]Department of Chemistry, Lahore Garrison University, Lahore, Pakistan
[3]Institute of Chemistry, Khwaja Fareed University of Engineering and Information Technology 64200, Rahim Yar Khan, Pakistan
[4]Dairy and Food technology, Pakistan Council of Scientific and Industrial Research (PCSIR), Lahore, Pakistan
[5]Department of Chemistry, Forman Christian College (A Chartered University) Lahore, Pakistan
[6]Department of Chemistry, University of Sahiwal, Sahiwal, Pakistan

Abstract: Present study was conducted to investigate the nutritional study of cow' milk of various breeds from Bhatta Chowk Lahore. Different cow's breeds were found to possesses variable amounts of nutritional contents, i.e., highest moisture and ash in Cholistani cow, highest fat in Sahiwal cow, highest calcium and specific gravity in Holstein cow and highest contents of protein, solid-not-fat and total solid in Red Sindhi. Red Sindhi cow's milk was found to be more nutritious in terms of its richness in proteins, solid-not-fat and total solids whereas Holstein cow was rich in calcium. Calcium was found to be in a range of 550 to 630 ppm with the decrease of concentration in the following order: Sahiwal > Holstein Frisian = Red Sindhi > Cholistani. The Cholistani cow milk showed the presence of 3.126 % protein, 3.5 % fat, 88.2 % moisture, 8.3 % solids-not fat, 11.8 % total solids, 0.791 % ash, 30.5° lactometer reading and 1.0305 kg/m^3 specific gravity. Sahiwal cow milk showed 3.318 % of protein, 4.1 % fat, 87.5 % moisture, 30.1° lactometer reading, 1.03 kg/m^3 specific gravity, 8.4 % solids-not-fat, 12.5 % total solids and 0.79 % ash. Holstein Frisian's milk demonstrated the presence of 3.33 % protein, 3.8 % fat, 87.35 % moisture, 31° lactometer reading, 1.03 kg/m^3 specific gravity, 8.85 % solids-not-fat, 12.65 % total solids and 0.77 % ash. Red Sindhi's milk revealed the presence of 3.38 % protein, 3.95 % fat, 85.65 % moisture, 28° Lactometer reading, 1.028 kg/m^3 specific gravity, 10.4 % solids-not-fat, 14.35% total solids and 0.705 % ash.

Keywords: Red Sindhi, Sahiwal, Cholistani, Holstein Frisian breeds, Cow Milk, Bhatta Chowk Lahore, Nutritional analysis.

1. INTRODUCTION

Dairy products are an important food source throughout the world, for which the milk is mainly produced by four ruminants, i.e., cows, buffaloes, goat and sheep. Milk has special significance due to its nutritional value and its role in growth and resistance to the diseases. It is an important source of magnesium, calcium, phosphorus, potassium and vitamins [1]. Water, proteins, fats, lactose, minerals and other dissolved ingredients (vitamins and white blood cells) are important components of cow milk. Cow milk is the major source of calcium but the amount of calcium and other constituents varies from a breed to another breed [2]. Milk is a dilute emulsion which is comprised of fat/oil dispersed in aqueous colloidal continuous phase. Physical properties of milk are similar to those of water but the difference lies in the concentration of solutes (salts, lactose and proteins) [3]. The specific gravity of cow's milk is 1.029; its viscosity is significantly lower as compared to the camel

Received: July 2022; Accepted: September 2023
* Corresponding Author: Shabbir Hussain <shabchem786@gmail.com>

and buffalo's milk [4]. Cow's milk contains fat globules; lipid metabolic differences produce small or large fat globules [5]. It has been reported that the amount of saturated fatty acids, trans fatty acid, linoleic acid and conjugated linolenic acid is lower in cow's milk as compared to that in the buffalo's milk [6]. Milk and dairy products are good sources of fat-soluble vitamins, i.e., A, E, D, and K [7]. Raw milk can be separated into fat-enriched and fat-depleted phases, i.e., cream and skim milk, respectively by gravitational separation. It occurs due to differences in densities of milk serum and emulsified fat globules [8]. Different types of carbohydrates such as lactose, galactose, glucose and other oligosaccharides are found in milk. Cow milk generally contains 4.8 % anhydrous lactose (on average) whereas lactose concentration depends upon the type of milk [9]. Cow's milk is three to four times richer in protein than human milk, [10]. Lingathurai et. al., [11] collected sixty samples of cow's milk in Madurai and found 6.14 % fat, 3.77 % protein, 18.10 % of total solids and 0.08 % ash. Mahdian and Tehrani [12] analyzed total solids in milk by adding bacteria and found the increasing amount of total solids from 14 % to 27 % in milk with the increasing growth of bacteria.

The composition of cow's milk varies with season. The highest level of main components (e.g., solids not fat: 96.4±0.04 g/L; lactose: 53±0.02 g/L; protein: 35.3±0.01 g/L, minerals: 7.8±0.04 g/L) of milk were observed in winter. Moreover, the nutritional components of raw milk were found in higher quantity as compared to the sterilized and pasteurized milk [13]. For macronutrient estimation, 40 milk samples of cow and buffalo were tested and there was a lower concentration of total solids, fat, protein, lactose and ash contents in cow milk than buffalo milk [14]. Dora found the highest significant correlation between total solids, fats and solid-not-fats in cow's milk [15]. Mineral fraction is about 8-9 g/L in cow's milk [16]. The mineral composition varies according the lactation phase, environmental factor, eating and nutritional status of animal and its genes [17]. With the climate changes, it was observed that the Se, Mg and Zn concentrations were fluctuating [18]. A larger fraction of milk contains calcium and phosphorus which take part in bone growth and nurturing of newborns [19]. Calcium is very important as it involves in many metabolic processes in body, helps in bone growth and prevents from osteoporosis [20]. 0.019 g/liter of calcium, 0.029 g/liter potassium and 0.010 g/liter sodium were estimated through atomic absorption in cow's milk samples in a study [21]. Zinc, magnesium and copper can be determined directly by using atomic absorption spectroscopy according to Association of Official Agricultural Chemists (AOAC) 2000 [22]. For estimating the strength of oxidant or reductant, titration method is used by using a sensitive indicator to analyze the biomolecular interaction specifically calcium milk interaction [23].

With an expected 65.7 million tons of milk produced in 2021–2022, Pakistan is among the top 5 milk-producing nations in the world [24]. Farmers are involved in Milk production in Pakistan. In mixed farming system, farmers keep 1-2 milk animals and are responsible for the production of about 38% of total milk [25].

Sahiwal cattle are considered as one of the best cow breed across the world [26]. Sahiwal cattle are found in parts of districts Sahiwal, Okara, Pakpattan, Multan, and Faisalabad. Sahiwal cow weighs 400–500 kg and is medium-sized with a thick body [27] The average lactation production of a Sahiwal cow is 1475 ± 651 kg [28]. The Red Sindhi breed emerges from a mountainous region (called Mahal Kohistan) and is extended to Thattha and Dadu districts in Sindh. It is a medium in size and has red colour body [29]. Its milk yield is observed to be the highest (1220 liters) in 3rd lactation [30]. Cholistani cattle breed is found in Cholistan tract (a desert area), different areas of Bahawalnagar, Bahawalpur, and Rahimyar Khan districts. In males, it's body weight is 450-500 and in females it is 350-400 kg [31]. Cholistani cattle is as an excellent heat tolerant animal with high milk potential even in desert conditions and is commonly found Cholistan desert in Pakistan [32].

Current studies were performed to investigate the qualitative and quantitative determination of moisture, ash, protein, fat, solids-not-fat, total solids, specific gravity and calcium in milk samples of four cow breeds, i.e., Red Sindhi, Holstein Frisian, Cholistani and Sahiwal breeds.

2. MATERIALS AND METHODS

The present work was performed in Food and Biotechnology Research Center (FBRC) at Pakistan Council of Scientific and Industrial Research (PCSIR), Lahore, Punjab Pakistan. The milk samples of four cow breeds (Red Sindhi, Holstein Frisian, Cholistani and Sahiwal breeds) were collected from Bhatta Chowk Lahore which is situated beyond the Cantt area of Lahore, Pakistan. All chemicals were purchased from *BDH.* Distilled water was used for washing all glassware which (after washing) were dried in an oven at 100 ºC. Polarized Zeeman Atomic Absorption Spectrophotometer, Hitachi High Technologies America, Inc with model Z-8000 was used. Electronic balance (OHAUS Pioneer Analytical Balance, with Draftshield, 210 g capacity, 0.1 mg Readability, Model Number 80251552) was used in this study.

Gerber's Centrifuge (0-4000 rpm) was used with WTW 1F10-220 Inolab Level 1 Multiparameter Meter without Probe, 110 V. Muffle furnace having temperature range of 0-1000 °C was used. Borosil Gerber milk Pipette (Pyrex) having capacity 10.75 mL and Standard Gerber milk test butyrometers were used.

2.1 Determination of calcium contents using permanganate titration method

Calcium was determined by permanganate titration. Solutions containing milk samples were titrated against standard potassium permanganate solution to get persistent pink color (at least 30 sec) with heating.

$$\text{Calcium, percent by weight} = \frac{1.002 \times V}{W}$$

2.2 Determination of calcium contents using atomic absorption spectrophotometer

Milk Ash (0.5 g) was mixed with 1 ml concentrated nitric acid and then distilled water was added to make the total volume to 100 mL. Samples were analyzed by Hitachi Polarized Zeeman Atomic Absorption Spectrophotometer, Z-8000. Three readings were taken for precise calculations.

2.3 Estimation of Moisture (%)

Moisture was estimated by measuring the difference between weight of dried empty petri dish and sample containing petri dish. The weight of dishes with dried milk samples was noted by analytical balance and % moisture was calculated by following relation:

$$\text{Moisture \%} = \frac{W_1 - W_2}{W}$$

Where,
W = Weight (gram) of milk sample
W_1 = Initial weight (gram) of the dish with sample taken for analysis
W_2 = Final weight (gram) of the dish with sample after drying

2.4 Determination of Ash (%)

10 mL milk sample was placed and charred in muffle furnace at 550 °C for 4 hours to get ash. Weight of each crucible was noted to measure the ash percentage.

$$\text{Ash (\%)} = \frac{W_2 - W_1}{W} \times 100$$

Where,
W = Weight (gram) of milk sample
W_1 = Weight (gram) of the empty crucible
W_2 = Weight (gram) of the crucible with sample after ashing.

2.5 Evaluation of Fat (%) by Gerber Method

Fat content was determined by Gerber's method using Gerber's Butyrometer as per AOAC methods [33].

2.6 Determination of Total Solid (%)

Total solids were determined as per AOAC method.

$$\text{Total solid (\%)} = \frac{W_2 - W}{W_1 - W} \times 100$$

Where,
W = Weight (gram) of dish
W_1 = Weight (gram) of the dish with sample taken for analysis
W_2 = Weight (gram) of the dish with sample after drying

2.7 Determination of Solid-not-fat (%)

Total solid and fat were determined by above-described two methods. Then solid-not-fat was determined for each sample by subtracting fat (%) from total solid (%).
Solid Not Fat (%) = Total solids (%) - Fat (%)

2.8 Determination of Nitrogen (%) by Kjeldahl Method

Total nitrogen was determined by standard Kjeldahl's method.

$$\text{Protein (\%)} = \frac{\text{Titre used x 0.4 x 6.38}}{\text{Volume of sample}}$$

2.9. Evaluation of Specific gravity

Specific gravity was determined by lactometer method.

$$\text{Specific gravity} = \left(\frac{\text{Lactometer reading}}{1000} \right) + 1$$

3. RESULTS AND DISCUSSION

The milk samples of four cow breeds (Red Sindhi, Holstein Frisian, Cholistani and Sahiwal breeds) were analyzed for the presence of various parameters (moisture, ash, protein, fat, solids-not-fat, total solids, specific gravity and calcium); the obtained results are summarized in Table 1a whereas the statistical analysis (two-way ANOVA) data has been shown in Table 1b.

3.1 Calcium

By potassium permanganate titration method, it was found that Sahiwal, Cholistani, Holstein Frisian and Red Sindhi breeds contain 0.063, 0.055, 0.063 and 0.056 % calcium, respectively. The slight differences between the observed calcium values may be owed to the differences in their habits such as grazing habit, reproductive habit etc.

Atomic absorption spectroscopy was performed to verify the results of calcium concentration as obtained by potassium permanganate method. The Holstein Frisian cow and Sahiwal cow contained 0.06 % and 0.059 % calcium, respectively. The obtained results are thus very close to those obtained by permanganate method.

3.2 Moisture percentage

Sahiwal cow, Cholistani cow, Holstein Frisian cow and Red Sindhi cow were found to possess the moisture contents of 87.5, 88.2, 87.35 and 85.65 %, respectively in their milk samples. Red Sindhi cow possessed the lowest moisture content while Cholistani cow demonstrated the highest amount of moisture content in its milk. The moisture content resembles closely with that (82-90%) reported earlier in different milk samples [34].

3.3 Ash percentage

Sahiwal cow, Cholistani cow, Holstein Frisian cow and Red Sindhi cow had shown the presence of 0.709, 0.791, 0.77 and 0.705 % ash in their milk. Thus Cholistani cow possessed the highest ash content (0.791 %) as compared to the other three breeds whereas the lowest ash content (0.705 %) was observed in Red Sindhi cow.

3.4 Fat percentage

A fat content of 3.8, 4.1, 3.5 and 3.95% was observed in the milk samples of Holstein Frisian cow, Sahiwal cow, Cholistani cow and Red Sindhi cow, respectively. Milk sample of Sahiwal cow has shown the highest fat content (4.1 %) and Cholistani cow possessed the least amount (3.5 %) of fat. However, the obtained fat range 3.5-4.1 % in the investigated samples lies within the range 3.3-4.4 % already reported for the cow's milk [35]. Various factors such as period of lactation, individual traits, nutrition and breed govern the concentration of fat in a milk [35] because various kinds of plant diets govern their nutritional contents [36-38].

3.5 Total Solid Percentage

12.5, 11.8, 12.65 and 14.35 % total solids were found in milk samples of Sahiwal cow, Cholistani cow, Holstein Frisian cow and Red Sindhi cow, respectively. Red Sindhi cow possessed the highest percentage (14.35 %) of total solids whereas in Cholistani cow, the lowest percentage (11.8 %) of total solid was observed. The difference in breeds may be due to fodder difference, difference of lactation period, climate and health status of the breed. Actually, different plants have variable amounts of phytochemical and nutritional

ingredients [39-41] and thus affect the nature of milk when they are used as food for cattle.

3.6 Solid-not-fat Percentage

It was found that Sahiwal, Cholistani, Holstein Frisian and Red Sindhi breeds have solid-not-fat of 8.4, 8.3, 8.85 and 10.4 %, respectively. Red Sindhi cow contained the highest amount (10.4 %) of Solids-not-fat whereas Cholistani cow demonstrated the lowest value of solids-not-fat (8.3 %) in its milk.

3.7 Protein percentage

Sahiwal, Cholistani, Holstein Frisian and Red Sindhi breeds have shown the protein contents of 3.318, 3.126, 3.33 and 3.38 %, respectively in their milk samples. From the above results, it is concluded that Red Sindhi cow has the highest protein content while Cholistani cow shows lowest quantity of protein in its milk sample. Earlier reports verify that beta-lactoglobulin is present in elevated concentrations in cow milk whey protein [42].

3.8 Lactometer reading and specific gravity

Lactometer reading and specific gravity were found to be 31 and 1.031 in Holstein Frisian cow, 28 and 1.028 in Red Sindhi cow, 30.5 and 1.0305 in Cholistani cow and 30 and 1.03, in Sahiwal cow as shown in Table 1a. So, it can be concluded that Holstein Frisian possessed the highest value of lactometer reading and specific gravity. Red Sindhi has shown the lowest value of lactometer reading and specific gravity.

4. CONCLUSIONS

Nutritional parameters such as calcium, specific gravity, protein, fat, moisture, solid-not-fat, total solids and ash were analyzed in cow milk of four breeds (Red Sindhi, Sahiwal, Cholistani and Holstein Frisian). Calcium in the investigated milks samples was found to be in the range of 0.06-0.05 % as determined by potassium permanganate titration and atomic absorption spectrometry. Protein was observed in the range of 3.312-3.38 % whereas fat contents were found in the range of 3.5-4.1 % in the

Table 1a. The values of various parameters in investigated milk samples

	Breeds			
Parameters	**Cholistani cow**	**Sahiwal cow**	**Holstein Friesian**	**Red Sindhi**
Calcium %	0.055	0.059	0.063	0.056
Protein %	3.126	3.318	3.33	3.38
Fat %	3.5	4.1	3.8	3.95
Moisture%	88.2	87.5	87.35	85.65
Lactometer	30.5	30	31	28
Solid-not-fat	8.3	8.4	8.85	10.4
Total solid	11.8	12.5	12.65	14.35
Ash%	0.791	0.709	0.77	0.705
Specific Gravity	1.030	1.030	1.031	1.028

Table 1b. Statistical analysis by using two-way ANOVA was performed which showed significant results in rows (P<0.05) and non-significant in columns P>0.05

Source of Variation	**Rows**	**Columns**	**Error**	**Total**
SS	25346.14	0.16	15.12	25361.43
df	8	3	24	35
MS	3168.27	0.05	0.63	
F	5027.89	0.09		
P-value	0.0000	0.9675		
F crit	2.36	3.01		

milk samples. Moreover, moisture (85.65- 88.2 %), solids-not-fat (8.3-10.4 %), total solids (11.8- 14.35 %) and ash (0.705- 0.791 %) were observed in the tested milk of cow breeds. Lactometer reading of cow milk was shown in the range of 28-31°. Specific gravity in cow milk of four breeds was in range of 1.028-1.03 %. A little difference in investigated parameter values is due to the differences in the cow breeds as they vary in their genetics, body and habitat. However, it can be concluded that milk of different cow breeds possesses variable amounts of nutritional contents i.e., highest moisture and ash in Cholistani cow, highest fat in Sahiwal cow, highest calcium and specific gravity in Holstein cow and highest contents of protein, solid-not-fat and total solid in Red Sindhi cow. Red Sindhi cow's milk was found to be more nutritious in terms of its richness in proteins, solid-not-fat and total solids whereas Holstein cow was rich in calcium as compared to other breeds.

5. CONFLICT OF INTEREST

The authors declare no conflict of interest.

6. REFERENCES

1. K. Mayilathal, K. Thirumathal, N. Thamizhselvi, and D. Yasotha. A comparative study on the chemical parameters of milk samples collected from cow, buffalo and goat at Dindigul district, Tamil Nadu, India. *International Journal of Recent Scientific Research* 8(4): 16612-16614 (2017).
2. T.L. Tyasi, M. Gxasheka, and C. Tlabela. Assessing the effect of nutrition on milk composition of dairy cows: A review. *International Journal of Current Science* 17: 56-63 (2015).
3. P. Fox, T. Uniacke-Lowe, P. McSweeney, J. O'Mahony, P. Fox, T. Uniacke-Lowe, P. McSweeney, and J. O'Mahony. Physical properties of milk. *Dairy Chemistry and Biochemistry*: 321-343 (2015).
4. J. Yoganandi, B.M. Mehta, K. Wadhwani, V. Darji, and D.K. Aparnathi. Comparison of physico-chemical properties of camel milk with cow milk and buffalo milk. *Journal of Camel Practice and Research* 21(2): 253-258 (2014).
5. L. Walter, P. Shrestha, R. Fry, B. Leury, and A. Logan. Lipid metabolic differences in cows producing small or large milk fat globules: Fatty acid origin and degree of saturation. *Journal of Dairy Science* 103(2): 1920-1930 (2020).
6. O. Ménard, S. Ahmad, F. Rousseau, V. Briard-Bion, F. Gaucheron, and C. Lopez. Buffalo vs. cow milk fat globules: Size distribution, zeta-potential, compositions in total fatty acids and in polar lipids from the milk fat globule membrane. *Food Chemistry* 120(2): 544-551 (2010).
7. M.V. Calvo, J. Fontecha, A. Pérez-Gálvez, and L.M. Rodríguez-Alcalá. Milk lipids and their nutritional importance, in Bioactive Lipids. *Elsevier*. p. 269-295 (2023).
8. T. Huppertz, T. Uniacke-Lowe, and A. Kelly. Physical chemistry of milk fat globules. *Advanced Dairy Chemistry: Lipids 2:* 133-167 (2020).
9. P.L. McSweeney, N.F. Olson, P.F. Fox, A. Healy, and P. Højrup. Proteolytic specificity of chymosin on bovine α s1,-casein. *Journal of Dairy Research* 60(3): 401-412 (1993).
10. S. Kumar, K. Kumar, S. Suman, and P. Kumar. Cow milk and human health-a review. *Research & Reviews: Journal of Dairy Science and Technology* 3(3): 1-3 (2014).
11. S. Lingathurai, P. Vellathurai, S.E. Vendan, and A.A.P. Anand. A comparative study on the microbiological and chemical composition of cow milk from different locations in Madurai, Tamil Nadu. *Indian Journal of Science and Technology* 2(2): 51- 54 (2009).
12. E. Mahdian and M.M. Tehrani. Evaluation the effect of milk total solids on the relationship between growth and activity of starter cultures and quality of concentrated yoghurt. *Agriculture and Environmental Sciences* 2(5): 587-592 (2007).
13. A. Belkhemas. *A* comparative study of different types of cow's milk marketed in tiaret region. 2022, Ph.D. Thesis, Université IBNKHALDOUN-Tiaret. http://dspace.univ- tiaret.dz/handle/123456789/8321
14. M. Salman, M. Khaskheli, A.R.T. Israr-Ul- Haq, P. Khuhro, M. Rauf, H. Hamid, and A. Aziz. Comparative studies on nutritive quality of buffalo and cow milk. *International Journal of Research in Applied, Natural and Social Sciences* 2(12): 69-78 (2014).
15. D.S. Dora, S.K. Chourasia, S.S. Sahu, D. Paikra, and S. Bara. Relationship between different milk constituents of GIR cow. *Journal of Entomology and Zoology Studies* 8(2): 551-553 (2020).
16. F. Gaucheron. The minerals of milk. *Reproduction Nutrition Development* 45(4): 473-483 (2005).
17. Š. Zamberlin, N. Antunac, J. Havranek, and D. Samaržija. Mineral elements in milk and dairy products. *Mljekarstvo: časopis za unaprjeđenje proizvodnje i prerade mlijeka* 62(2): 111-125 (2012).
18. E.M. Rodriguez, M. Sanz Alaejos, and C. Diaz Romero. Mineral concentrations in cow's milk from the Canary Island. *Journal of food composition and analysis* 14(4): 419-430 (2001).
19. S. Dandare, I. Ezeonwumelu, and M. Abubakar. Comparative analysis of nutrient composition of milk from different breeds of cows. *Scholars Research Library European Journal of Applied Engineering and Scientific Research* 3(2): 33-36 (2014).

20. A.E. Ratajczak, A. Zawada, A.M. Rychter, A. Dobrowolska, and I. Krela-Kaźmierczak. Milk and dairy products: good or bad for human bone? practical dietary recommendations for the prevention and management of osteoporosis. *Nutrients* 13(4): 1329 (2021).
21. G. Murthy, and U. Rhea. Determination of major cations in milk by atomic absorption spectrophotometry. *Journal of Dairy Science* 50(3): 313-317 (1967).
22. G. Lutfullah, A.A. Khan, A.Y. Amjad, and S. Perveen. Comparative study of heavy metals in dried and fluid milk in Peshawar by atomic absorption spectrophotometry. *The Scientific World Journal* 2014: 715845 (2014).
23. L.-S. Canabady-Rochelle, C. Sanchez, M. Mellema, and S. Banon. Thermodynamic characterization of calcium-milk protein interaction by isothermal titration calorimetry. *Dairy Science & Technology* 89(3-4): 257-267 (2009).
24. M. Tariq, and P.S.-C.T.T. Singh, Sustainable Dairy Production in Pakistan: Lesson Learned and Way Forward. https://sdgs.un.org/sites/default/files/2023-05/B65%20-%20Tariq%20-%20Sustainable%20Dairy%20Production% 20in%20Pakistan.pdf.
25. M.A. Chaudhry, M. Rafiq, M.A. Hanjra, M. Ahmad, and S. Hassan. Economic analysis of milk production in district okara. *Pakistan Veterinary Journal* 17 (3): 135-138 (1997).
26. A. Kumar, B. Chandel, A. Dixit, S. Tiwari, K. Haritha, and M. Kumar. Distribution and Preference of Selected Dairy Breeds among Farmers of Bihar: A Socio-economic Analysis. *Indian Journal of Extension Education* 59(3): 85-89 (2023).
27. R.M. Uddin, M.E. Babar, A. Nadeem, T. Hussain, S. Ahmad, S. Munir, R. Mehboob, and F.J. Ahmad. Genetic analysis of prolactin gene in Pakistani cattle. *Molecular Biology Reports* 40(10): 5685-5689 (2013).
28. S. Banik, and R. Gandhi. Animal model versus conventional methods of sire evaluation in Sahiwal cattle. *Asian- Australasian Journal of Animal Sciences* 19(9): 1225-1228 (2006).
29. D.M.J. Aftab. *Pak Dairy Info Pakistan's 1st Online Dairy Farming Guide.* 2012.
30. P. Khatri, K.B. Mirbahar, and U. Samo. Productive performance of Red Sindhi cattle. *Journal of Animal and Veterinary Advances* 3(6): 353-355 (2004).
31. F.N. Talpur, M. Bhanger, and M. Khuhawar. Comparison of fatty acids and cholesterol content in the milk of Pakistani cow breeds. *Journal of Food Composition and Analysis* 19(6-7): 698-703 (2006).
32. A. Qayyum, J.A. Khan, R. Hussain, T.I. Ahmad, I. Zahoor, M. Ahmad, M. Awais, N. Ahmed, Z. Ahmad, and M. Mubeen. Correlations of blood serum and milk biochemical profiles with subclinical mastitis in Cholistani cattle. *Pakistan Journal of Agricultural Sciences* 55(4): 959-964 (2018).
33. D.H. Kleyn, J.M. Lynch, D.M. Barbano, M.J. Bloom, M.W. Mitchell and Collaborators. Determination of fat in raw and processed milks by the Gerber method: collaborative study. *Journal of AOAC International* 84(5): 1499-1508 (2001).
34. B. Puga-Torres, D. Salazar, M. Cachiguango, G. Cisneros, and C. Gómez- Bravo. Determination of aflatoxin M1 in raw milk from different provinces of Ecuador. *Toxins* 12(8): 498 (2020).
35. M. Markiewicz-Kęszycka, G. Czyżak- Runowska, P. Lipińska, and J. Wójtowski. Fatty acid profile of milk-a review. *Bulletin of the Veterinary Institute in Pulawy* 57(2): 135-139 (2013).
36. N. Mahmood, M.A. Muazzam, M. Ahmad, S. Hussain, and W. Javed. Phytochemistry of Allium cepa L.(Onion): An Overview of its Nutritional and Pharmacological Importance. *Scientific Inquiry and Review* 5(3): 41-59 (2021).
37. S.Z. Butt, S. Hussain, K.S. Munawar, A. Tajammal, and M.A. Muazzam. Phytochemistry of Ziziphus Mauritiana; its Nutritional and Pharmaceutical Potential. *Scientific Inquiry and Review* 5(2): 1-15 (2021).
38. S. Hussain, M. Javed, M.A. Abid, M.A. Khan, S.K. Syed, M. Faizan, and F. Feroz. Prunus Avium L.; Phytochemistry, Nutritional and Pharmacological Review. *Advancements in Life Sciences* 8(4): 307-314 (2021).
39. R. Anwar, S. Hussain, M.A. Abid, M. Ahmad, M. Javed, and M. Pervaiz. Pharmacological and Phytochemical Potential of Aleo Barbadensis (A Comprehensive Review). *Lahore Garrison University Journal of Life Sciences* 6(02): 107-123 (2022).
40. S. Hussain, W. Javed, A. Tajammal, M. Khalid, N. Rasool, M. Riaz, M. Shahid, I. Ahmad, R. Muhammad, and S.A.A. Shah. Synergistic Antibacterial Screening of Cymbopogon citratus and Azadirachta indica: Phytochemical Profiling and Antioxidant and Hemolytic Activities. *ACS Omega* 8(19): 16600-16611 (2023).
41. M. Javed, M. Shoaib, Z. Iqbal, M.A. Khan, S. Hussain, and M. Amjad. Phytochemical and Biological Studies on Curcuma longa L. in Pattoki (Kasur), Pakistan: Chemical and Biological studies of Curcuma longa. *Proceedings of the Pakistan Academy of Sciences: B. Life and Environmental Sciences* 57(2): 59-66 (2020).
42. G. Niero, M. Franzoi, C.L. Manuelian, G. Visentin, M. Penasa, and M. De Marchi, Protein profile of cow milk from multibreed herds and its relationship with milk coagulation properties. *Italian Journal of Animal Science* 20(1): 2232-2242 (2021).

Proceedings of the Pakistan Academy of Sciences: A Physical and Computational Sciences 60(3): 57-61 (2023)

ISSN (Print): 2518-4245; ISSN (Online): 2518-4253
https://doi.org/10.53560/PPASA(60-3)822

Pakistan Academy of Sciences

Research Article

Evaluation of Bending Length, Rigidity and Modulus of Woven and Knitted Fabrics

Mehreen Ijaz*, Namood-e-Sahar, and Zohra Tariq

Department of Home Economics, Lahore College for Women University, Lahore, Pakistan

Abstract: Performance evaluation of textile materials is necessary to determine the use of an end-product. Woven and knitted materials are most preferred manufacturing techniques due to their certain characteristics suitable for apparel and upholstery. The present study aims at determining the bending length, rigidity and modulus of fabrics through standardized test procedures to measure the draping behaviour of an end-product. The results identified the phenomenon that specimens manufactured with woven fabrics were better in drapability compared with knitted fabrics. Moreover, it was identified that type of fiber also plays an important role in determining stiffness of fabrics such as silk fiber showed excellent results. A comprehensive comparison was made between various types of fabrics. The study can be helpful for the textile producers to make amendments in their construction parameters to present acceptable stiffness and draping qualities of fabrics to the end consumers.

Keywords: Bending, Rigidity, Modulus, Draping, Woven, Knitted

1. INTRODUCTION

The evaluation of textile materials such as fiber, yarn or fabric plays an important role in describing the performance behaviour of an end-product [1]. An assessment of mechanical characteristics such as tensile strength, tear strength, bending rigidity, elongation and flexibility etc. needs to be expanded to obtain better results. Th evaluation process of fabrics is quite complex in theoretical terms and must be verified through experiments in laboratory settings [2]. Several testing instruments are used to measure the physical characteristics of fabrics such as its dimensional stability, handle, drape, elongation, lustre and fineness through standardized testing procedures [3]. There are certain indicators that can be used to depict the draping qualities of textile materials. To determine the drape of a product, it is important to consider the factors such as dimensions, stiffness, and elasticity of fabrics. A number of studies have revealed that drape coefficient is highly associated with the mechanical and structural characteristics of fabrics [4].

Drapability of fabric along with its other characteristics like color, texture, lustre or smoothness are taken as criterion to understand the appearance as well as performance. There are multiple factors that can affect the draping quality such as the surface on which it hangs, type of fiber, finish applied over its surface and surrounding environment. Fabric stiffness is an important quality to be considered by textile manufacturers before designing apparel or upholstery products [5]. Fabric rigidity is the ability of the fabric to bend under its own weight. It describes the way a fabric drapes when hang in vertical position. It is largely depending on its ability to resist bending or presents stiffness. Fabric stiffness has a direct relationship with its bending length; high stiffness results in higher bending length and vice versa [6]. Fabric modulus is one of the intrinsic qualities of stiffness of fabric related to its thickness and mass. It is used to measure the compactness and closeness of the fabric geometry made with fibers and yarns. Fibers having low modulus are considered as soft and high modulus as crisp to withstand their position [7].

Received: May 2023; Accepted: September 2023
* Corresponding Author: Mehreen Ijaz <mehreenijaz@hotmail.com>

This current study focuses on identifying the bending length, bending rigidity, and bending modulus of selected woven and knitted fabrics. A comprehensive comparison was made between the samples to understand their requirements for draping in any end-product used for apparel or upholstery.

2. MATERIALS AND METHODS

Samples of woven and knitted fabrics were collected from Nishat Mills Private Limited. Their construction parameters were identified, and these were grouped and labelled accordingly. Two groups were formed; woven and knitted. Five samples from each category were taken and assessed for their bending behaviour. The construction specifications of specimens are given in the Table 1.

The determination of fabric stiffness was measured by ASTM D1388 test procedure. The specimens were preconditioned for 24 hours in a standard atmosphere according to the guidelines provided in ASTM-D1776 testing procedure [8]. Test was conducted in a testing atmosphere having 21°±1°C temperature and 65%±2% relative humidity, as per the instructions given in the test procedure. The bending length, rigidity and modulus was identified. Cantilever principle was employed to measure the stiffness behaviour of fabrics. Shirley fabric stiffness tester was used [9].

A rectangular specimen from each category was cut with the dimensions of 6×1 inches. It was then mounted on a horizontal platform from where it overhung. The tested specimen was moved slowly along with the template to bend downwards under its own weight. It was extended to the point where the specimen's edge intersected with the index lines, which were visible in the mirror. The bending length was read off from the template engraved in centimetres. Each specimen was tested three times in both warp and weft directions with their right and wrong sides.

Bending rigidity was determined through Eq. (1) [10].

$$BR(\mu\text{Nm}) = \text{W}\,(\text{g/m}^2) \times BL^3\,(\text{mm}) \times 9.807 \times 10^{-6} \quad (1)$$

Bending modulus was determined through Eq. (2) [10].

$$BM(\text{Kg/cm}^2) = 12 \times BL^3(\text{mm}) \times \text{W}\,(\text{g/m}^2) \times 10^{-7} / T100^3(\text{mm}) \quad (2)$$

3. RESULTS AND DISCUSSION

The Statistical Package for Social Sciences (SPSS) was used to analyze the collected data for the determination of bending length, rigidity, and modulus. Mean ± S.D were calculated. The bending length of woven and knitted fabrics (face side) is shown in Figure 1. It is measured in centimeters. It is depicted from the calculated data that specimen A-2 showed the highest value for the bending length in both warp and weft directions. One possible reason is that it was composed of silk fiber that has inherent ability to drape better as compared to other fibers. It was investigated [6] that characteristics of fibers, yarns and fabrics can significantly impact the way fabrics drape. It can be said that various construction parameters such as thread count, ends/picks, yarn type, mass would manufacture fabrics with varied drape qualities. It was investigated [11] that yarn density, thickness and space ratio have significant effect on the mechanical behaviour of fabrics. On the other hand, specimen B-1 showed good draping quality due to the viscose yarn used in knitting process. A-3 and B-2 (Figure 1) specimen showed less values for the bending ability both in face and reverse sides of woven and knitted fabrics.

Table 1. Construction specifications of samples

Sample code	Construction type	Type of weave/knit	Fiber content	Thread count	Course / inch	Yarn count	Mass (gsm)
A-1	Woven	Plain	Cotton-100	105×80	-	115	155
A-2	Woven	Plain	Silk-60 Polyester-40	120×135	-	220	145
A-3	Woven	Twill	Cotton-60 Polyester-40	85×125	-	130	125
B-1	Knitted	Rib	Viscose-100	-	65	110	137
B-2	Knitted	Jersey	Cotton-50 Polyester-50	-	70	120	185
B-3	Knitted	Jersey	Cotton-100	-	80	105	229

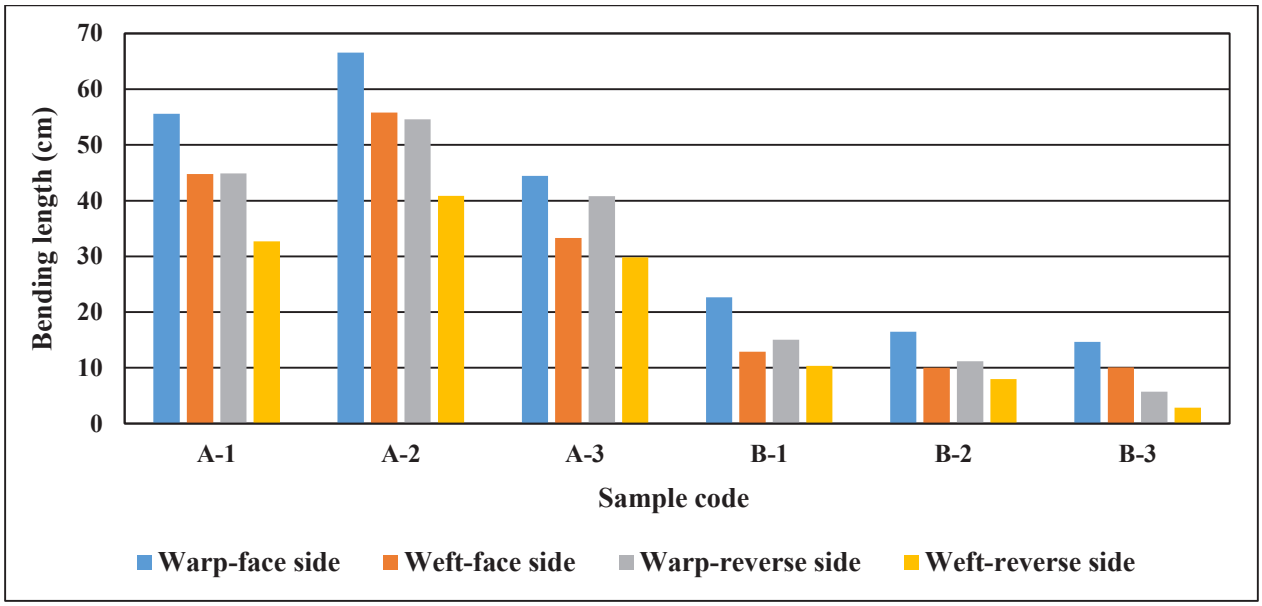

Fig. 1. Bending length of specimens

Low draping affect was investigated due to the long floats and fewer number of interlacing per inch in woven fabrics [12].

Low mass of fabrics can be the cause of high drape coefficient. It can be seen that specimen B-1 has the lowest mass compared with B-2 and B-3 results in high draping rating for knitted fabrics. Thickness of the fabrics did not show any significant effect on the draping ability [13]. The generic class of fibers is important to know the draping behaviours of most of the fabrics. The fiber content along with its percentage ratio has strongly affect the stiffness of knitted materials [14]. Fine fibers had better draping quality compared to coarse fiber [15]. Knitted fabrics manufactured with viscose micro denier fibers were stiffer than viscose regular denier fibers. One possible reason is the low bending rigidity and increased tightness and twisting factor of the resultant fiber [16].

Figure 2 explains that woven fabrics had better bending rigidity compared with knitted fabrics. Yarn interlacing pattern can change the draping ability of fabrics. It was found [6] that there was a positive strong relationship between tightness and compactness of weave and bending rigidity of the observed fabric. Similar phenomenon was observed

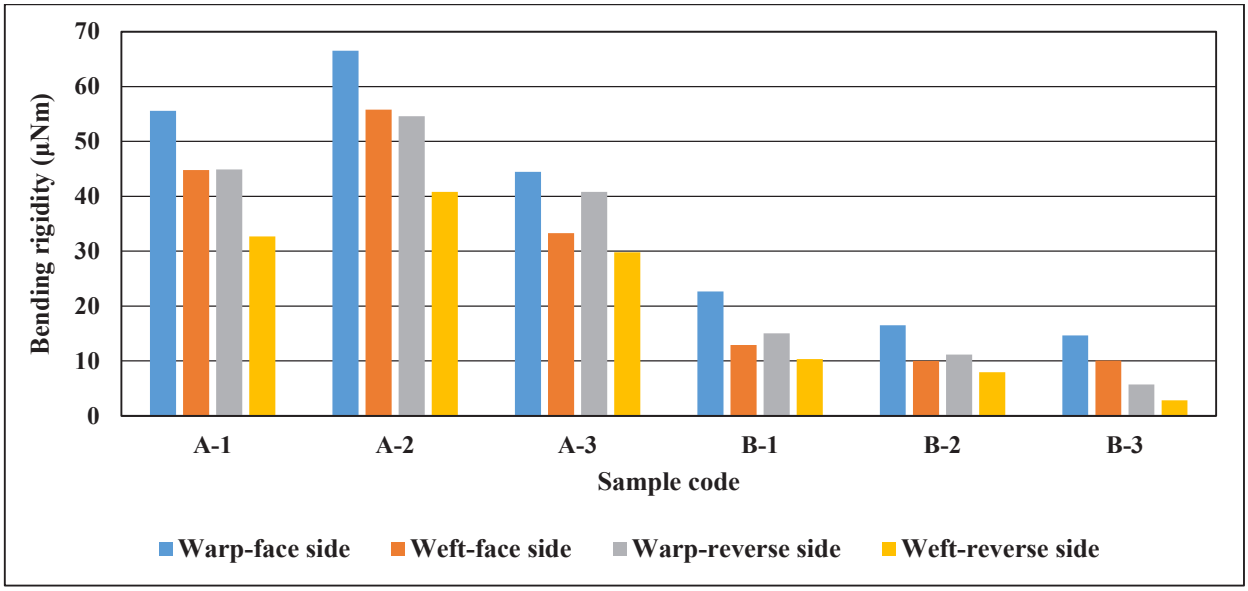

Fig. 2. Bending rigidity of specimens

in the current study that specimen A-1 and A-2 made with plain weave had better draping ability compared with twill weave having long floats in specimen A-3. Finishing treatments applied to the surface of woven fabrics in the relaxation form can reduce the frictional pressure between lengthwise and crosswise yarns, thus results in reduced bending length and rigidity and lowers the draping affect [17].

Elastomeric finishing agents can help in increase the bending strength and draping of fabrics as compared to treatments such as starch that make the fabric stiff in its behaviour [18]. The interlacing pattern of woven materials affect the bending rigidity of tested fabrics. It was found that fabrics made with basket weave presented less bending length than twill weave. It may be due to its long floats and less number of interlacings throughout its surface area [19, 20].

The tested specimens A-2 and A-1 had greater bending modulus for woven and knitted fabrics. (Figure 3). Cross section of fibers may impact the mechanical behaviour of manufactured fabrics. It was found [21] that high space ratio in the cross section makes the fabric more inelastic and soft. Other parameters including yarn count or linear density show higher impact on mechanical properties of fabric than its cross section. The density area was increased in the coarse yarns and decreased in the fine and smooth yarns [22]. It was found that fabrics with high density ratio were more prone to abruptly change the weave density in terms of measuring drapability. It was investigated that weave density significantly increase the drape coefficient of woven fabrics [11].

Woven fabrics had significantly higher bending modulus compared with knitted fabrics. These were ranked as follows A-2, A-1 and A-3 in the woven group from highest to the lowest rank. Whereas, B-1 showed the highest range followed by B-2 and B-3 in the knitted group of specimens. The bending modulus of woven fabrics was highly dependent on the direction in which the specimens were placed. It has been suggested that an increase in the number of covers in a particular direction causes a significant decrease in the bending rigidity of the same orientation. It was also observed that an increase in number of crossings in warp and weft direction and stiffening of liners in between significantly increased the bending rigidity of the tested samples [23].

4. CONCLUSIONS

From the present study, it can be concluded that woven fabrics depicted better draping quality in terms of length, rigidity and modulus as compared

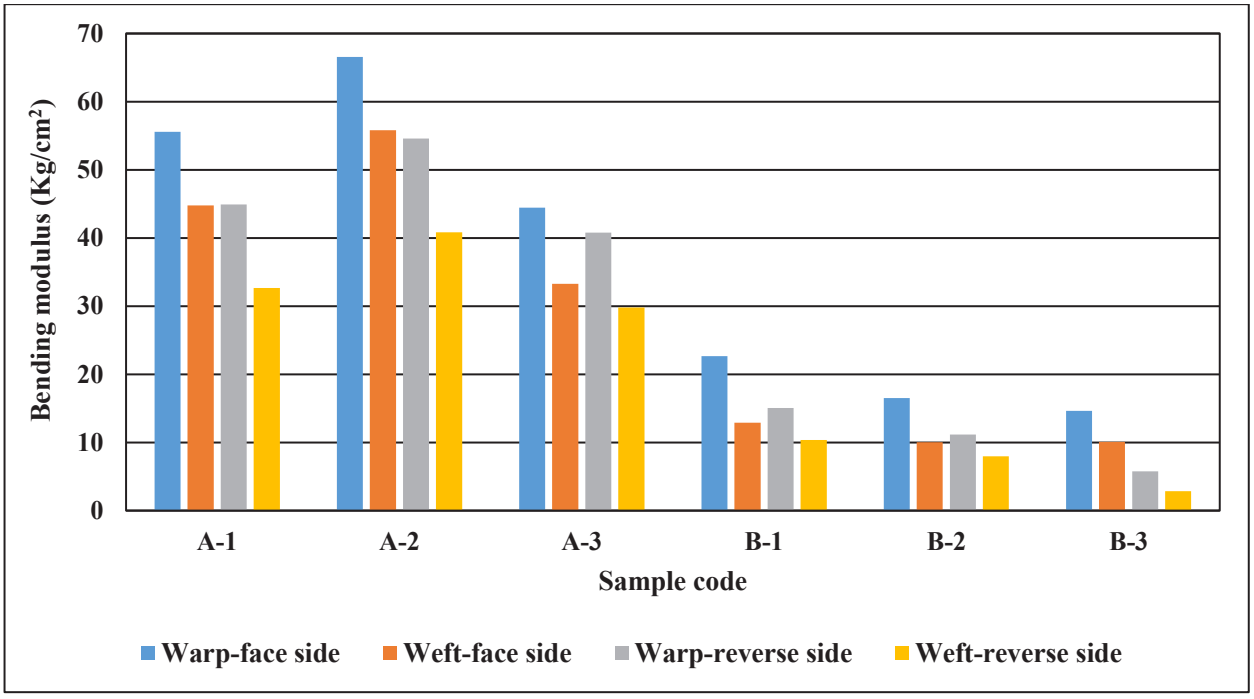

Fig. 3. Bending modulus of specimens

to the knitted fabrics. A2 specimen made with silk was better able to drape due to the inherent characteristics of the fiber and lesser number of interlacings per inch during the weaving. Specimen B1 showed good results in all aspects from the knitted group of fabrics attributed to the rib knit stitch and the inclusion of the viscose yarns. The study can be helpful for the textile producers to make the amendments in their manufacturing parameters for improved results of an end-product either used for apparel or upholstery. Follow up studies can focus on other mechanical properties of woven and knitted to improve their performance.

5. CONFLICT OF INTEREST

The authors declare no conflict of interest.

6. REFERENCES

1. J. Hu. Introduction to fabric testing. *Fabric Testing, Woodhead Publishing Series in Textiles.* 1-26 (2008).
2. R.J. Bassett, R. Postle, and N. Pan. Experimental methods for measuring fabric mechanical properties: A review and analysis. *Textile Research Journal* 69(11): 866-875 (1999).
3. P. Bishop, Testing for Fabric Comfort. *Woodhead Publishing Limited, CRC Press* (2008).
4. T. Sarac, J. Stepanovic, G. Demboski, and V. Petrovic. Fabric draping and cotton fabric structure relation analysis. *Advanced Technologies* 4(1): 84-88 (2015).
5. P. Pandurangan, J. Eischen, N. Kenkare, and T.A. Lamar. Enhancing accuracy of drape simulation. Part II: Optimized drape simulation using industry-specific software. *Journal of the Textile Institute* 99(3): 219-226 (2008).
6. R.A.E. Sanad. The measurement of drape for nonwoven and conventional textile fabrics. *PhD Thesis. University of Leeds* (2013).
7. M. Ijaz. Performance criteria of chemical protective clothing. *PhD Thesis. University of the Punjab.* (2017).
8. ASTM International. ASTM D1388. Standard test method for stiffness of fabrics. *West Conshohocken; PA: ASTM International* (2018).
9. ASTM International. ASTM D 1776. Standard practice for conditioning and testing textiles. *West Conshohocken; PA: ASTM International* (2015).
10. A.D. Boos, and D. Tester. Fabric assurance by simple testing. *CSIRO, Textile and Fiber Technology, Report No. WT92.02* (1994).
11. M. Matsudairaa, S. Yamazaki, and Y. Hayashi. Changes in dynamic drapability of polyester fabrics with weave density, yarn twist and yarn count obtained by regression equations. *Indian Journal of Fibre and Textile Research* 33(3): 223-229 (2008).
12. M.M. Quirk, T.L. Martin, and M.T. Jones. Inclusion of fabric properties in the e-textile design process. *In 2009 International Symposium on Wearable Computers* 37-40 (2009).
13. I. Frydrych, G. Dziworska, and A. Cieslinska. Mechanical fabric properties influencing the drape and handle. *International Journal of Clothing Science and Technology* 3(1): 171-183 (2000).
14. A. Telli, and N. Ozdil. Effect of recycled PET fibers on the performance properties of knitted fabrics. *Journal of Engineered Fibers and Fabrics* 10(20): 47–60 (2015).
15. M.E. Yuksekkaya, T. Howard, and S. Adanur. Influence of the fabric properties on fabric stiffness for the industrial fabrics. *Textiles and Apparel Technology* 18(4): 263-267 (2008).
16. G. Ramakrishnan, B. Dhurai, and S. Mukhopadhyay. An investigation into the properties of knitted fabrics made from viscose microfibers. *Journal of Textile and Apparel, Technology and Management* 6(1):1-9 (2009).
17. B.J. Collier. Measurement of fabric drape and its relation to fabric mechanical properties and subjective evaluation. *Clothing and Textiles Research Journal* 10(1): 46-52 (1991).
18. I. Frydrych, G. Dziworska, and M. Matusiak. Influence of the kind of fabric finishing on selected aesthetic and utility properties. *Fibres & Textiles in Eastern Europe* 3(42): 31-37 (2003).
19. R. Chattopadhyay. Design of Apparel Fabrics: Role of fibre, yarn and fabric parameters on its functional attributes. *Journal of Textile Engineering* 54(6): 179-190 (2008).
20. G. Agarwal, L. Koehl, and A. Perwuelz. Interaction of wash- ageing and use of fabric softener for drapeability of knitted fabrics. *Textile Research Journal* 81(11): 1100-1112 (2011).
21. P. Chidambaram, R. Govindan, and K.C. Venkatraman. Study of thermal comfort properties of cotton/regenerated bamboo knitted fabrics. *African Journal of Basic & Applied Sciences* 4(2):60-66 (2012).
22. Z.B. Sayed, T. Islam, N.H. Chawdhury, and M. Ahmed. Effect of knitted structures and yarn count on the properties of weft knitted fabrics. *Journal of Textile Science and Technology* 4(2): 67-77 (2018).
23. E. Witczak, I. Jasinska, and I. Krawczynska. The influence of structure of multilayer woven fabrics on their mechanical properties. *Materials* 14(5): 1315-1321 (2021).

Proceedings of the Pakistan Academy of Sciences: A Physical and Computational Sciences 60(3): 63-66 (2023)

ISSN (Print): 2518-4245; ISSN (Online): 2518-4253
https://doi.org/10.53560/PPASA(60-3)663

Pakistan Academy of Sciences

Research Article

Mathematical Analysis on Spherical Shell of Permeable Material in NID Space

Saeed Ahmed[1*], Muhammad Akbar[2], Muhammad Imran Shahzad[3], Muhammad Ahmad Raza[4], and Sania Shaheen[3]

[1]Department of Physics, Quaid-i-Azam University, Islamabad, Pakistan
[2]Department of Electronics, Quaid-i-Azam University, Islamabad, Pakistan
[3]Department of Applied Physics, Federal Urdu University of Arts, Science and Technology Islamabad, Islamabad, Pakistan
[4]Department of Statistics, Federal Urdu University of Arts, Science and Technology Islamabad, Islamabad, Pakistan

Abstract: In this paper, we have studied the magnetic shielding effect of a spherical shell analytically in fractional dimensional space (FDS). The Laplacian equation in fractional space predicts the complex phenomena of physics. This is a boundary value problem that has been solved by the separation variable method mathematically by taking low frequency $\omega = 0$. Electric potential is obtained in fractional dimensional space for the three regions, namely outside the spherical shell, between the shell and hollow sphere and inside the sphere. Also, the induced dipole moment has been derived. We obtain a general solution that reduces to the classical results by setting fractional parameter $\alpha = 3$ which takes its value $(2 < \alpha \leq 3)$.

Keywords: Variable Method, Magnetic Shielding Effect, Fractional Dimensional Space, Spherical Shell.

1. INTRODUCTION

The novel idea of fractional-dimensional space (FDS) is essential in different disciplines of physics worked by numerous researchers [1-18]. Like the researcher, Wilson [3] has investigated quantum field theory (QFT) in FDS. Furthermore, the FDS can be employed as an indicator in the Ising limit of the QFT [6]. Stillinger [4] has defined an axiomatic basis for this idea for the development of Schrödinger wave mechanics and Gibbsian statistical mechanics in the α-dimensional space. The runtime operational category of space-time dimension shown by Zeilinger and Svozil [10] provides a likelihood of determination of space-time dimension empirically. It is also acknowledged that the fractional dimension of space-time should be less than 4. The α-dimensional fractional space has also been modelled in the last few decades [11]. Moreover, the solution of electro-static problems [13-18], has also been investigated in the FDS $(2 < \alpha \leq 3)$.

We have extended the problem of a spherical shell of highly permeable material which is derived by Baleanu *et al.* [17]. We have solved it in fractional dimensional space analytically. The primary aim is to use the Laplacian equation to find electric potential and induced dipole moment in FDS. For the integer order $\alpha = 3$, the original solution is reproduced.

2. MATERIALS AND METHODS

We consider here a spherical shell of permeable material which is placed in fractional space shown in Figure 1**.** We have studied the spherical shell of the inner radius '*a*' and the outer radius '*b*' for the

Received: January 2023; Accepted: September 2023
*Corresponding Author: Saeed Ahmed <saeedqau@gmail.com>

phenomenon of magnetic shielding. This problem has been extended from Jackson [13]. The core is made of material of permeability, μ, and placed in a fractional space. B_0 is the uniform magnetic field applied on the surface. We need to discover the fields B and H everywhere in space, but most specifically in the cavity (r < a**)** as a function of μ. The magnetic field H is determined from a scalar potential H = -∇Ψ, as there are no currents present. Thus, the potential Ψ satisfies the Laplacian in fractional space having fractional α-dimension in "spherical polar coordinate systems" which is described by Baleanu *et al.* [17]:

$$\left(\frac{d^2}{dr^2}+\frac{\alpha-1}{r}\frac{d}{dr}+\frac{1}{r^2}\left[\frac{d^2}{d\theta^2}+(\alpha-2)cot\theta\frac{d}{d\theta}\right]-\frac{1}{r^2sin\theta}\left[\frac{d^2}{d\phi^2}+(\alpha-3)cot\phi\frac{d}{d\phi}\right]\right)\Psi=0. \quad (1)$$

where the fractional parameter α lies in the range $(2 < \boldsymbol{\alpha} \leq 3)$

In this case, the Laplace equation for the potential independent of angle ϕ can be expressed as:

$$\nabla^2\Psi=\left(\frac{\partial^2}{\partial r^2}+\frac{\alpha-1}{r}\frac{\partial}{\partial r}+\frac{1}{r^2sin^{\alpha-2}\theta}\frac{\partial}{\partial\theta}sin^{\alpha-2}\theta\frac{\partial}{\partial\theta}\right)\Psi=0 \quad (2)$$

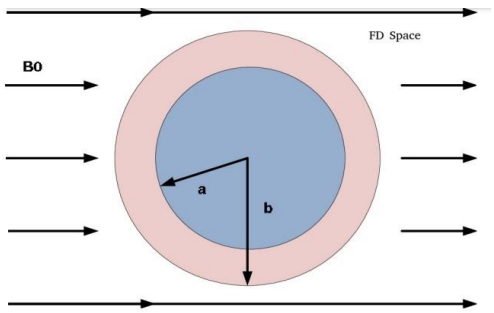

Fig. 1. Spherical Shell of Highly Permeable Material Placed in FDS

Eq (3) is separable and suppose.

$$\Psi(r,\theta)=R(r)\Theta(\theta) \quad (3)$$

The differential equation (3) followed by the published article [17], can be decoupled into two different parts namely angular and radial which are written as:

$$\left[\frac{d^2}{d\theta^2}+(\alpha-2)cot\theta\frac{d}{d\theta}+l(l+\alpha-2)\right]\Theta(\theta)=0 \quad (4)$$

$$\left[\frac{d^2}{dr^2}+\frac{\alpha-1}{r}\frac{d}{dr}+\frac{l(l+\alpha-2)}{r^2}\right]R(r)=0 \quad (5)$$

Therefore, the combined solutions of Ψ (r, θ) in α-dimensional fractional space, can be expressed as

$$\Psi(r,\theta)=\sum_{l=0}^{\infty}\left(a_lr^l+\frac{b_l}{r^{l+\alpha-2}}\right)C_l^{\alpha/2-1}(cos\theta) \quad (6)$$

Here, the unknown constants a_l and b_l can be determined by using the boundary conditions (B.Cs.) on Ψ (r, θ).

We construct here the solution for three different regions by satisfying the B.Cs., at r = a and r = b.

For the outer region r > b, the potential must be of the form,

$$\Psi(r,\theta)=-H_0rcos\theta+\sum_{l=0}^{\infty}\frac{A_l}{r^{l+\alpha-2}}C_l^{\alpha/2-1}(cos\theta) \quad (7)$$

where $H = H_0$ is the uniform field, at large distance.

For the inner regions, a < r < b the potential can be written as:

$$\Psi(r,\theta)=\sum_{l=0}^{\infty}\left(B_lr^l+\frac{C_l}{r^{l+\alpha-2}}\right)C_l^{\alpha/2-1}(cos\theta) \quad (8)$$

For r<a

$$\Psi(r,\theta)=\sum_{l=0}^{\infty}D_lr^lC_l^{\alpha/2-1}(cos\theta) \quad (9)$$

All coefficients for $l \neq 1$ vanish. Then we can construct the solutions for different regions given below:

$$\Psi_e(r,\theta)=\left[-H_0r+Ar^{-(\alpha-1)}\right](\alpha-2)(cos\theta), r>b \quad (10)$$

$$\Psi(r,\theta)=\left[Br+Cr^{-(\alpha-1)}\right](\alpha-2)(cos\theta), a<r<b \quad (11)$$

$$\Psi(r,\theta)=Dr(\alpha-2)(cos\theta), r<a \quad (12)$$

The boundary conditions, at r = a and r = b, are that H_θ and B_r be continuous for l = 1, the coefficients satisfy the four simultaneous equations.

$$\frac{\partial\Psi(r,\theta)}{\partial\theta}\frac{\partial\Psi(r,\theta)}{\partial\theta}(b_-)=\frac{\partial\Psi(r,\theta)}{\partial\theta}(b_+) \quad (13)$$

$$\frac{\partial\Psi(r,\theta)}{\partial\theta}(a_-)=\frac{\partial\Psi(r,\theta)}{\partial\theta}(a_+) \quad (14)$$

$$\mu_1\frac{\partial\Psi(r,\theta)}{\partial r}(b_-)=\mu_0\frac{\partial\Psi(r,\theta)}{\partial r}(b_+) \quad (15)$$

and

$$\mu_0\frac{\partial\Psi(r,\theta)}{\partial r}(a_-)=\mu_1\frac{\partial\Psi(r,\theta)}{\partial r}(a_+) \quad (16)$$

From the above four boundary conditions, we find four simplified equations:

$$A-b^\alpha B-C=a_0 \quad (17)$$

Where, $\alpha_0=H_0b^\alpha$

$$a_1A+\kappa b^\alpha B-a_1\kappa C=-a_0 \quad (18)$$

Where $\alpha_1=\alpha-1$ and $\kappa=\mu/\mu_0$.

$$a^{\alpha}B + C = a^{\alpha}D \tag{19}$$

$$a^{\alpha}\kappa B - a_1\kappa C = a^{\alpha}D \tag{20}$$

By eliminating the unknown constant D from Eq. (19) and Eq. (20), we find

$$C = \frac{(\kappa-1)}{(a_1\kappa+1)}a^{\alpha}B \tag{21}$$

By substituting the value of C in Eq. (18) from Eq. (21), we obtain

$$C = \frac{(a_1+\kappa)}{a_1(\kappa-1)} + \frac{a_0\alpha}{a_1(\kappa-1)} \tag{22}$$

Now we find the value of B by comparing Eq. (21) and Eq. (22).

$$B = \frac{a_0\alpha(a_1\kappa+1)}{(a_1a^{\alpha}(k-1)^2-(a_1+k)(a_1\kappa+1))b^{\alpha}} \tag{23}$$

Similarly,

$$C = \frac{a_0\alpha a^{\alpha}(\kappa-1)}{(a_1a^{\alpha}(k-1)^2-(a_1+k)(a_1\kappa+1))b^{\alpha}} \tag{24}$$

Solving for Constant A, substituting the value of unknown coefficients B and C in Eq. (18), we obtain the simplified coefficient A:

$$A = H_0\frac{[(a_1\kappa+1)(\kappa-1)(b^{\alpha}-a^{\alpha})]}{\left[(a_1+k)(a_1\kappa+1)-a_1\left(\frac{a}{b}\right)^{\alpha}(k-1)^2\right]} \tag{25}$$

Where, α_1=α-1 and κ=μ/μ_0.

Finally, we solve for coefficient D by substituting the value of B and C in Eq. (20), we obtain:

$$D = H_0\frac{\alpha(a_1\kappa+1+\kappa-1)}{\left[(a_1+k)(a_1\kappa+1)-a_1\left(\frac{a}{b}\right)^{\alpha}(k-1)^2\right]} \tag{26}$$

Which is simplified as:

$$D = H_0\frac{\alpha^2\kappa}{\left[(a_1+k)(a_1\kappa+1)-a_1\left(\frac{a}{b}\right)^{\alpha}(k-1)^2\right]} \tag{27}$$

To retrieve the results for integer order we set $\boldsymbol{\alpha}$ = 3.

Special Case

The potential outside the spherical shell is uniform and the dipole moment equal to the magnitude A. Inside the cavity of highly permeable material, there is a uniform magnetic field parallel to H_0 and equal to magnitude D. For μ >> μ_0, the dipole moment A and the inner field D become as:

$$A = b^{\alpha}H_0 \tag{28}$$

$$D = \frac{\alpha^2\mu_0}{\mu\left(1-\left(\frac{a}{b}\right)^{\alpha}\right)} \tag{29}$$

3. RESULTS AND DISCUSSION

We have investigated a closed-form solution in non-integer dimensional space (NID) for a spherical shell which is made of magnetic materials. Here, the potential for three regions of the spherical shell has been calculated through induced dipole moment in fractional dimensional space. Its results are very interesting. We find that the field due to the core that is inversely proportional to μ, it means the shielding effect is because of the highly permeable material μ/ $\mu_0 \approx 10^3 - 10^6$ that causes enough reduction in the field inside the sphere, although, the spherical shell is thin. Moreover, this general solution can be applied for various materials by replacing permeable materials like lossless metamaterials DNG, ENG, DPS, MNG, ENZ, MNZ, DNZ and plasmas (isotropic, anisotropic, uniaxial, bi-axial, magnetized and un magnetized plasmas). Further, it can be applied for lossy mediums like dry sand, wet sand, water, soil and petroleum etc.

4. CONCLUSIONS

Fractional space plays a key role to describe the complex phenomena of Physics. In this study, the Laplace equation has been analyzed in α-dimensional fractional space (FS). The potential for three regions of the spherical shell is calculated in (FS). Induced dipole moment has been also derived. The shielding effect is because of the highly permeable material μ/μ0 ≈ $10^3 - 10^6$ that causes enough reduction in the field inside sphere, although, the spherical shell is thin. A general solution has been investigated in this article that can be applied for different materials inside and outside the spherical shell. For all investigated cases when α = 3 the classical results are retrieved.

5. CONFLICT OF INTEREST

The authors declare no conflict of interest.

6. REFERENCES

1. C.G. Bollini, and J.J. Giambiagi. Dimensional renormalization: The number of dimensions as a regularizing parameter. *Nuovo Cimento B* 12: 20-26 (1972).
2. J.F. Ashmore. On renormalization and complex spacetime dimensions. *Communications in Mathematical Physics* 29: 177-187 (1973).
3. K.G. Wilson. Quantum Field - Theory Models in Less Than 4 Dimensions. *Physical Review D* 7(10): 2911-2926 (1973).

4. F.H. Stillinger. Axiomatic basis for spaces with noninteger dimension. *Journal of Mathematical Physics* 18(6): 1224-1234 (1977).
5. X.F. He. Excitons in anisotropic solids: The model of fractional-dimensional space. *Physical. Review B* 43(3): 2063-2069 (1991).
6. C.M. Bender, and S. Boettcher. Dimensional expansion for the Ising limit of quantum field theory. *Physical Review D* 48(10): 4919-4923 (1993).
7. C.M. Bender, and K.A. Milton. Scalar Casimir effect for a D-dimension sphere. *Physical Review D* 50 (10): 6547-6555 (1994).
8. V.E. Tarasov. Fractional generalization of Liouville equations. *Chaos: An Interdisciplinary Journal of Nonlinear Science* 14(1): 123-127 (2004).
9. V.E. Tarasov. Electromagnetic fields on fractals. *Modern Physics Letters A* 21(20): 1587-1600 (2006).
10. A. Zeilinger, and K. Svozil. Measuring the dimension of spacetime. *Physical Review Letters* 54(24): 2553-2555 (1985).
11. S. Muslih, and D. Baleanu. Fractional multipoles in fractional space. *Nonlinear Analysis: Real World Applications* 8(1): 198-203 (2007).
12. C. Palmer, and P.N. Stavrinou. Equations of motion in a noninteger-dimensionspace. *Journal of Physics A: Mathematical and General* 37(27): 6987-7003 (2004).
13. J.D. Jackson. Classical Electrodynamics. 3rd Ed. *John Wiley, New York, USA,* pp. 201-202 (1999).
14. J.A. Stratton. Electromagnetic Theory. *Wiley-IEEE Press,* pp-640 (1941).
15. T. Myint-U, and L. Debnath. Linear Partial Differential Equations for Scientists and Engineers, (4th ed.). *Springer Science & Business Media* (2007).
16. V.E. Tarasov. Gravitational field of fractals distribution of particles. *Celestial Mechanics and Dynamical Astronomy* 94: 1-115 (2006).
17. D. Baleanu, A.K. Golmankhaneh, and A.K. Golmankhaneh. On electromagnetic field in fractional space. *Nonlinear Analysis: Real World Applications* 11(1): 288-292 (2010).
18. V.E. Tarasov. Vector Calculus in Non-Integer Dimensional Space and its Applications to Fractal Media. *Communications in Nonlinear Science and Numerical Simulation* 20(2): 360-374 (2015).

Instructions for Authors

Manuscript Format

The manuscript may contain Abstract, Keywords, INTRODUCTION, MATERIALS AND METHODS, RESULTS, DISCUSSION (or RESULTS AND DISCUSSION), CONCLUSIONS, ACKNOWLEDGEMENTS, CONFLICT OF INTEREST and REFERENCES, *and any other information that the author(s) may consider necessary*.

Abstract (font size 10; max 250 words)**:** Must be self-explanatory**,** stating the rationale, objective(s), methodology, main results, and conclusions of the study. Abbreviations, if used, must be defined on the first mention in the Abstract as well as in the main text. Abstract of review articles may have a variable format.

Keywords (font size 10)**:** Three to eight keywords**,** depicting the article.

INTRODUCTION: Provide a clear and concise statement of the problem, citing relevant recent literature, and objectives of the investigation.

MATERIALS AND METHODS: Provide an adequate account of the procedures or experimental details, including statistical tests (if any), concisely but sufficient enough to replicate the study.

RESULTS: Be clear and concise with the help of appropriate Tables, Figures, and other illustrations. Data should not be repeated in Tables and Figures, but must be supported with statistics.

DISCUSSION: Provide interpretation of the RESULTS in the light of previous relevant studies, citing published references.

ACKNOWLEDGEMENTS: (font size 10)**:** In a brief statement, acknowledge the financial support and other assistance.

CONFLICT OF INTEREST: State if there is any conflict of interest.

REFERENCES (font size 10)**:** Cite references in the text **by number only** in **square brackets**, e.g. "Brown et al [2] reported ..." or "... as previously described [3, 6–8]", and list them in the REFERENCES section, in the order of citation in the text, Tables and Figures (not alphabetically). Only published (and accepted for publication) journal articles, books, and book chapters qualify for REFERENCES.

Declaration: Provide a declaration that: (i) the results are original; (ii) the same material is neither published nor under consideration elsewhere; (iii) approval of all authors have been obtained; and (iv) in case the article is accepted for publication, its copyright will be assigned to *Pakistan Academy of Sciences*. Authors must obtain permission to reproduce, where needed, copyrighted material from other sources and ensure that no copyrights are infringed upon.

Manuscript Formatting

Manuscripts must be submitted in Microsoft Word (2007 Version .doc or .docx format); **pdf** files not acceptable. Figures can be submitted in Word format, TIFF, GIF, JPEG, EPS, PPT. Manuscripts, in *Times New Roman*, 1.15spaced (but use single-space for Tables, long headings, and long captions of tables & figures). The text must be typed in a double-column across the paper width. The Manuscript sections must be numbered, i.e., **1. INTRODUCTION, 2. MATERIALS AND METHODS,** and so on… (a) **Title** of the article **(**Capitalize initial letter of each main word; font-size 16; **bold**), max 160 characters (no abbreviations or acronyms), depicting article's contents; (b) Author' first name, middle initial, and last name (font size 12, **bold**), and professional affiliation (i.e., each author's Department, Institution, Mailing address and Email; but no position titles) (font size 12); (c) Indicate the corresponding author with *; (d) **Short running title**, max 50 characters (font size 10).

Headings and Subheadings (font size 11): All flush left

LEVEL-1: **ALL CAPITAL LETTERS; Bold**

Level-2: **Capitalize Each Main Word (**Except prepositions**); Bold**

Level-3: Capitalize each main word (Except prepositions)***; Bold, Italic***

Level-4: *Run-in head*; *Italics*, *in the normal paragraph position. Capitalize the initial word only and end in a colon (i.e., :)*

List of REFERENCES must be prepared as under:

a. Journal Articles *(Name of journals must be stated in full)*

1. I. Golding, J. Paulsson, S.M. Zawilski, and E.C. Cox. Real time kinetics of gene activity in individual bacteria. *Cell* 123: 1025–1036 (2005).
2. W. Bialek, and S. Setayeshgar. Cooperative sensitivity and noise in biochemical signaling. *Physical Review Letters* 100: 258–263 (2008).
3. R.K. Robert, and C.R.L.Thompson. Forming patterns in development without morphogen gradients: differentiation and sorting. *Cold Spring Harbor Perspectives in Biology* 1(6) (2009).
4. D. Fravel. Commercialization and implementation of biocontrol. *Annual Reviews of Phytopathology* 43: 337359 (2005).

b. Books

5. W.R. Luellen. Fine-Tuning Your Writing. *Wise Owl Publishing Company, Madison, WI, USA* (2001).
6. U. Alon, and D.N. Wegner (Ed.). An Introduction to Systems Biology: Design Principles of Biological Circuits. *Chapman & Hall/CRC, Boca Raton, FL, USA* (2006).

c. Book Chapters

7. M.S. Sarnthein, and J.D. Stanford. Basal sauropodomorpha: historical and recent phylogenetic developments. In: The Northern North Atlantic: A Changing Environment. P.R. Schafer, & W. Schluter (Ed.), *Springer, Berlin, Germany*, pp. 365–410 (2000).
8. J.E. Smolen, and L.A. Boxer. Functions of Europhiles. In: Hematology, 4th ed. W.J. Williams., E. Butler and M.A. Litchman (Ed.), *McGraw Hill, New York, USA*, pp. 103–101 (1991).

d. Reports

9. M.D. Sobsey, and F.K. Pfaender. Evaluation of the H2S method for Detection of Fecal Contamination of Drinking Water, Report WHO/SDE/WSH/02.08, *Water Sanitation and Health Programme, WHO, Geneva, Switzerland* (2002).

e. Online references

These should specify the full URL for reference and give the date on which it was consulted. Please check again to confirm that the work you are citing is still accessible:

10. L. Branston. SENSPOL: Sensors for Monitoring Water Pollution from Contaminated Land, Landfills and Sediment (2000). http://www.cranfield.ac.uk/biotech/senspol/ (accessed 22 July 2005)

Tables and Figures

Insert all tables as editable text, not as images. Number tables consecutively following their appearance in the text, Figures should appear in numerical order, be described in the body of the text, and be positioned close to where they are first cited. Each figure should have a caption that describes the illustration, and that can be understood independently of the main text (Caption Table 1. and Fig 1. font size 10; Bold; Captions should be in sentence case; left-aligned). All Figures should have sufficiently high resolution (minimum 1000 pixels width/height, or a resolution of 300 dpi or higher) to enhance the readability. Figures may be printed in two sizes: column width of 8.0 cm or page width of 16.5 cm; number them as **Fig. 1**, **Fig. 2**, … in the order of citation in the text. Parts in a figure can be identified by A, B, C, D, ... and cited as Figure 2A, Figure 2B, Figure 2C. Captions to Figures must be concise but self-explanatory. Laser printed line drawings are acceptable. Do not use lettering smaller than 9 points or unnecessarily large. Photographs must be of high quality. A scale bar should be provided on all photomicrographs.

Tables: with concise but self-explanatory headings must be numbered according to the order of citation (like **Table 1.**, **Table 2.**). *Do not* abbreviate the word "Table" to "Tab.". Round off data to the nearest three significant digits. Provide essential explanatory footnotes, with superscript letters or symbols keyed to the data. Do not use vertical or horizontal lines, except for separating column heads from the data and at end of the Table.

Figures: Figures may be printed in two sizes: column width of 8.0 cm or page width of 16.5 cm; number them as **Fig. 1**, **Fig. 2**, … in the order of citation in the text. Captions to Figures must be concise but self-explanatory. Laser printed line drawings are acceptable. Do not use lettering smaller than 9 points or unnecessarily large. Photographs must be of high quality. A scale bar should be provided on all photomicrographs.

Note: The template of the manuscript is available at http://www.paspk.org/proceedings/; http://ppaspk.org/

Reviewers: Authors may suggest four relevant reviewers, two National and two International (with their **institutional E-mail** addresses).

SUBMISSION CHECKLIST

The following list will be useful during the final checking of an article before sending it to the journal for review.

Ensure that the following items are present:

One author has been designated as the corresponding author with contact details:

• E-mail address (Correct and valid)

• Full address of Institute/organization

• Keywords

• All figure captions

• All tables (including title, description, footnotes)

Further considerations

• Manuscript has been 'spell-checked' and 'grammar checked'

• References are in the correct format for this journal

• All references mentioned in the Reference list are cited in the text, and vice versa

• Permission has been obtained for the use of copyrighted material from other sources (including the Internet)

In case of any difficulty while submitting your manuscript, please get in touch with:

Editor
Pakistan Academy of Sciences
3-Constitution Avenue, Sector G-5/2
Islamabad, Pakistan
Email: editor@paspk.org
Tel: +92-51-920 7140
Websites: http://www.paspk.org/proceedings/; http://ppaspk.org/

PROCEEDINGS OF THE
PAKISTAN ACADEMY OF SCIENCES: PART A
Physical and Computational Sciences

CONTENTS

Volume 60, No. 3, September 2023 **Page**

Review Article

Blockchain in Healthcare: A Comprehensive Survey of Implementations and a Secure Model Proposal 1
— *Mehak Maqbool Memon, Manzoor Ahmed Hashmani, Filmann Taput Simpao, Anthony Cinco Sales, Neil Quinones Santillan, and Dodo Khan*

Research Articles

Acoustical Analysis of Insertion Losses of Ceiling Materials 15
— *Enobong Patrick Obot, Rufus Chika Okoro, Daniel Effiong Oku, Christian Nlemchukwu Nwosu, and Michael Ugwu Onuu*

Practical Analysis of Tap Water Dissolved Solids Efficient Reduction 27
— *Muhammad Imran Majid, and Naeem Shahzad*

An Intelligent Decision Support System for Crop Yield Prediction Using Machine Learning and Deep Learning Algorithms 37
— *Maryum Bibi, Saif-Ur-Rehman, Khalid Mahmood, and Rana Saud Shoukat*

Nutritional Study of Various Cow Breeds from Bhatta Chowk Lahore (Punjab), Pakistan 49
— *Asad Gulzar, Bisma Sher, Shabbir Hussain, Abdul Ahad Rasheed, Muhammad Salman, Shazma Massey, and Abdur Rauf*

Evaluation of Bending Length, Rigidity and Modulus of Woven and Knitted Fabrics 57
— *Mehreen Ijaz, Namood-e-Sahar, and Zohra Tariq*

Mathematical Analysis on Spherical Shell of Permeable Material in NID Space 63
— *Saeed Ahmed, Muhammad Akbar, Muhammad Imran Shahzad, Muhammad Ahmad Raza, and Sania Shaheen*

Instructions for Authors

Websites: http://www.paspk.org/proceedings/; http://ppaspk.org

PAKISTAN ACADEMY OF SCIENCES, ISLAMABAD, PAKISTAN

HEC Recognized, Category Y; Scopus Indexed